

**Geotechnical Characterisation and Design Processes for Anisotropic
Rock Masses in Open Pits: A Case Study of an Iron Ore Deposit in
Orientation Biased Anisotropic Host Rocks.**

by

Siyamazi Zamagatsheni Ndlovu

Submitted in fulfilment of the requirements for the degree
Master of Engineering and Environmental Geology

in the

Department of Geology
Faculty of Natural and Agricultural Sciences

UNIVERSITY OF PRETORIA

Supervisor: Prof J Louis van Rooy

Date of submission: February 2018

Declaration

“I declare that the dissertation which I hereby submit for the degree MSc Engineering and Environmental Geology at the University of Pretoria, is my own work and has not previously been submitted by me for a degree at another university”

ACKNOWLEDGEMENTS

First and foremost, all praise and glory be to God, my strength giver. To my parents thank you so much for your consistent support, be it emotionally, financially and at times physically. I will always be eternally grateful for being blessed with parents like you. Mom and Dad, we did it, we finished our Masters.

To my supervisor Prof J Louis van Rooy, thank you so much for your guidance on the subject matter.

ABSTRACT

Slope design and mining in foliated in-situ rock masses can be a major logistical and geotechnical hindrance. The Rock Mass Classification parameters need to be considered in relation to the anisotropic rock masses. What data acquisition methods should be considered, how much geotechnical data is needed and how should the data be represented so have to produce an optimum design which considers all the classification parameters? Data collected in foliated rock masses needs to be characterized along with specific laboratory rock testing to give an accurate indication of the extent and effect the anisotropy will exhibit on the rock mass. Geotechnical logging parameters gathered on site are dependent on the classification system to be applied for the geotechnical design requirements. Rock Mass Rating system (RMR), Mining Rock Mass Rating system (MRMR) as well as Geological Strength Index (GSI) are used, however the addition of the In-situ Rock Mass Rating system (IRMR) and the Japanese Geological Society Engineering Classification System (JGS) can allow for a downgrading of the rating value to account for the presence of foliation or other anisotropy in the rock masses. The geotechnical investigation done on this project area in Mozambique undertakes defining these additional data parameters required for adjusting rating systems for anisotropy as well as a holistic pit slope design consisting of geotechnical models such as geological model, structural model, rock mass model (material properties and classifications), kinematic, Swedge and limit equilibrium analyses. Limit equilibrium modeling of isotropic models inherently shows overall slopes being more stable than those of anisotropic models where the failure of the slope occurs due to the orientation (dip and dip direction) of the exposed rock material fabric on the slope in relation to the direction and angle of the overall slope. Application of anisotropic slope model designs would produce worst-case scenario outcomes, which if used to generate final slope geometries would result in more conservative slope parameters being applied in the slope design.

LIST OF ABBREVIATIONS

AMCG	Anorthosite- Mangerite-Charnockite-Granite
BFA	Base Friction Angle
FoS	Factor of Safety
GAB	Gabbro (Unweathered)
GABMW	Gabbro (Moderately Weathered)
GABW	Gabbro (Weathered)
GAN	Anorthosite (Unweathered)
GANW	Anorthosite(Weathered)
GDO	Dolerite
GSI	Geological Strength Index
HB	Hoek-Brown
IRMR	In-situ Rock Mass Rating
IRMS	In-situ rock mass Strength
IRS	Intact Rock Strength
JC	Joint condition rating adjustment
JCS	Joint Wall Compressive Strength
JGS	Japanese geological Society Engineering Classification System
JRC	Joint Roughness Coefficient
JS	"cemented" joint adjustment
MRMR	Mining Rock Mass Rating
OFX	Iron-Ore (Unweathered)
OFXMW	Iron-Ore (Moderately Weathered)
OFXW	Iron-Ore (Weathered)
PoF	Probability of Failure

RBS	Rock Block Strength
RMR	Rock Mass Rating
RMS	Rock Mass Strength
RQD	Rock Quality Designation
TCB	Tete-Chipata belt
TCS	Triaxial Compressive Strength
UCM ratio	Uniaxial Compressive Strength with Young's Modulus and Poisson's ratio
UCS	Uniaxial Compressive Strength
UTB	Uniaxial Indirect Tensile Strength (Brazilian Method)

TABLE OF CONTENTS

CHAPTER 1	INTRODUCTION	1
1.1	PROBLEM STATEMENT	1
1.2	OVERVIEW OF STUDY	4
CHAPTER 2	LITERATURE STUDY	5
2.1	CHARACTERIZATION AND CLASSIFICATION OF ANISOTROPIC ROCK MASS	6
2.1.1	Mining Rock Mass Rating System (MRMR)	7
2.1.2	In situ Rock Mass Rating System (IRMR)	11
2.1.3	Joint and foliation strength parameters	14
2.1.4	Geological strength Index (GSI)	15
2.1.5	Japanese Geological Society (JGS) Engineering Classification System	19
2.2	ANISOTROPIC ROCK MASS GEOMECHANICAL TESTING	24
2.3	GEOTECHNICAL DESIGN IN ANISOTROPIC/FOLIATED ROCK MASSES. 27	
2.4	LITERATURE REVIEW FINDINGS	29
CHAPTER 3	METHODOLOGY	31
3.1	GEOTECHNICAL DRILLING	31
3.2	GEOTECHNICAL LOGGING	32
3.3	LABORATORY TESTING	32
3.4	CLASSIFICATION SYSTEMS	33
3.5	ROCK MASS STRENGTH ESTIMATION	33
3.5.1	In situ rock strength	34
3.5.2	Estimation of mi	34
3.5.3	Estimation of GSI	34
3.5.4	Disturbance factor (D) estimation	35
3.5.5	Mohr-Coulomb strength parameters for rock mass	35
3.5.6	Joint and foliation strength parameters	35
3.5.7	Joint Rough Coefficient (JRC) values	35
3.5.8	Joint Compressive Strength (JCS)	36
3.5.9	Mohr-Coulomb strength parameters for joints and foliation	36
3.6	GEOTECHNICAL SECTIONS AND DOMAINS	36

3.7 SLOPE STABILITY ANALYSIS	37
3.7.1 Acceptance Criteria.....	38
3.7.2 Structural Data Analysis	38
3.7.3 Kinematic Analysis	38
3.7.4 SWEDGE Analysis.....	39
3.8 LIMIT EQUILIBRIUM ANALYSIS.....	41
3.8.1 Limit Equilibrium Input Parameters	41
3.8.2 Deterministic and Probabilistic Analysis.....	41
CHAPTER 4 CASE STUDY	43
4.1 REGIONAL GEOLOGY	43
4.2 LOCAL GEOLOGY	45
4.3 STRUCTURAL GEOLOGY	46
4.4 GROUNDWATER MODEL	47
CHAPTER 5 RESULTS.....	49
5.1 GEOTECHNICAL INVESTIGATION RESULTS.....	49
5.2 LABORATORY TESTING RESULTS.....	50
5.2.1 Density and strength properties of in situ rock	50
5.3 ROCK MASS CLASSIFICATION RESULTS	53
5.4 SLOPE STABILITY ANALYSIS RESULTS.....	56
5.4.1 Structural Data Analysis	56
5.4.2 Kinematic Analysis Results	59
5.4.3 SWEDGE Analysis Results	62
5.4.4 Limit Equilibrium Analysis Results.....	64
CHAPTER 6 DISCUSSION AND CONCLUSION.....	65
REFERENCES	69
APPENDICES	73

LIST OF FIGURES

Figure 2-1 Joint Frequency (Laubscher and Taylor 1976).....	10
Figure 2-2 In situ Rock Mass Rating adjustment flow chart (Jakubec, 2000)	12
Figure 2-3 Scale concept used for the IRMR classification system.....	13
Figure 2-4 Problems with RQD and classification systems that include RQD (Jakubec 2013)	14
Figure 2-5 Suggested proportions of parameters σ_{ci} and m_i for estimating rock mass properties for flysch (Marinos, P. Hoek, E, 2001).....	18
Figure 2-6 System for Engineering Classification of Rock Mass (Masahiko, 2005) after JGS 2004	21
Figure 2-7 Influence of loading direction on strength results (Saroglou, 2003)	24
Figure 3-1 Geotechnical domains (Red line showing division of North from South Study Area.) .	37
Figure 4-1 Simplified geological map of the Tete Suite and surroundings (Westerhof et al, 2008) .	44
Figure 4-2 Interpretation of the dykes through the project area (SRK 2015)	47
Figure 4-3 Conceptual hydrogeological model of the project area (SRK 2014).....	48
Figure 5-1 Plan of geotechnical boreholes where black labels indicate the research holes in the project area.	49
Figure 5-2 Correlation of RMR, MRMR and IRMR with depth	54
Figure 5-3 Stereographic projection of discontinuities in Northern section of the Study Area	58
Figure 5-4 Stereographic projection of discontinuities in the Southern section of the Study Area .	58
Figure 5-5 Probability of occurrence of stack scale failure in the Northern Study Area	60
Figure 5-6 Probability of occurrence of bench scale failure in Project area North.....	60
Figure 5-7 Probability of occurrence of stack scale failure in the Southern Study Area	61
Figure 5-8 Probability of occurrence of bench scale failure in the Southern Study Area.....	61
Figure 6-1 Anisotropic rock mass geotechnical investigation and design flow chart.	65

LIST OF TABLES

Table 2-1 Geotechnical Parameters and Ratings (Laubscher and Taylor 1976).	8
Table 2-2 Assessment of Joint Conditions (Laubscher and Taylor 1976).	9
Table 2-3 Geological Parameters and Ratings (Laubscher and Taylor 1976).....	11
Table 2-4 GSI Characterisation (Hoek and Brown 1998).....	16
Table 2-5 Foliated/laminated/sheared rock mass category in the GSI system.....	17
Table 2-6 Classification and Classes of Hard Rock Mass (Masahiko, 2005) after JGS 2004	22
Table 2-7 Classification parameters and classes of Soft Rock Mass (Masahiko, 2005) after JGS 2004.....	23
Table 2-8 Classification of foliation and anisotropy of rock material (Tsidzi 1990).....	25
Table 2-9 Classification of Anisotropy (Singh et al. 1989)	26
Table 2-10 Acceptance Criteria (Read and Stacey, 2009)	28
Table 3-1 Limit Equilibrium Input parameters	41
Table 5-1 Geotechnical units used in the research study	50
Table 5-2 Densities of in situ rock masses	51
Table 5-3 Rock Strength Summary	51
Table 5-4 Base friction angle results.....	52
Table 5-5 Summary of Elastic properties.....	53
Table 5-6 Laubscher's (1990) MRMR and Bieniawski (1989) RMR Results.....	55
Table 5-7: GSI Estimate.....	55
Table 5-8 Summary of input parameters and results from RocData	56
Table 5-9 Minimum, mean and maximum discontinuity set orientation data.....	57
Table 5-10 SWEDGE results Northern Study Area.....	62
Table 5-11 SWEDGE results Southern Study Area.....	62
Table 5-12 Slope geometries.....	63
Table 5-13 Overall slope stability results.....	64

CHAPTER 1 INTRODUCTION

Rock masses that have been foliated or sedimentary rocks which have well-developed bedding planes which typically exhibit high strength anisotropy are very challenging to describe using rock mass classification systems. Current mainstream rock mass classification systems do not account for the rock mass foliation/anisotropy other than open joints. The foliations in the rock mass should be analysed separately so that anisotropy of in situ rock mass rating can be quantified and incorporated into the geotechnical analysis being undertaken. Data acquisition and correct data processing will result in the appropriate parameters and adjustments being made to the current classification methods that will yield an accurate rock mass classification of the anisotropic materials, which will be a true representation of the in-situ rock mass.

This dissertation will address which methods of data collection are best and compare the rock mass classification methods required for open pit geotechnical design and the additional analysis methods and calculations that are required for the analysis of foliated/ anisotropic rock masses.

1.1 PROBLEM STATEMENT

In most geotechnical investigations little attention is paid to the problem of foliation and or anisotropy. These variations in the rock mass may affect and limit the geotechnical design within a project area. However, surface mapping of natural outcrops, core logging and investigation trenches can produce data on the foliation and structural history for the in-situ rock mass. Although this data may be valuable and sound it is generally not incorporated into the design process.

The use of sophisticated numerical modelling techniques to estimate the rock mass strength does not nullify the importance of the widely used classification systems for rock masses. These systems are still fundamental tools for rock mass characterisation,

When it comes to anisotropic rock masses, such as foliated rock masses the applied current rock mass classifications neglect rock mass closed discontinuities especially those outside the category known as “open joints” category (Jakubec, 2001). Closed or cemented discontinuities considering this dissertation have the potential of opening and being weakness planes (open discontinuities /joint/ bedding/ banding planes of weakness).

The two most well-known and used rock mass classification systems, namely the Rock Quality Designation System (Barton, 1974) and Geomechanics or Rock Mass Rating (RMR) System (Bieniawski, 1976) evolved from earlier classification systems and were primarily developed for use in the tunnel design and construction fields. Laubscher (1990) adjusted the RMR system specifically for use in the mining environment and introduced the Mine Rock Mass Rating (MRMR) system. The MRMR system however does not address anisotropic rock mass conditions as found in foliated rock masses. Current rock mass classification systems do not consider anisotropic rock masses or rock masses with distinct alignment of minerals and consequently fabric. The general systematic joint sets rock masses may also contain many other discontinuities which may be closed, and which may or may not impact the rock mass strength. These may include schistosity, bedding planes, foliation, etc. and these structures (discontinuities) needs to be considered in the rock mass to be accurately characterized.

To address the issue Jakubec and Laubscher (2000) introduced a modified MRMR Classification System, termed the In-Situ Rock Mass Rating (IRMR) System. The IRMR is a recent addition to classification systems which is still not widely implemented in industry in slope design. The implementation of this system results in less over estimation of the rock mass strengths applied in design resulting in more conservative design approaches.

The current practice for geotechnical investigations regarding geomechanical laboratory testing does not take into consideration the anisotropic nature of the rock mass being tested, resulting in an over estimation of the rock strength as strength test results on failure planes of foliation structures are usually disregarded in the strength analysis to obtain a Hoek-Brown curve. Other fundamental properties of the rock mass such as thermal conductivity

and resistivity would vary according to the direction in which they are measured, relative to the axis of symmetry (Nasseri et al. 2003). The problem solution that would be associated with anisotropy of in situ rock masses may result in more complicated engineering, numerical modelling and design. It is therefore important that detailed analysis is carried out specifically on foliation and is incorporated in the geological model.

The preferred alignment of platy minerals such as those found in mica rich and chloritic schists results in directional differences in mechanical strengths in rock masses (Palmstrom, 1995)

The role of rock anisotropy and its interaction with the numerical analyses boundary conditions and the geotechnical design are based on the following factors in relation to foliation (Nasseri et al. 2003).

- Orientation of foliation: The orientation and variation in orientation must be known so that the axis of the transverse anisotropy and the direction of strength weakening are known.
- Intensity of foliation: A more intense foliation will have a greater effect on the elastic properties and the strength variation.
- Type of foliation: If there are geological differences in the foliation type, these should be specified because they will have different effects on the rock elasticity and strength.
- Foliation in metamorphic rocks may have a profound influence on ground water movement (Singhal, 2010).

The primary objectives of this dissertation are to:

- Define anisotropy/foliation in relation to petrography
- Document the classification systems which incorporate foliation/ anisotropic data.
- Analyses of laboratory tests in relation to foliated rock masses and
- Application of classification systems and laboratory test results in the design process for open pit models.

1.2 OVERVIEW OF STUDY

In Chapter 2 Literature Review; is a critical literature review of the research topic,

In Chapter 3 Methodology; covers the methodology of the geotechnical investigation and analysis methods for an open pit design of an anisotropic rock mass.

In Chapter 4 Case Study; is a case study of an iron ore deposit in an orientation biased anisotropic host rock

In Chapter 5 Results; details the results of the geotechnical investigation and analysis of the case study area.

In Chapter 6. Discussion and Conclusions; discusses the major findings of the results of the case study and conclusions of the dissertation.

In Chapter 7 References

In Chapter 8 Appendices

CHAPTER 2 LITERATURE STUDY

Foliation is a general term for the planar arrangement of small-scale textural, crystallographic and/or structural features and presents a “planar fabric”. The “planar fabric” is applied, for example, to cleavage in slates, to schistosity or gneissic structure in metamorphic rock masses (Passchier & Trouw 1996). The intensity of the foliation is in turn a function of the type and intensity of the deformation by which it was formed. (Akesson, 2001)

The definition of foliation is also used alone in defining planar fabrics in deformed and metamorphosed crystalline rocks. The fundamental analysis of foliation character and foliation orientation is based on recognized principles of structural analysis (Turner, 1963).

There are three main foliation types namely:

- Stylolitic foliation which forms typically in calcareous or argillaceous sandstones,
- Disjunctive foliation which develops in quartz-rich sandstones and form rough to smooth foliations and
- Crenulation foliation which forms in rock masses with high proportions of platy minerals or at times in finely laminated rock masses.

Foliation structures are caused during ductile flattening of a rock mass coupled with mechanical rotation, solution, precipitation and recrystallisation of minerals in the rock. This is also influenced by the mineralogical composition of the rock which would result in the different types of foliation occurring (Singhal, 2010).

Foliation belongs to the group of geological structures which are called pervasive, meaning that these structures do not occur as individual features unlike (ie fractures or bedding planes) but rather affects the intact rock, usually as a preferred shape and/or crystallographic orientation of mineral grains and/or aggregates of mineral grains. Foliation planes are often referred to as S- planes (from the original German nomenclature), and tectonites which show

a single pervasive foliation which is mesoscopically recognisable and constantly oriented (e.g. in hand-specimen or on outcrop surfaces) are often referred to as S-tectonites (Barker 1990).

Metamorphism of rock masses with a high micaceous and chlorite content would most likely result in anisotropic mineral orientations. Most metamorphic changes in rock masses result in harder minerals, but the preferred orientation of platy minerals due to shearing movements results in considerable directional differences in mechanical properties. Rocks with gneissic texture are generally not strongly anisotropic whereas slaty rock masses would be highly anisotropic. (Singhal, 2010).

2.1 CHARACTERIZATION AND CLASSIFICATION OF ANISOTROPIC ROCK MASS

The aim of geotechnical mapping/ logging pervasive structures such as foliation is a means to obtain representative orientation values for areas of outcrop or borehole sections in which the structure is judged to be entirely homogeneous.

Pervasive structures are not individual features, but are bulk properties and cannot be treated statistically, except for obtaining mean values and variation ranges. Parameters such as width, length, spacing, aperture and frequency which are important in fracture system analysis, do not come into consideration in foliation or anisotropic investigations. The three parameters that are important in anisotropic studies are:

- Orientation
- Intensity
- Type

The foliation in the in-situ rock seems to pre-determine the orientation of the dominant discontinuity set (Äikäs et al. 2003), and possibly also the preferred orientation of any possible major discontinuity set of fracture zones. The data acquisition process needs to incorporate the above mentioned fundamental parameters with the Rock Mass Rating and

well as the Mining Rock Mass Rating mapping and logging parameters, to produce an adequate design that is related to the anisotropic rock mass.

Äikäs et al. (2003) mention a program of foliation characterization and measurement that considers the systematic foliation investigations which consisted of tunnel mapping, as well as core logging, which are standard methods of data acquisition. The degree of foliation can be quantified by using optical microscopy to count the linear traverses on thin sections, orientated perpendicular to the foliation (Akesson, 2001).

The geotechnical logging parameters gathered on site are dependent on the classification system to be applied for the design requirements. RMR, MRMR is used in underground mining design whereas the GSI system is prominently used in open pit and tunneling design. In addition, to the above-mentioned classification systems, the IRMR and JGS can be utilised to allow for downgrading of these rating value for the presence of foliation in the rock mass. All these classification systems are discussed in further in the sub-sections below.

2.1.1 Mining Rock Mass Rating System (MRMR)

Rock mass classification, which is a useful tool for rock engineering, was initiated in Europe in the 1940s. Terzaghi (1946) proposed nine categories of rock mass associated with the applied rock load on tunnel supports. The Q-system (Barton et al. 1974), RMR (Bieniawski, 1973) and others were proposed in the 1970s and Laubscher's (1975) Mining Rock Mass rating (MRMR) was derived from the system proposed by Bieniawski (1978).

The main purpose of rock mass classification systems is to classify rock masses into zones based on similar behaviour; provide a basis of understanding between different mining sectors and to formulate design parameters for the actual mine design (Jakubec, 2000)

The MRMR system considers the same rock mass parameters as the RMR classification, but also incorporates groundwater and joint condition parameters. (Laubscher and Taylor 1976).

The rock mass parameters utilized in this classification system are:

- Intact Rock Material Strength (IRS) referring to the Uniaxial Compressive Strength of the in-situ rock
- Rock Quality Designation (RQD)
- Joint spacing

- Groundwater in conjunction with the Joint condition

Each parameter is rated separately and is added up to result in rating ranges between 0 to 100. The rating allocation for each parameter is shown in Table 2-1, Table 2-2 and Figure 2-1 below and the calculated rating and classification of the rock mass are shown in Table 2-3.

Table 2-1 Geotechnical Parameters and Ratings (Laubscher and Taylor 1976).

Parameter and Ratings					
IRS=M Pa Rating (%)			RQD Rating (%)		Joint Spacing (m)
Extremely hard	> 185	20	97-100	15	0 < -> 25
	165-185	18	64-96	14	
Very Hard	145-164	16	71-83	12	
Hard	125-144	14	56-70	10	
	105-124	12	44-55	8	
	85-104	10	31-43	6	
Soft	65-84	8	17-30	4	Matrix Type
	45-64	6	4-16	2	M1 Fault
	35-44	5	0-3	0	M2 Shears
Very Soft	25-34	4			M3 Intense Fracturing
	12-24	3			M4 Intense Mineralisation
	5-11	2			M5 Deformable Material
	1-4	1			

Table 2-2 Assessment of Joint Conditions (Laubscher and Taylor 1976).

Assessment of Joint Conditions					
Parameters	Accumulative percentage adjustment of possible rating of 40				
	Description	Dry	Adjustment Percentage		
			Moist	Moist, Pressure 25- 125 1/m	High pressure >25 1/m
MICRO- small scale joint expression	1. Polished	0.55	0.50	0.45	0.40
	2. Smooth Planar	0.60	0.55	0.50	0.45
	3. Rough Planar	0.65	0.60	0.55	0.50
	4. Slickensides Undulating	0.70	0.65	0.60	0.55
	5. Smooth Undulating	0.75	0.70	0.65	0.60
	6. Rough Undulating	0.80	0.75	0.70	0.65
	7. Slickensides Stepped	0.85	0.80	0.75	0.70
	8. Smooth Stepped	0.90	0.85	0.80	0.75
	9. Rough Stepped/Irregular	0.95	0.90	0.85	0.80
MACRO- large scale joint expression	1. Planar	0.75	0.70	0.65	0.60
	2. Undulating	0.80	0.75	0.70	0.65
	3. Rough Planar	0.85	0.80	0.75	0.70
	4. Curved	0.95	0.90	0.85	0.80
	5. Irregular	1.00	1.00	0.95	0.90
Joint wall alteration weaker than wall rock, only if it is weaker than the filling		0.75	0.70	0.65	0.60
Joint Filling	1. Gouge Thickness > Amplitude of Irregularities	0.30	0.20	0.15	0.10
	2. Gouge Thickness < Amplitude of Irregularities	0.45	0.40	0.35	0.30
	3. Soft Sheared Material- Fine	0.50	0.45	0.40	0.35
	4. Soft Sheared Material- Medium	0.60	0.55	0.50	0.45
	5. Soft Sheared Material- Coarse	0.70	0.65	0.60	0.55
	6. Non- Softening Material- Fine	0.80	0.75	0.70	0.65
	7. Non-Softening Material- Medium	0.85	0.80	0.75	0.70
	8. Non-Softening Material- Course	0.90	0.85	0.80	0.75

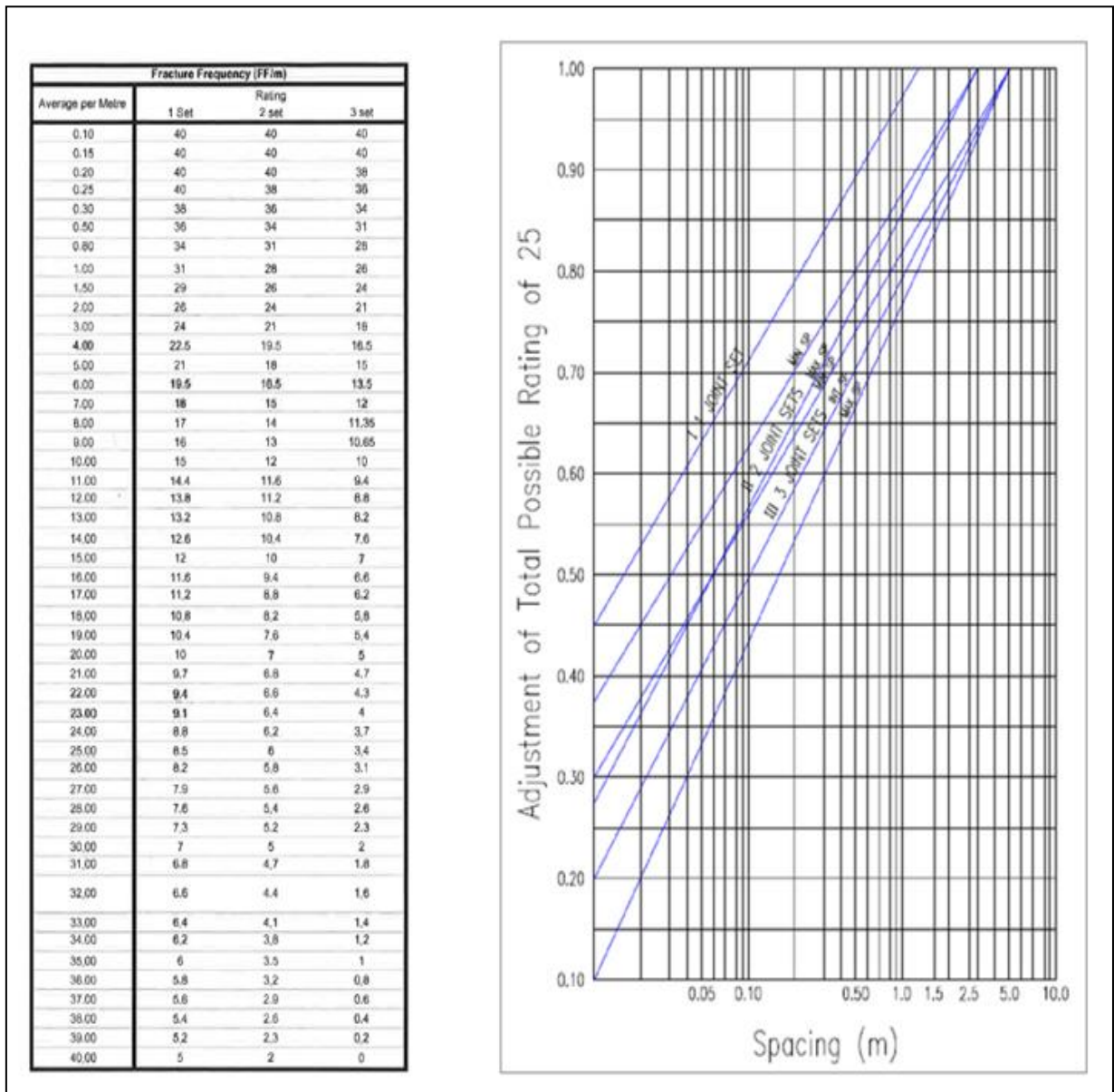


Figure 2-1 Joint Frequency (Laubscher and Taylor 1976).

Table 2-3 Geological Parameters and Ratings (Laubscher and Taylor 1976).

Geological Parameter Rating					
Class	1	2	3	4	5
	B	A B	A B	A B	A B
Rating	100-81	80-61	60-41	40-21	20-0
Description	Very Good	Good	Fair	Poor	Very Poor
Colour	Blue	Green	Yellow	Brown	Red
Distinguish between A and B sub-classes by colouring the A sub classes full and cross-hatch the B					

The main shortcoming of the MRMR system in relation to foliation anisotropy is that it only accounts for open joints. Foliation structures are not accounted for and neither is their effect on RQD and the IRS.

2.1.2 In situ Rock Mass Rating System (IRMR)

In 2000 Laubscher's Mining Rock Mass Rating (MRMR) classification system was modified to the in-situ Rock Mass Rating (IRMR), which introduced the rock block strength concept and suggested a method to capture and incorporate discontinuities other than open joints (Laubscher and Jakubec, 2000). The impact of discontinuities on rock mass strength estimates and the challenges of current data collection techniques are discussed by Jakubec (2013). The following changes were introduced to the MRMR system resulting in the IRMR system (Jakubec, 2000):

- Rock Block Strength (RBS);
 1. RBS as described in Jakubec and Laubscher (2000) is the strength of the primary rock block (bounded by joints), corrected for non-continuous fractures and veins. To arrive at a value for the RBS, the measured IRS value must be adjusted for sample size, such that the conversion from core or hand specimen to rock block is approximately 80 per cent of the IRS. For example, where the in-situ rock strength (IRS) is 100 MPa, the rock block strength (RBS) is 80 MPa, in the absence of fractures and veins. Where such discontinuities are present, a further adjustment is required to more accurately determine the RBS. The strength of closed structures, and their frequency, is used to determine this adjustment.

- “cemented” joint adjustment (JS);
2. Is the downgrading of RBS in relation to the joint spacing of cemented joints where the strength of the cementing material is less than that of the host rock?
 - changes in joint condition rating (JC) adjustment
 3. An adjustment in accordance to the strength of the least favourable joint set (orientation of the joint with regards to the disturbing stress applied)
 - Water impact as an MRMR adjustment.
 4. The water / ice adjustment is an addition that reduces the frictional properties and effective stress of the rock mass as follows:
 - water generally decreases rock mass strength;
 - ice generally increases rock mass strength;
 - rock mass strength increases with lower ice temperatures; and
 - ice in the rock mass could cause creep.

The changes and additions are shown in Figure 2-2. The In-situ Rock Mass Strength (IRMS) are reduced by:

- Material Strength;
- Quality of discontinuities and
- Strength of discontinuities.

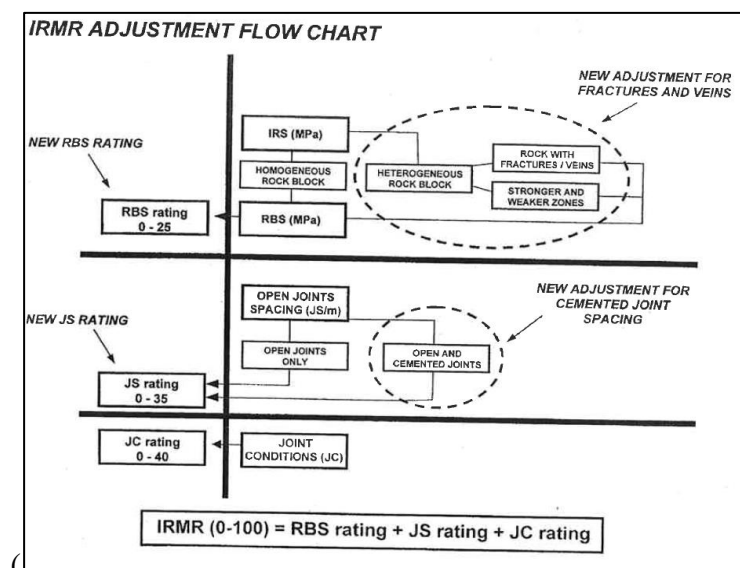


Figure 2-2 In situ Rock Mass Rating adjustment flow chart (Jakubec, 2000)

The IRMR classification system addresses the importance of discontinuities in rock mass classification in relation to strength adjustments to rock block and rock mass as shown in Figure 2-3. The weakening factor presented by the discontinuities influences the strength categories which include;

- Intact Rock Strength (IRS):
- Rock Block Strength (RBS) and
- Rock Mass Strength (RMS).

In relation to foliated rock masses sampling bias resulting from core testing of just the stronger materials/sections of the rock mass is considered. Therefore, accurate sampling and testing that would be more representative of the foliated/ anisotropic rock mass would include discontinuities which will result in a reduced IRS estimation.

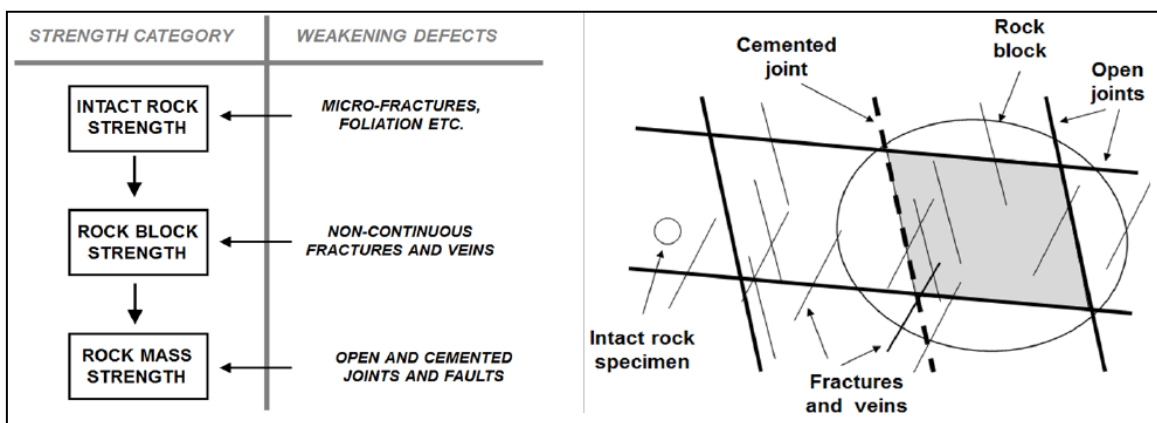


Figure 2-3 Scale concept used for the IRMR classification system

Defect persistence, large scale geometry, and orientation are usually misinterpreted in core logging. The geotechnical logging should separately log open joints and foliation structures, to calculate the anisotropy of in situ rock mass ratings, with or without taking foliation into consideration (Jakubec 2013).

The downside of classification systems which include RQD is that when considering discontinuities, the estimation of RQD is based on the measurement of the total measurement of all pieces is longer than 10 cm divided by the total core recovered in the interval. The RQD and fracture frequency in IRMR are now part of the RBS and should not be counted twice in the calculation of IRMR (Jakubec, 2000).

In both cases shown in Figure 2-4 the RQD = 0. The different degree of fragmentation is significantly different and will result in different mining and ground support environments. The IRMR produces a more appropriate estimation in relation to the degree of fragmentation.



Figure 2-4 Problems with RQD and classification systems that include RQD (Jakubec 2013)

The joint strength adjustment assumes that the strength of the least favorable joint set is applied in the IRMR calculation (Jakubec, 2000).

Dyke (2008) compared values of MRMR and IRMR and found a correlation coefficient that indicates a linear relationship and an imperfect, yet significant, correlation between the MRMR and IRMR. A general regression equation is derived to be used to predict equivalent IRMR

values from MRMR values,

where:

$$\mathbf{IRMR} = 1.0376\mathbf{MRMR} - 1.3655 [\pm 0.24]$$

2.1.3 Joint and foliation strength parameters

Barton (1973) suggested a criterion to estimate the peak shear strength by introducing the roughness component, JRC, and the joint wall strength, JCS, as functions of the normal stress. The envelop of the failure criterion obtains an appearance of a slightly curved line, representing the gradually changing shear strength due to decreasing JRC and JCS over high stresses.

Barton Bandis failure criterion (1990): is an empirical relationship utilised to model the shear strength of rock discontinuities (e.g. joints or foliation). The Barton-Bandis criterion is non-linear, and relates the shear strength to the normal stress using the equation below:

$$\tau = \sigma_n \tan \left[\phi_b + JRC \log_{10} \left(\frac{JCS}{\sigma_n} \right) \right]$$

where ϕ_b is the basic friction angle of the failure surface?

JRC is the joint roughness coefficient, and

JCS is the joint wall compressive strength [

2.1.4 Geological strength Index (GSI)

The Geological Strength Index (GSI) is the observation of a rock mass made by a qualified and experienced geologist or engineering geologist for a visually estimated strength index used in the calculation of the generalization Hoek-Brown Failure criterion (Dyke 2002).

The Geological Strength Index (GSI) was introduced by Hoek et al (1994) as an alternative method to classify rock mass quality due to difficulties in applying Bieniawski's (1978) Rock Mass Rating (RMR) to very poor rock masses. The GSI is an important tool to estimate parameters such as cohesion, friction angle and deformation modulus of rock masses.

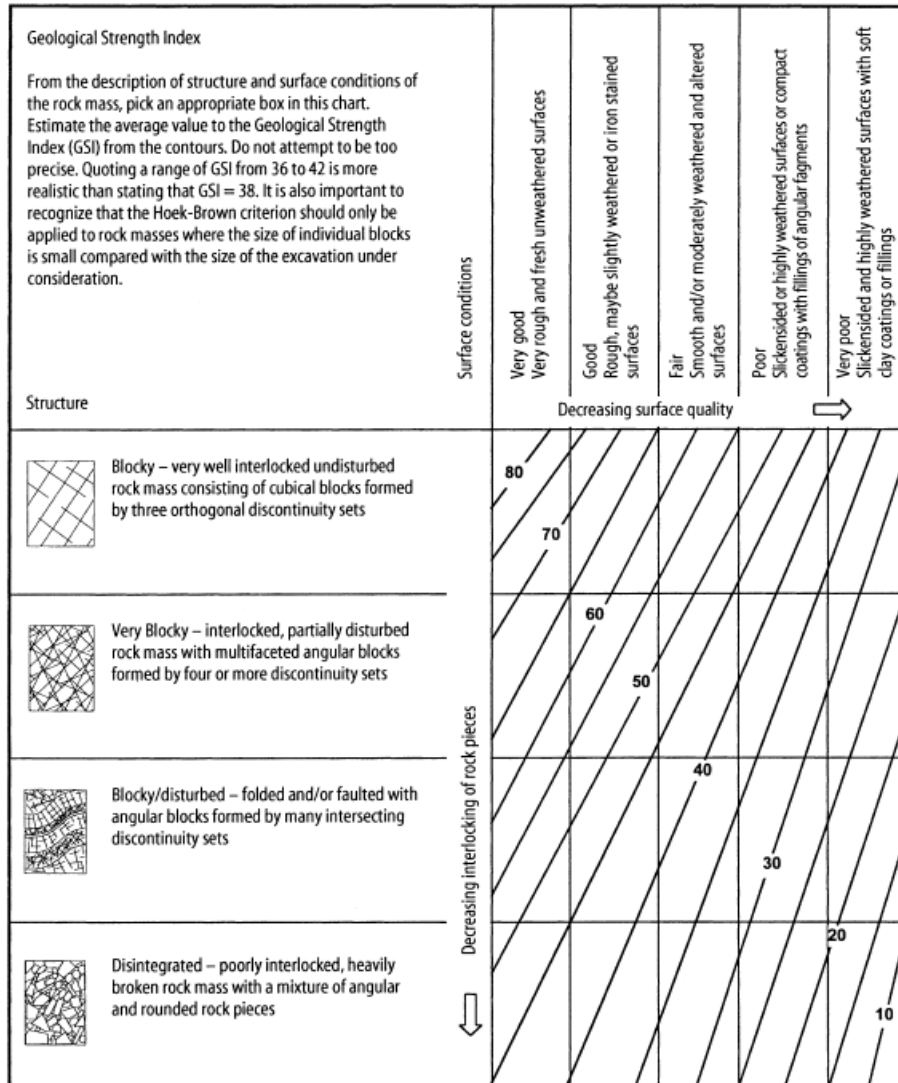
GSI is based upon an assessment of the lithology, structure and condition of discontinuity surfaces in the rock mass and it is estimated from visual inspection? of the rock mass exposed in surface excavations or outcrops. There are two fundamental parameters of geological processes, namely:

- The blockiness of the rock mass, and
- The surface conditions of the discontinuities.

The combination of these two parameters provides a basis for the description of a wide range of rock masses from which the GSI is estimated.

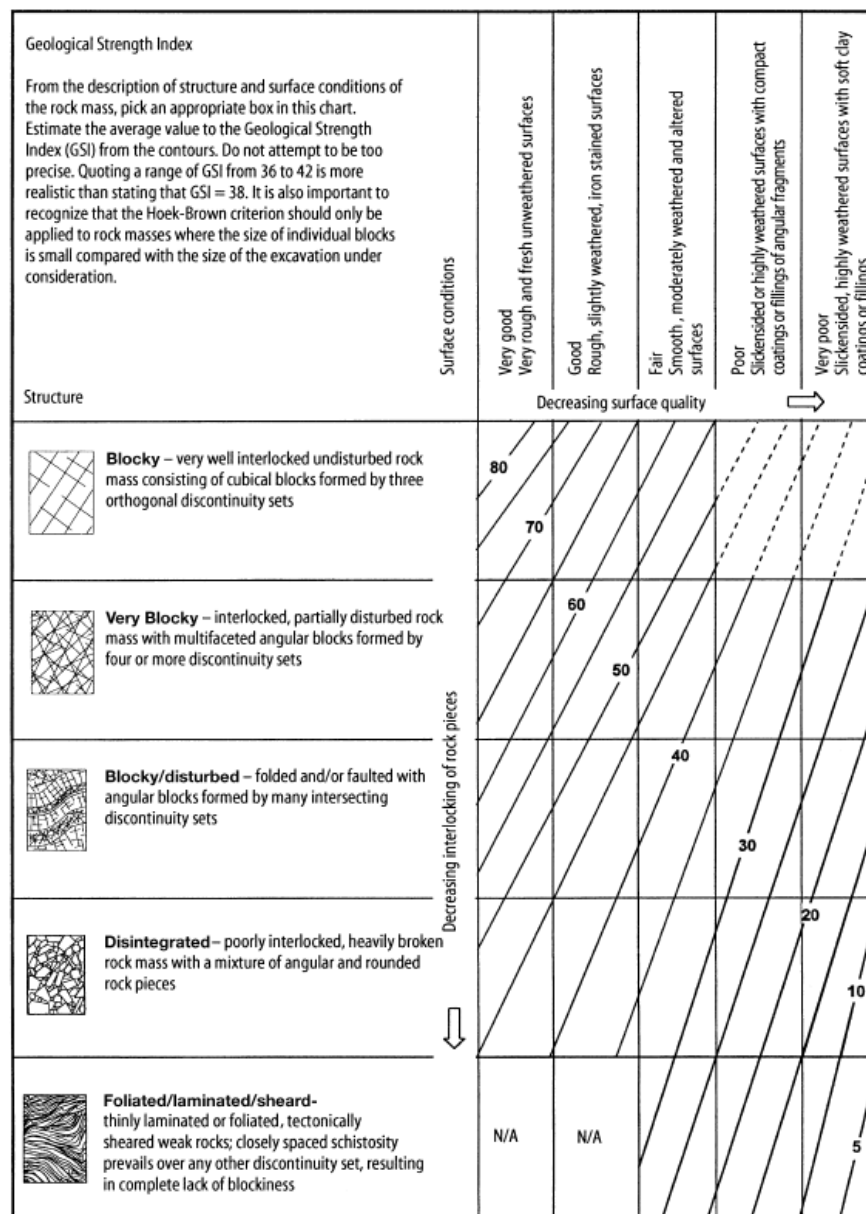
Table 2-4 illustrates the Hoek and Brown (1998) characterization of rock masses based on interlocking and joint alteration.

Table 2-4 GSI Characterisation (Hoek and Brown 1998)



In the application of the GSI system to foliated rock masses the foliation forms the predominant structure over a specific discontinuity/defect description with a lack of blockiness, however the rock mass cannot be entirely described as ‘good or very good as the foliation/anisotropy results in a degree of weakness along the foliation/anisotropic planes. The foliated rock mass category accommodates the rock masses in the lowest range of applicability of the GSI system (Table 2-5). These rock masses feature controlling strength and deformability is not on the rock to rock contacts but rather on the shear strength of the infill material along the foliation planes (Hoek, 1998).

Table 2-5 Foliated/laminated/sheared rock mass category in the GSI system



The behavior of strongly anisotropic rock masses will be controlled by the fact that the mineral alignment of the planes is an order of magnitude weaker than any other features. For foliated rock masses a lower GSI value is needed even if the rock mass does look competent. GSI values for anisotropic rock masses where the alignment of platy minerals originated from alteration or dynamic metamorphosis become lower and move towards the right-hand corner (Category H) in the GSI chart (Figure 2-5). Gneiss compared to sound granitic rock masses shows a slight displacement of the assigned range downward and to the

right of the GSI chart may be seen. Same comments as for the granite apply when gneiss is weathered. Schists may vary from strong micaschists and calcitic schist types to weak chloritic, talcic schists and phyllites. The persisting schistosity planes and their usually “poor” surface conditions restrain the range of GSI values. However, the shaded areas illustrated in the charts are indicative and should not be used for design purposes as deviations may occur. But even for indicative cases or for rough estimations? the use of mean values is not, recommended. For design purposes it is obviously necessary to base the assessment on detailed site inspection and evaluation of all geological data derived from site investigation (Hoek; 2013)

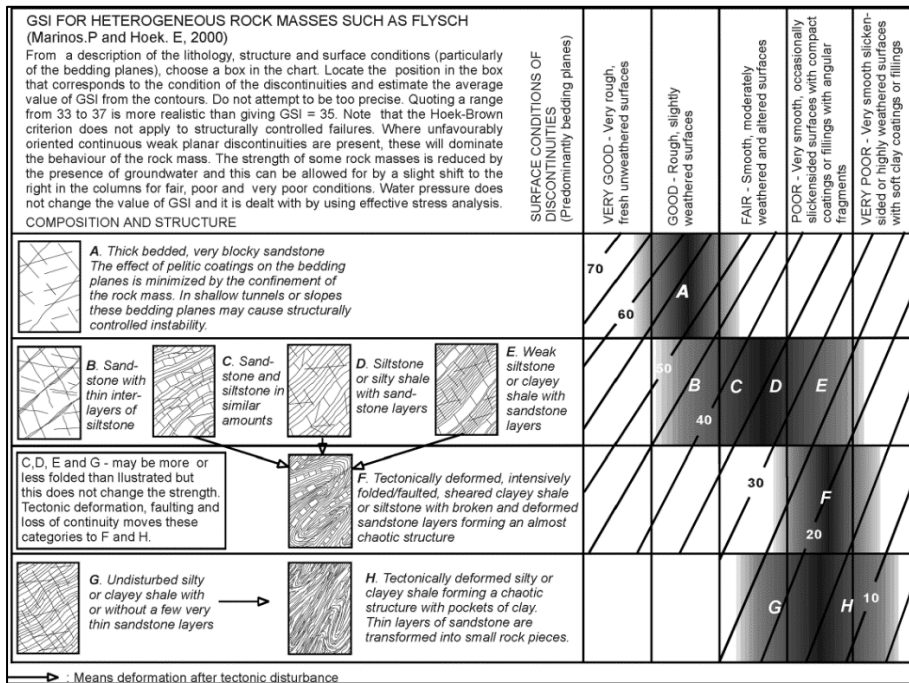


Figure 2-5 Suggested proportions of parameters σ_{ci} and m_i for estimating rock mass properties for flysch (Marinos, P. Hoek, E, 2001)

The estimation of the Geological Strength Index (GSI) was based on RQD and the Joint Condition (JCond89) rating defined by Bieniawski (1989) in the formulas shown below:

$$GSI_{\text{Bieniawski89}} = 1.5J\text{Cond}_{89} + RQD/2$$

$$GSI = RMR - 5$$

2.1.5 Japanese Geological Society (JGS) Engineering Classification System

The aim of JGS classification is to assign the classification of rock masses based on their fundamental characteristics which specifically determine the essential behavior of rock mass. The JGS classification can be used to (Masahiko, 2005):

- understand the actual state of rock mass;
- share information about the rock mass among the various fields of engineers;
- estimate the geotechnical properties in preliminary investigation stage, as well as for;
- plan the methods of investigation / testing to determine the design parameters, making the analysis model and for
- supply basic information to assess the rock mass in the advanced stages of a project where the design, construction and monitoring are concerned.

The JGS is based on the relation between physical properties of rock masses and internationally recognized identification and description of rock and rock masses such as in ISO 14689-1:2003. The following identification and descriptions of rock mass properties are considered:

- Strength of rock material, the uniaxial strength;
- Foliation;
- Discontinuities;
- Grain size of constituting rock material;
- Content of large fragments;
- Layer Thickness; and
- Weathering/ Alteration state.

In anisotropic rock masses the existence of foliation can be investigated through the laminations/banding and spacing of planes in the petrography of rock material. Foliation in rock masses have a strong influence on the anisotropy of the mechanical parameters of the rock mass. The foliation planes can quite easily open by uplifting and stress release during excavation.

The classification of the rock masses in the JGS classification system is based on three steps with one additional sub step. The steps are as follows:

- First step the rock mass is classified according to its uniaxial strength. If the strength is equal to or greater than 25 MPa the rock mass is classified as Hard rock mass (H). Fresh unweathered rock with an Uniaxial Compressive Strength (UCS) of less than 25 MPa is classified as Soft rock mass (S)
- In the second step the hard rock mass is further classified into Massive (M) and Foliated (f) depending on the fabric. In the case of Soft rock masses if the minerals are homogenous the rock mass is classified as (M) and if the material is fragmented and has matrix the rock mass is classified as rudaceous (R) and if the rock mass is thinly bedded it is classified as interbedded (B)
- The third step considers the indices of classes from the combination of two classification parameters. The parameters are shown in Table 2-6 and
- This classification system is currently being used in the geotechnical sector in Japan and has of yet not been applied to mining geotechnics or designs. It is important to note that the prior mentioned mining classification systems e.g. MRMR etc. are modifications of earlier derived civil engineering and tunneling classification systems which means there is a possibility for the development of the JGS classification system to into a mining focused system.

- **Table 2-7.** The detailed roughness and weathering classes are shown in Figure 2-6 and Table 2-6 below. The final sub step is the classification of the fracture zones (Masahiko, 2005).

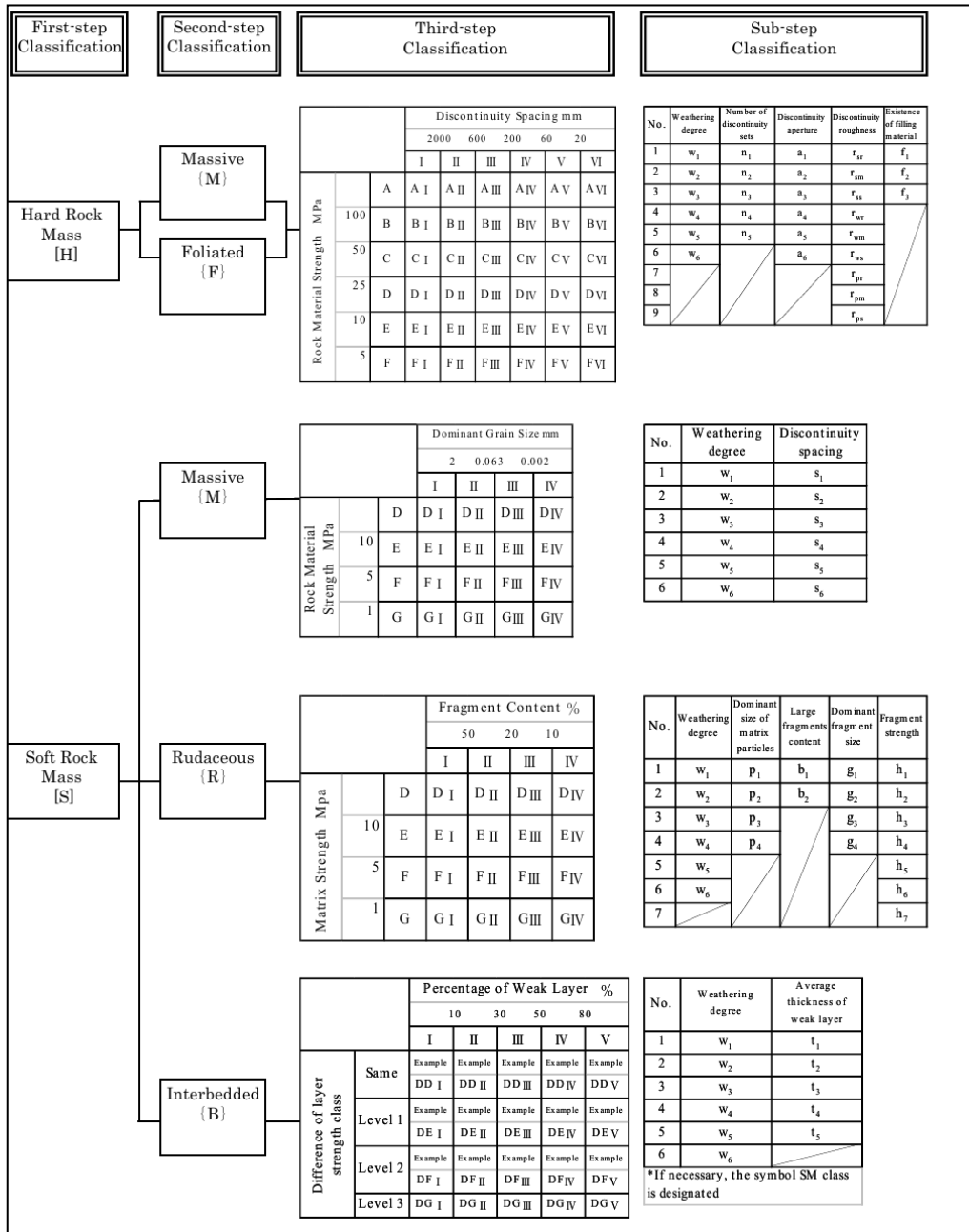


Figure 2-6 System for Engineering Classification of Rock Mass (Masahiko, 2005) after JGS

2004

Table 2-6 Classification and Classes of Hard Rock Mass (Masahiko, 2005) after JGS 2004

Classification Parameter	Class					
Rock Material strength (MPa)	A	B	C	D	E	F
	More than 100	100-50	50-25	25-Oct	05-Oct	less than 5
Discontinuity Spacing (mm)	I	II	III	IV	V	VI
	More than 2000	2000-600	600-200	200-60	0-20	Less than 20
Weathering degree	W1	W2	W3	W4	W5	W6
	Figure 2.6					
Number of discontinuity sets	n1	n2	n3	n4		n5
	1 set	2 sets	3 set	4 sets and above		Random
Discontinuity aperture (mm)	a1	a2	a3	a4	a5	a6
	Less than 0.1	0.1-0.25	0.25-0.50	0.50-2.5	2.5-10	More than 10
Discontinuity roughness	Figure 2.6					
Existence of filling Material	f1		f2		f3	
	None		Partially filled		Fully filled	

This classification system is currently being used in the geotechnical sector in Japan and has of yet not been applied to mining geotechnics or designs. It is important to note that the prior mentioned mining classification systems e.g. MRMR etc. are modifications of earlier derived civil engineering and tunneling classification systems which means there is a possibility for the development of the JGS classification system to into a mining focused system.

Table 2-7 Classification parameters and classes of Soft Rock Mass (Masahiko, 2005) after JGS 2004

Classification parameters	Class							
Rock material strength (MPa)	D		E		F		G	
	25-10		10-5		5-1		Less than 1	
Matrix strength (MPa)	D		E		F		G	
	25-10		10-5		5-1		Less than 1	
Difference of layer strength class	DD/EE/FF/GG		DE/EF/FG		DF/EG		DG	
	Same		Level 1		Level 2		Level 3	
Dominant grain size (mm)	I		II		III		IV	
	More than 2		2-0.063		0.063-0.002		Less than 0.002	
Fragment content (%)	I		II		III		IV	
	More than 50		50-20		20-10		Less than 10	
Percentage of weak layers (%)	I		II	III		IV	V	
	More than 10		10-30	30-50		50-80	Less than 10	
Weathering degree	W1	W2		W3		W4	W5	W6
	Figure 2.6							
Discontinuity spacing (mm)	S1	S2		S3		S4	S5	S6
	More than 2000	2000-600		600-200		200-60	0-20	Less than 20
Dominant size of matrix particles (mm)	P1	P2		P3		P4		
	More than 2	2-0.063		0.063-0.002		Less than 0.002		
Large fragment content (%)	b1		b2					
	More than or equal to 10		less than 10					
Dominant fragment size (mm)	g1	g2		g3		g4		
	More than 630	630-200		200-63		Less than 63		
Fragment strength (MPa)	h1	h2	h3		h4	h5	h6	h7
	More than 100	100-50	50-25		25-10	10-5	5-1	Less than 1
Average thickness of weak layers (mm)	f1		f2		f3		f4	f5
	More than 600		600-200		200-60		60-20	less than 20

2.2 ANISOTROPIC ROCK MASS GEOMECHANICAL TESTING

Foliation results in the arrangement of minerals in a rock material which may result in orientated planes of weakness. The in-situ rock material will be weaker when loaded in one direction, and stronger when loaded in another direction (Yasar, 2001). The differential loading direction on foliated samples results in the type of strength locus illustrated in Figure 2-7. The strength of the rock material strength will be dependent on the orientation of the foliation and the applied compressive stress exerted on the sample upon testing. If the principal applied stress is normal to the foliation orientation the failure of the sample would be caused by the foliation as it would be along that plane and not be of the in-situ rock material itself. If the compressive or tensile stress applied on a test sample is in the same orientation as that of the foliation in the sample will result in the reduction in strength caused by foliation such as schistosity and gneissic banding which is determined by the arrangement and amount of flaky and elongated minerals (Palmstrom, 1995).

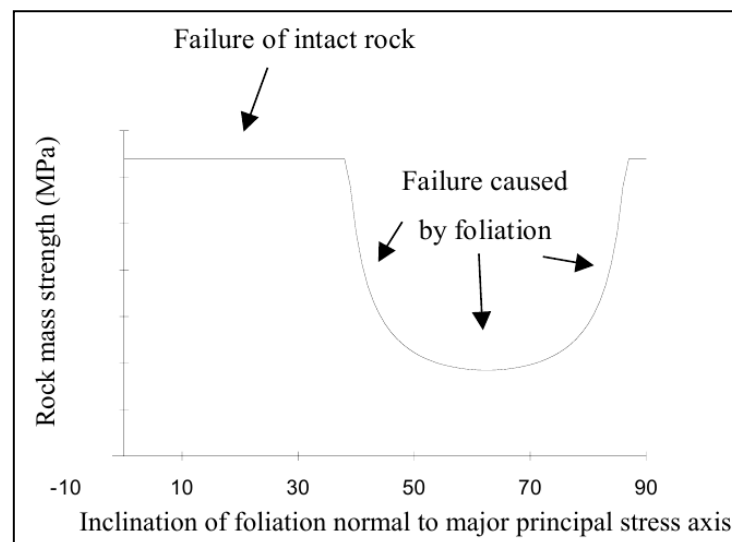


Figure 2-7 Influence of loading direction on strength results (Saroglou, 2003)

Strength anisotropy in foliated rocks materials, together with measurements of their intrinsic anisotropic foliation fabric shows that the lowest strength value results evident when the foliation anisotropy is in the same orientation as the applied stress.

Tsidzi (1990) derived the following expression to account for the anisotropic factor when considering the uniaxial compressive strength:

$$fA = 0.95 + 0.17 Fi$$

Where: Fi is the foliation index with the ratings indicated in Table 2-8.

Table 2-8 Classification of foliation and anisotropy of rock material (Tsidzi 1990)

Foliation Classification Anisotropy Classification	Description	Foliation Anisotropy Factor (fA)
Very weakly foliated (or non- foliated) $Fi < 1.5$ Isotropic	Platy and prismatic minerals <10%, which may occur as discontinuous streaks or may be randomly oriented. Rock fractures are curved or folded. Usually found in high-grade regional metamorphic regions or in contact metamorphic zones.	1-1.2
Weakly foliated (or non-foliated) $Fi = 1.5-3$ Fairly anisotropic	Platy and prismatic minerals 10-20%, Compositional layering is evident, but mechanically insignificant, usually found in high-grade regional metamorphic regions. Typical rocks: Quartzofeltspatic gneiss, mylonitic, migmatite	1.2-1.5
Moderately foliated (or non- foliated) $Fi = 3-6$ Moderately anisotropic	Platy and prismatic minerals 20-40%, Thin to thick folia occasionally discontinuous. Foliation is usually mechanically passive. Found in rocks formed by medium to high-grade regional metamorphism. Typical rocks: Schistose gneiss, quartzose schist.	1.5-2
Strongly foliated (or non-foliated) $Fi = 6-9$ Highly anisotropic	Platy and prismatic minerals 40-60%. Thin wavy continuous folia which may be mechanically significant. Usually formed under medium-grade regional metamorphic conditions. Typical rocks: Mica schist, hornblende schist	2-2.5
Very strongly foliated (or non- foliated) $Fi = 9$ very highly anisotropic	Platy and prismatic minerals > 60% occurring as very tin continuous folia. Foliation is perfect and mechanically significant. Found in rocks formed by dynamic or low-grade regional metamorphism. Typical rocks: Slate, small folded phyllite	>25

The foliation index can be determined from thin section analysis by measuring the mineral composition and the shape of the minerals. The following are noted from the equation:

- the strength anisotropy index fA is directly proportional to foliation orientation
- The minimum compressive strength of the foliated rock material can roughly be assessed as;

$$\sigma c \min = \sigma c \max / fA = \sigma c \max / (1 + 2.5 c/100)$$

According to Singh et al. (1989) the anisotropy ratio is defined as:

$$Rc = \sigma c 90 / \sigma c \min ,$$

Where: $\sigma c 90$ is the uniaxial compressive strength measured at right angle to the foliation plane. The associated reduction for strength (Rc) is shown in Table 2-9. This reduction factor is higher than the fA factor suggested by Tzidzi (1990). The difference in reduction factor may be as a result of different rock masses used in the tested samples. Further investigations are required to derive a more accurate expression of rock material anisotropy.

Table 2-9 Classification of Anisotropy (Singh et al. 1989)

Anisotropy ratio Rc	Classification	Rock type
1-1.1	Isotropic	
1.11-2.0	Low anisotropy	Shale
2.01-4.0	Medium anisotropy	
4.01-6.0	High anisotropy	Slate
>6.0	very High anisotropy	Phyllites

For a field strength estimate of anisotropic and weathered/altered rock masses the uniaxial compressive strength can be calculated from:

$$\sigma c = \sigma c 50 / (fA \times fW)$$

where: $\sigma c 50$ can be found for fresh rocks from published strength tables,

fA , is the foliation anisotropy (Table 2-8)

fW is the weathering/alteration factors.

In relation to the foliation planes, the grain differences within the planes of the foliated rock mass are in the same orientation as of the overall foliation planes which can also subsequently control the material strength of the rock material. (Saroglou, 2003)

2.3 GEOTECHNICAL DESIGN IN ANISOTROPIC/FOLIATED ROCK MASSES.

The aim of an open pit design is to provide an optimal excavation configuration in the context of safety, ore recovery and financial return (Stacey, 2008). The underestimation of the rock mass behaviour in relation to foliation anisotropy may result in compromising the safety of the pit and therefore the ore recovery which will affect the financial viability of the mine.

The application of the open pit design process requires the formulation of different the parameters and aspects that need to be investigated to achieve a holistic design. According to Stacey (2008) the following parameters and aspects in the investigation need to be undertaken to complete a geotechnical design:

- Geotechnical models which would consist of the:
 - -Geological model
 - -Structural model
 - -Rock mass model (material properties and classifications)

These above-mentioned procedures form part of the outcome from the analysed data that has been acquired during the site investigation.

- Slope design methods consisting of:
 - -Kinematic and Swedge analysis
 - -Limit equilibrium

The kinematic and Swedge analysis determines the likely failure mechanisms and probability of failure (PoF), whereas the 5limit equilibrium analysis determine the factor of safety (FoS). This is summarised in the internationally accepted design criteria (Table 2-10) derived from *The Guideline for Open Pit Slope Design* (Read and Stacey, 2009).

Table 2-10 Acceptance Criteria (Read and Stacey, 2009)

Slope Scale	Consequence of Failure	Acceptance Criteria		
		FoS (min) Static	FoS (min) Dynamic	% PoF (max) P (FoS < 1)
Bench	Low-High	1.1	N/A	25 - 50
Inter-ramp	Low	1.15 - 1.2	1.0	25
	Medium	1.2	1.0	20
	High	1.2 - 1.5	1.1	10
Overall	Low	1.2 - 1.3	1.0	15 - 20
	Medium	1.2	1.05	5 - 10
	High	1.3 - 1.5	1.1	≤ 5

In the case of a design methodology developed from the failure at the Trout Lake Mine in Hudson Bay where the foliation anisotropy was considered, the classification and laboratory results in relation to the foliation direction determined the failure strength criteria. The empirical design utilized the Mathews stability graph in conjunction with field observations. Boundary-element techniques, Displacement –discontinuity techniques and finite -element models were used to design the slope and investigated the 2D and 3D interactions (Eberhardt, 1997).

The design of the Jwaneng Mine’s south-eastern wall that is characterized by foliation planes which dip and daylight into the mining face consisted of the following steps being undertaken for the geotechnical design process (Contreras, 2009):

- Determining geotechnical domains for design utilizing structural and geological data to divide the Project area into design sectors. The different geotechnical domains have different slope designs;
- Determine the geotechnical rock mass parameters consisting of MRMR and the Joint strength properties using Barton-Bandis strength curve.
- Analysis of the Hydrogeological Regime;
- Conducting a stability analysis including limit Equilibrium analyses via RocScience® software SLIDE and Numerical modelling using Itasca modelling code

Udec. The Udec modeling assumed explicit joints are foliation and sub vertical joints are open.

The application of these design steps resulted in the optimization of the slope as the risks in each geotechnical domain were analysed and were well understood.

2.4 LITERATURE REVIEW FINDINGS.

- The three parameters that are important in foliation/ studies are:
 - -Orientation;
 - -Intensity' and
 - -Type.
- The foliation type is a function of mineral composition and degree of small- scale heterogeneity. The foliation intensity is in turn a function of the type and intensity of the deformation by which it was formed.
- The geotechnical logging parameters gathered on site are dependent to the classification system to be applied and the purpose of the design requirements.
- The MRMR system considers the same rock mass parameters as RMR but also incorporates ground water and joint condition parameters.
- The main function of the MRMR system is to classify rock masses into zones based on similar behaviour; provide a basis of understanding between different mining professionals/divisions? and to formulate design parameters for the actual mine design.
- The most commonly use rock mass rating system in mining, the MRMR, does not account for foliation/anisotropy, it only accounts for open joints.
- Foliation structures are not accounted for in the effect that they have on RQD and the IRS
- The IRMR classification system addresses the importance of discontinuities in rock mass classification in relation to strength adjustments to rock block and rock mass.
- Barton Bandis failure criterion is an empirical relationship utilised to model the shear strength of rock discontinuities (e.g. joints or foliation).

- The Geological Strength Index (GSI) was introduced by Hoek et al (1994) as an alternative method to classify rock mass quality due to difficulties in applying the Bieniawski's Rock Mass Rating (RMR) to very poor rock masses. The GSI is an important tool to estimate parameters such as cohesion, friction angle and deformation modulus of rock masses.
- GSI values for anisotropic rock masses where the alignment of weak minerals originated from alteration or dynamic metamorphism will result in a decrease in the GSI rating which would account for the inherent weakness within the foliation planes.
- The reduction in strength from anisotropy caused by foliation and schistosity is determined by the arrangement and amount of flaky and elongated minerals.
- Strength anisotropy in foliated rocks masses, together with measurements of their intrinsic anisotropic foliation fabric, show that the lowest strength values are due to? the orientation of the foliation.
- Design applications in foliated anisotropic rock masses need the classification and laboratory results to be analysed in relation to the foliation direction to determine the failure strength criteria so as to produce a more conservative design
- An empirical design in conjunction with field observation is needed with Boundary-element techniques, Displacement – discontinuity techniques and finite -element models to design mine slopes and investigate the 2D and 3D interactions of the discontinuities.

CHAPTER 3 METHODOLOGY

The geotechnical database from an open pit mining operation in Mozambique is utilized. The data was assimilated from the geotechnical borehole logs which were analysed and interpreted together with laboratory testing data. The data analysis and interpretation focused on:

- The geotechnical logging and classification of the rock masses.
- Laboratory test analysis
- Kinematic analysis.
- Swedge analysis.
- Limit equilibrium slope stability modelling.

3.1 GEOTECHNICAL DRILLING

Orientated core drilling was conducted in accordance with the following specifications:

- All boreholes were orientated using the ACTII orientation tool;
- Boreholes were rotary cored, using triple-tube core barrels to ensure maximum core recovery;
- The borehole core diameter was either HQ3 (61.1mm) or NQ3 (45.1mm) in fresh rock material and PQ (85.1mm) in the softer overburden material; and
- Boreholes were inclined at -60° to the horizontal.

Orientation of the core facilitated the measurement of alpha (α) and beta (β) angles of discontinuities, used to determine their true dip and dip direction.

3.2 GEOTECHNICAL LOGGING

All the different lithological units that will be exposed within the open pit excavation were logged as separate geotechnical zones.

The following parameters were logged for each zone:

- The extent and distribution of geotechnical zones;
- The Rock Quality Designation (RQD);
- The descriptions of matrix or rock material structures, i.e. faults, shear zones, intense fracturing and zones of deformable material;
- The Intact Rock Strength (IRS) / hardness estimate;
- The degree and nature of rock weathering;
- The relative orientation of rock structures (dip and dip direction of bedding, foliation joints, etc);
- The total number of structures, described as fracture frequency per metre; and
- The condition of structures, i.e. roughness profile, wall alteration and infilling.

The geotechnical logs are presented in Appendix A.

3.3 LABORATORY TESTING

Laboratory tests were conducted on representative lithological samples to obtain an indication of the in-situ rock strength. The laboratory testing programme consisted of the following geomechanical tests:

- Uniaxial Compressive Strength with Young's Modulus and Poisson's Ratio (UCM);
- Uniaxial Compressive Strength (UCS);
- Triaxial Compressive Strength (TCS);
- Uniaxial Indirect Tensile Strength (Brazilian Method) (UTB); and
- Base Friction Angle (direct shear test on saw-cut rock surface) (BFA).

Tests were conducted on the lithologies dominant in the hanging wall (anorthosite), footwall (gabbro) and orebody. All testing was conducted by Rocklab (Pty) Ltd., South Africa.

3.4 CLASSIFICATION SYSTEMS

Laubscher's (1990) Mining Rock Mass Rating Classification System evaluates discrete geotechnical domains based on Intact Rock Strength, (IRS), fracture frequency, joint condition and weathering characteristics. Each of the resultant domains is evaluated separately, through the allocation of rating values, within a specific range, for each parameter.

Bieniawski's (1989) Rock Mass Rating Classification was also calculated which includes the following parameters:

- Weathering;
- Uniaxial compressive strength of in situ rock;
- RQD;
- Joint spacing;
- Joint orientation;
- Joint separation;
- Joint roughness;
- Joint continuity; and
- Groundwater.

Jakubec's (2000) In situ Rock Mass rating was calculated by applying Dyke (2008) comparison of MRMR and IRMR general regression equation:

Where:

$$\mathbf{IRMR} = 1.0376\mathbf{MRMR} - 1.3655 [\pm 0.24]$$

3.5 ROCK MASS STRENGTH ESTIMATION

The assessment of rock mass strength parameters was based on the boreholes analysed in the study area. Hoek-Brown strength parameters (UCS, GSI, mi and D) were assessed to

represent the rock mass strength and equivalent Mohr-Coulomb parameters (c and ϕ) based on the Hoek-Brown criterion.

3.5.1 In situ rock strength

Uniaxial compressive strength test results were analysed and statistically grouped to be utilized in the slope stability analyses. The in-situ rock strength values were based on the laboratory testing database. Mean values for tests that failed on internal discontinuities were used. No test results for GANW were available, and use was made of the field estimates calibrated with known test results to estimate this unit's strength.

3.5.2 Estimation of m_i

The estimation of m_i values was based on fitting Hoek-Brown (HB) failure envelopes with the results of UCS, triaxial and Brazilian tensile strength tests for each geotechnical unit. The HB envelope is linear in this plot and a linear regression analysis provides the required values of UCS and m_i . UCS is calculated as the square root of the intercept, and m_i as the slope divided by the calculated UCS. Hoek indicates that this method is robust, reliable and has the advantage that it gives a good visual impression of the distribution and scatter of the data.

The method described was implemented in an Excel spreadsheet, where the linear relationship was plotted for each rock type according to failure mode of the samples.

3.5.3 Estimation of GSI

The estimation of the Geological Strength Index (GSI) was based on RQD and the Joint Condition (JCond89) rating defined by Bieniawski (1989) in the formulas shown below:

$$GSI_{\text{Bieniawski89}} = 1.5J\text{Cond}_{89} + RQD/2$$

$$GSI = RMR - 5$$

3.5.4 Disturbance factor (D) estimation

The Disturbance factor (D) is a representation of the degree of disturbance within a rock mass because of stress release and blasting. The D factor ranges from 0 for undisturbed in-situ rock masses to 1 for highly disturbed rock masses. A D factor of 0.7 was used for the analysis, this implies good controlled wall blasting with limited damage to the rock mass. A worst-case scenario of the entire slope having a D=0.7 was analysed to lower the effect of the high UCS values of the rocks tested.

3.5.5 Mohr-Coulomb strength parameters for rock mass

RocScience software RocData was used to calculate the equivalent Mohr-Coulomb strength parameters based on the Hoek-Brown approach, where deep (>50 m) and shallow (<50 m) rock mass conditions, were represented by a maximum normal stress (δ_{nmax}) of 1.0 MPa, whereas 0.2 MPa was considered for shallow rock mass conditions

3.5.6 Joint and foliation strength parameters

Joint strength parameters were determined using the Barton Bandis approach which is based on estimates of the joint roughness coefficient (JRC) joint compressive strength (JCS) and the base friction angle. These descriptors were used to determine equivalent Mohr-Coulomb strength parameters for input into the analyses. The summary of the calculations for these below mentioned parameters are in Appendix E.

3.5.7 Joint Rough Coefficient (JRC) values

Representative values of the joint roughness coefficient (JRC) were estimated from borehole log data. The small scale joint expression data from the logs was used to estimate the appropriate JRC values at log scale for each rock type. A scale dimension consistent with the bench height (20 m) was assumed for the estimation of the JRC values representative of field conditions.

3.5.8 Joint Compressive Strength (JCS)

The joint compressive strength (JCS) values representative of field conditions were estimated by applying the scale factor correction to the average values of UCS defined with the laboratory testing programme for each rock unit.

3.5.9 Mohr-Coulomb strength parameters for joints and foliation

Two sets of Mohr-Coulomb strength parameters for joints were estimated corresponding to deep (>50 m) and shallow (<50 m) rock mass conditions, Joint strengths within the deep rock mass conditions region were represented by a maximum normal stress (δ_{nmax}) of 1.0 MPa, whereas 0.2 MPa was considered for shallow rock mass conditions. These parameters were used to consider the effect of strength anisotropy due to foliation and the dominant structural orientation of the geology

3.6 GEOTECHNICAL SECTIONS AND DOMAINS

The following aspects were considered in defining the geotechnical domains with in the research area.

- The orientation data was divided on either side of the limbs of the local fold structure persisting in the project area; and
- Weathering depth

Based on the geometry of the fold limbs, two geotechnical domains (Northern study area and Southern study area) were analysed which are further subdivided along the representative section lines according to the depth of weathering and orientation of the pit wall. A database of 1431 and 475 joint data entries for the Northern study area and the Southern study area respectively were used, which comprised the global drilling dataset used in the kinematic analysis. The geotechnical domains analysed are shown in Figure 3-1.

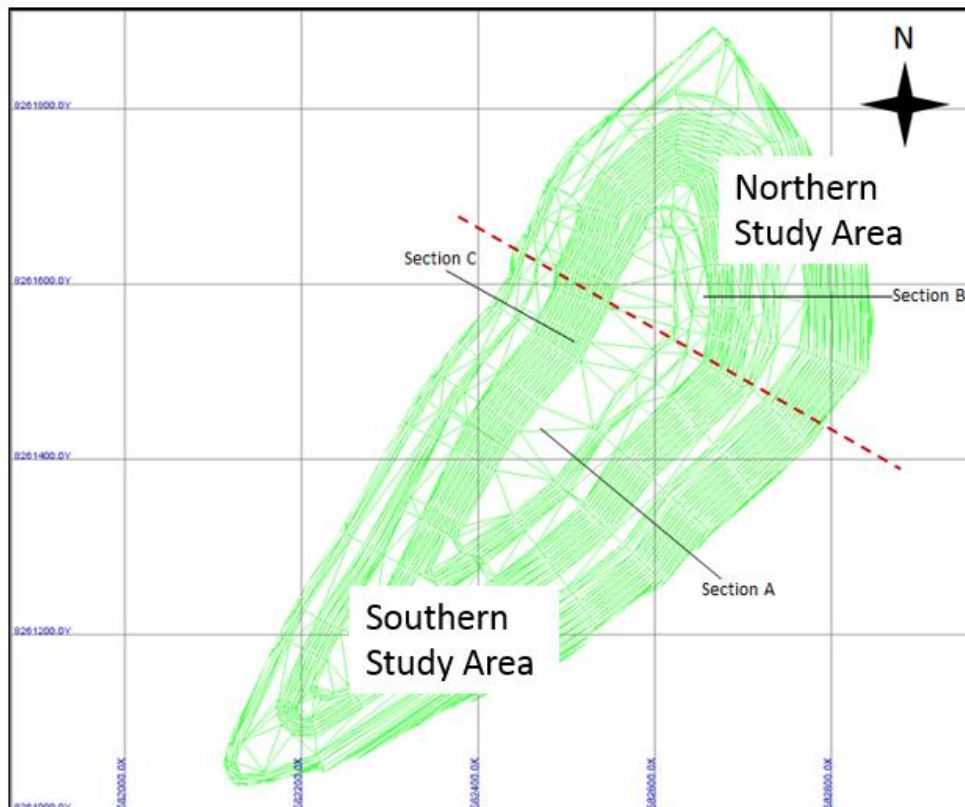


Figure 3-1 Geotechnical domains (Red line showing division of North from South Study Area.)

3.7 SLOPE STABILITY ANALYSIS

This analysis consisted of a kinematic study to determine the likely failure mechanisms, and a limit equilibrium analysis to determine the FoS and PoF of the individual design sections within each geotechnical domain. The results of these analyses were compared to internationally accepted design criteria derived from the Guideline for Open Pit Slope Design (Read and Stacey, 2009).

3.7.1 Acceptance Criteria

The acceptance criteria applied to the design analysis are summarised in Table 2-10 in Chapter 2 with the internationally acceptable PoF criteria described for the different slope scales.

3.7.2 Structural Data Analysis

A defect database was compiled utilising the logging data provided by the geotechnical drilling programme in the project area, with the natural discontinuities encountered (Joints, foliation and the dyke intrusions trend) in the orientated drill holes logged manually.

RocScience software DIPS was used to determine the major joint sets present in the proposed mining area. The grouping of the sets was based on the geological and structural trends of the discontinuities. The change in dip direction and dip in relation to the fold structure in the project area was taken into consideration.

3.7.3 Kinematic Analysis

Joint and foliation orientation data, assimilated from the recovered, orientated core will form the basis for the kinematic analysis. The aim of the kinematic analysis will be to identify potential modes of failure, specifically toppling, planar sliding and wedge sliding failures.

Representative slope orientations in the two geotechnical domains were kinematically analysed for the following failure modes:

- Toppling;
- Planar sliding; and
- Wedge sliding.

The kinematic analysis was carried out using RocScience software, DIPS, to determine stack and bench scale probability of occurrence for a certain mode failure. The analysis was carried out by varying stack angles and slope orientations, as well as varying bench face angles in a range of slope directions relevant to the northern section and southern sections in the study area. The following slope directions for each domain were analysed:

- Northern Study Area (East and West): 125°, 180°, 205° and 270°; and
- Southern Study Area (East and West): 045°, 125° and 310°.

The logged joints were analysed for planar, wedge and toppling failure. A friction angle of 35°, which is the mean calculated base friction angle obtained from the geomechanical testing results, was utilised for the analyses on a range of bench face angles of 70°, 80° and 90°, and stack angles of 40°, 50° and 60°. A lateral limit of 20° was placed for the planar failure analyses.

3.7.4 SWEDGE Analysis

Based on a study conducted by Gibson *et al.* (2006) which considers the optimisation of bench face angles and berm width geometries, two examples are given for the calculation of the radius of unstable material on a spill berm:

- **Pyramidal:** the wedge shape is considered and assumes that the unstable material is in the form of a pyramid, i.e. the symmetry of the wedge is reflected in the symmetry of the fallen wedge. The section of the pyramid in the plane of the spill berm is the radius (R); and
- **Conical:** the volume of unstable material is distributed in a symmetrical conical fashion, where the section of the cone in the plane of the spill berm is the radius (R).

The conical option was chosen as being the most applicable to this study in that it is believed that any unstable material will not strictly retain the shape of the wedge, but rather break into smaller rock fragments which will comprise the unstable spill material.

The calculus utilised for defining the radius of the conical expression of the volume of unstable material is:

$$R = \sqrt[3]{\frac{6KV}{\pi} \times \frac{\tan \alpha - \tan \phi}{\tan \phi \cdot \tan \alpha}}$$

Where:

K – 1.3 swelling factor

V – volume of material (m³)

α – the bench face angle ($^{\circ}$)

Φ – 38° the angle of repose

Having established a means of calculating the radius of the unstable material for a wedge sliding instabilities

The output of the probabilistic analysis included:

- The total number of iterations computed;
- The total number of wedge sliding instabilities that are possible based on the dip and dip direction of the slope and the variations in the dip and dip direction of the intersecting joints;
- The total number of wedges with an FoS <1.0 ;
- The mean FoS;
- The individual weight of each wedge evaluated; and
- The individual volume of each wedge evaluated (V).

The radius (R') of the conical expression of the volume of unstable material was calculated for each viable wedge iteration. From this point in the analysis, the following information was then calculated per wedge:

- The volume of the spill material anticipated if the radius exceeded the given bench width by 20% (V'');
- The remaining volume of the spill material on the bench which represents the 80% retention factor (V');
- The recalculated radius (R'') based on the remaining 80% volume (V'').

The following assumptions were applied in continuing with the analysis:

- Regardless of the FoS, all wedge iterations were utilised. Thus, even if the wedge has a FoS >1.1
- The friction and cohesion values remained static; and
- The bench height and the upper bench width remain static at 10m and 20m respectively, therefore defining the wedge size per bench. This study did not include multi-bench or stack geometry options.

Two scenarios (Northern Study Area and Southern Study Area) which consisted of bench scale and stack scale wedge failure in which kinematic wedge failure occurred were further analysed using RocScience software SWEDGE.

3.8 LIMIT EQUILIBRIUM ANALYSIS

3.8.1 Limit Equilibrium Input Parameters

The input parameters, derived from the geotechnical investigation programme and used for the design analyses are summarised in Table 3-1.

Table 3-1 Limit Equilibrium Input parameters

Geo. Unit	Unit Weight	UCS (Mpa)	GSI	mi	D	E (Gpa)	ν
GANW	26.8	105	22	20	0.7	-	-
GAN	29.1	105	59	11	0.7	78	0.26
GAB	28.7	156	62	8	0.7	85	0.27
GABMW and GABW	25.2	50	20	20	0.7	-	-
OFX	45.1	144	55	12	0.7	144	0.35
OFXMW and OFXW	43.5	47	23	25	0.7	-	-
GDO	29.7	176	30	11	0.7	105	0.27

3.8.2 Deterministic and Probabilistic Analysis

The FoS values were calculated using Hoek Brown parameters. The FoS calculations were generated with Bishop's, Simplified, General (GLE)/Morgenstern-Price and Janbu Corrected techniques.

The acceptance criteria (Read and Stacey, 2009) for the FoS values were utilised to identify areas of concern based on the calculated FoS.

The limit equilibrium analysis was carried out using SLIDE 6.0 software from RocScience. Three representative section lines were chosen for the limit equilibrium analysis (Figure 3-1). The sections were updated with their relative geological and structural intersections. The global mean values of the geomechanical properties, derived from the geotechnical drilling and laboratory testing programme for each geotechnical unit intersected were added into the model. Groundwater conditions for the analysis consisted of representative pore water pressure grids for each section line. The following two scenarios were analysed:

- Isotropic models, using Hoek-Brown which assumes homogeneous rock masses throughout the slope; and
- Anisotropic Linear models, using Anisotropic strength function which assumes heterogeneous rock masses and allows for a defined discrete angular range of slice base inclinations at varying cohesion and friction angles for each rock mass. The anisotropic model addresses the bias of the structure within the units (orientation bias of the banding and open joints of the gabbro host rock) which are in the same dip direction as the dip direction of the exposed ore deposit (North West) as well as the overall slope direction in the Northern study area (Section A) and Section B of the Southern study area. The Anisotropic Linear model is based on the Mohr-Coulomb criterion and assumes that the minimum shear strength occurs in the direction of the bedding planes and is given by cohesion and friction. (Rocscience 2013).

CHAPTER 4 CASE STUDY

A case study illustrating the shortcomings and solutions to rock mass classification in foliated/anisotropic rock masses is presented.

The project area is in the Northern Province of Tete, in Mozambique. The project area is characterised by a gently undulating topography with a prominent hill in the area forming part of the ore deposit.

4.1 REGIONAL GEOLOGY

The regional geology comprises mostly of gabbro, with subordinate anorthosite and magnetite, and relatively minor occurrences of pyroxenite/websterite and troctolite. This Tete (Gabbro-Anorthosite) Suite was formerly known as the Tete Gabbro-Anorthosite Complex (Westerhof et al,2008). Rock fabric are generally massive and medium to very coarse-grained or even pegmatitic. Widespread replacement of the original minerals and the imposition of planar fabric occur in various places throughout the Suite. but are most common along the contact with the crystalline basement (Evans et al, 1999; Maier et al, 2001). The crystalline basement of Tete Province can be attributed to three major Pan-African lithospheric plates, called East, West and South Gondwana (Figure 4-1). The Tete Suite was emplaced into the Tete-Chipata Belt (TCB), a newly defined multi-terrane structural domain that forms part of West Gondwana since its collision and amalgamation during the Grenvillian orogenic cycle at ~1.06 Ga (Westerhof et al,2008).

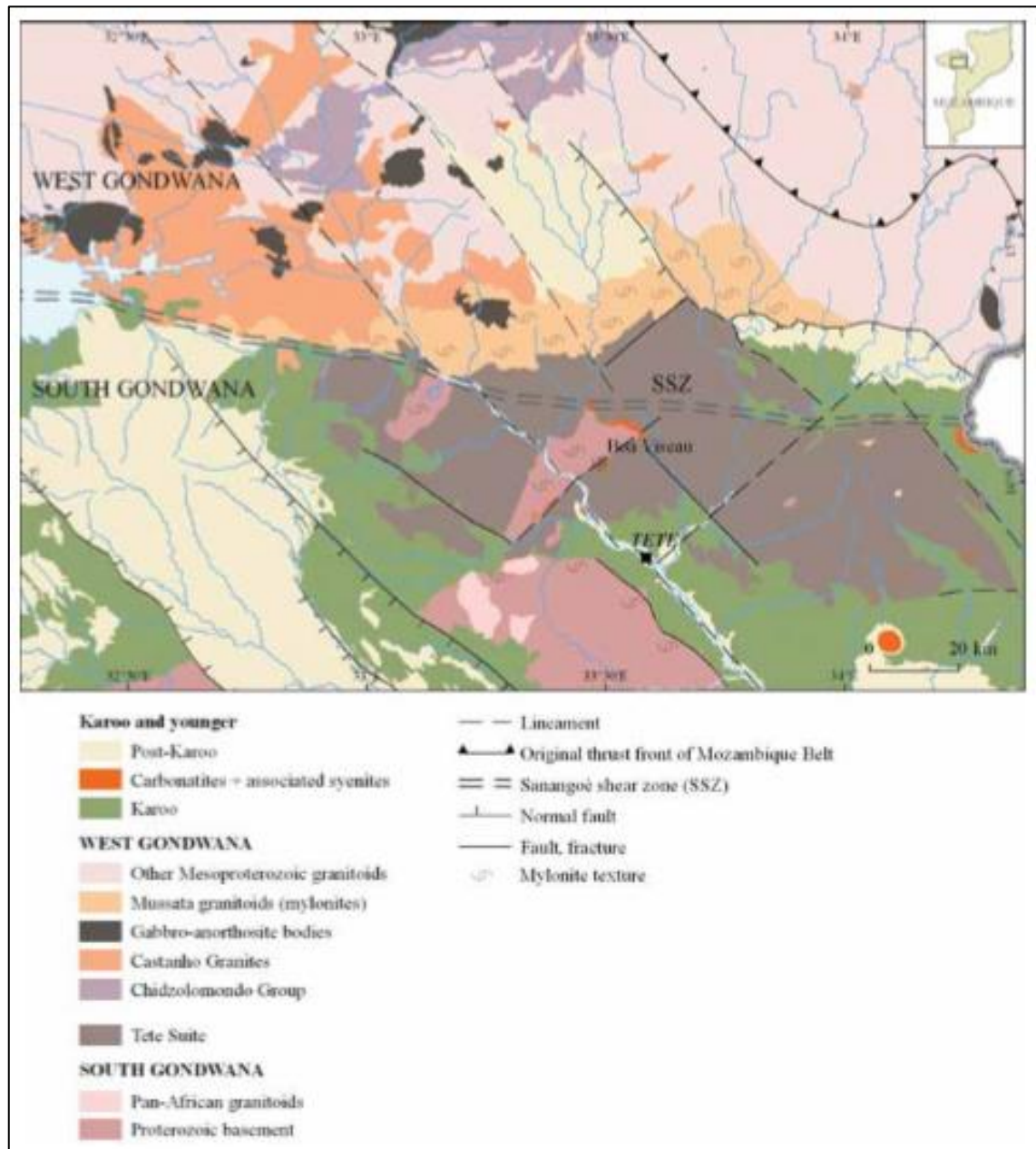


Figure 4-1 Simplified geological map of the Tete Suite and surroundings (Westerhof et al, 2008)

4.2 LOCAL GEOLOGY

The bedrock in the project area is predominantly gabbro, leucogabbro and norite, with subordinate anorthosite of the Luia Terrane and minor but widespread ultramafic rock types, mostly pyroxenite, and rocks that are mainly composed of iron-titanium oxides. The lithological units form a gentle syncline plunging to the west. The main ore deposit which is concentrated on the hill area is located on the fold axis (SRK, 2013).

Anorthosite occurs as pod shaped lensoid outcrops trending in the same direction as the gabbro, i.e. NNW-SSE and can be generally regarded as the host rock of the magnetite. The most distinguishing characteristic of the highly feldspathic anorthosite is its coarse-grained texture.

The anorthosite occurs in low lying areas as it is less resistant to weathering due to the presence of feldspars within its composition. The main rock outcrop occurs on the western side of the main ore deposit hill area. Some outcrops are found on the northern side of the Study area hill. Drilling results indicate that the anorthosite has a shallow dip to the SW on the northern limb and to the NW on the southern limb.

Anorthosite also exists as xenoliths in the gabbro terrain. This shows that the anorthosite is slightly older than the gabbro although both rocks are of Precambrian age.

Magnetite mainly outcrops near the summit of the hill and on the western side of the hill where it forms the topographically high profile. On the northern limb, the magnetite is trending NW-SE and generally dipping at approximately 42° towards South West. However, some magnetite outcrops show a NNW-SSE strike (SRK, 2013). The southern limb magnetite suffered strong metamorphic deformation especially at the contact with the foliated gabbro. Probably the tectonic intrusion of the gabbro was of a more violent nature resulting in a steep pressure and temperature gradient.

At the contact with the gabbro, magnetite has been transformed into magnetite gneiss with alternating lensoid mafic and felsic components, due to the compositional layering produced by metamorphic deformation. The thick magnetite eluvium deposits surround the magnetite outcrops (SRK, 2014).

Gabbro is mostly outcropping on the southern, eastern and north eastern parts of the hill. Gabbro also occurs as lensoid pod shaped topographically low profiles with outcrops trending N-S although NNE-SSW strike is common. Their low exposure is since they are easily weathered. Their general strike is about 340° dipping moderately at approximately 50° to the west.

4.3 STRUCTURAL GEOLOGY

The Project area Complex is cut by numerous fine to medium grained intrusive igneous rocks of basaltic origin, composed essentially of pyroxene, plagioclase and Fe-Ti oxides and commonly showing ophitic texture

Most of the dykes are very elongate continuous to sub-continuous bodies trending NE-SW to NNE-SSW. The dykes form swarms parallel or, in many cases oblique or at right angles (perpendicular) to the magmatic banding. Where they are intensely foliated and recrystallized, dykes are difficult to distinguish from the Gabbroic country rocks (SRK, 2013). The local dolerite dykes are in a series that is sub-vertical, striking northeast-southwest.

In the mineralised zone the dykes occupy about 10-15% of the total area whereas at other localities, 20% of the volume of the rocks is composed of dykes. Because these dykes do not extend beyond the layered intrusions, they are co-magmatic and genetically related to the Complex (Westerhof et al,2008).

During intrusion the dolerite dykes followed zones of weakness in the host rock such as fractures and zones of continental divergence. The magma emplacement is either by dilation or forceful emplacement. This conclusion is because some dyke host rock contact zones are well deformed while others show no evidence of deformation. Several faults have been interpreted from aeromagnetic imaging and can be seen to offset the Mineralisation (Figure 4-2).

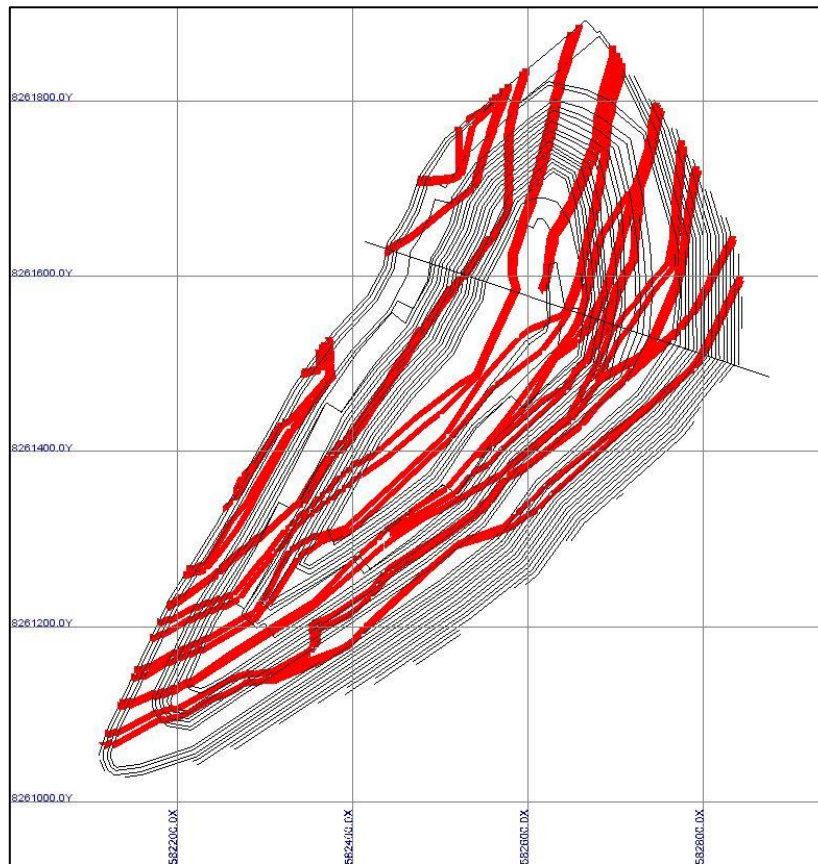


Figure 4-2 Interpretation of the dykes through the project area (SRK 2015)

4.4 GROUNDWATER MODEL

The depth to groundwater in the Project area ranges between 2.6 and 85 mbgl. The shallow water levels (2 – 16 mbgl) were measured at the foot of the hill closer to the main river which is adjacent to the project area, whereas the deeper water levels (60 – 85 mbgl) were measured on top of the study area hill.

The conceptual hydrogeological model of the project area indicates a shallow and a deeper aquifer system as shown in Figure 4-3.

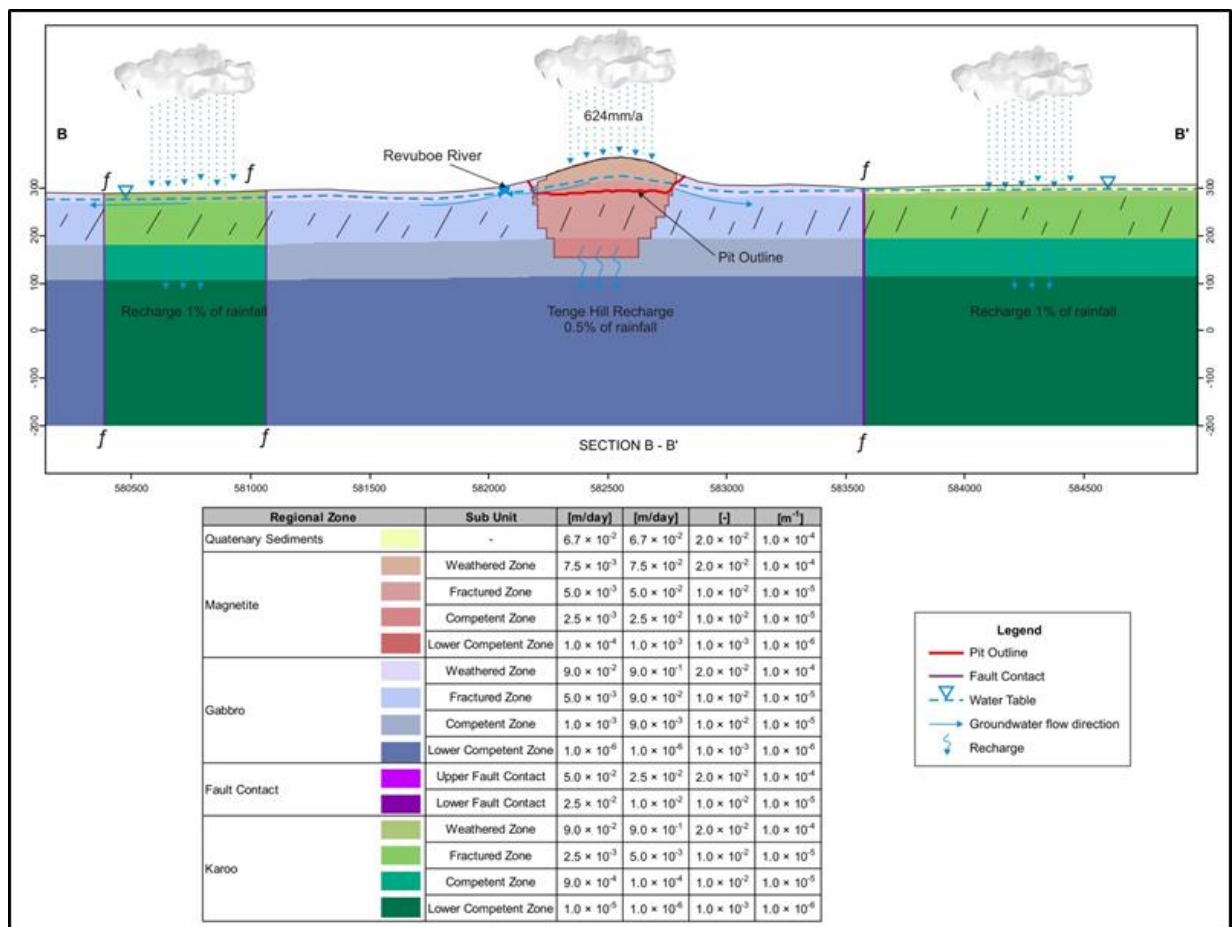


Figure 4-3 Conceptual hydrogeological model of the project area (SRK 2014)

The shallow groundwater aquifer is associated with the talus and conglomerate deposits and is actively recharged (SRK 2014). A fractured rock aquifer system occurs in the fractures, faults, joints and other lithological fabric such as the foliation of the Anorthosite and the anisotropy of the Gabbro. Most of the fractures are filled with secondary minerals reducing the permeability and connectivity of the fractured zone. The contact between the intruded dolerite dykes and the host rocks is tight showing very little or no evidence of deformation of the host rock. Therefore, dolerite dyke contacts are not considered as preferential flow pathways.

CHAPTER 5 RESULTS

5.1 GEOTECHNICAL INVESTIGATION RESULTS

Five Study area boreholes were logged during the drilling from the metallurgical test programme in 2012 and five orientated boreholes shown in Figure 5-1 were drilled in 2014. All these boreholes were utilized for the study.

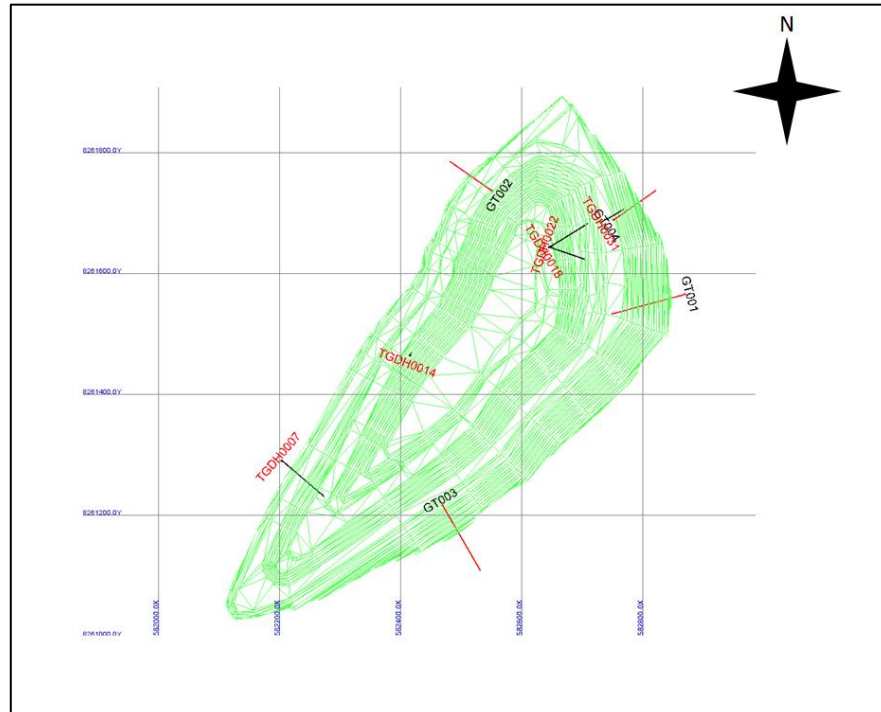


Figure 5-1 Plan of geotechnical boreholes where black labels indicate the research holes in the project area.

The logged data was sub-divided according to the lithological units (rock types) which were further sub-divided according to their grade of weathering. Units logged as completely, highly and moderately weathered were included in the weathered zones. The geotechnical units are summarised in Table 5-1.

Table 5-1 Geotechnical units used in the research study

Code	Geotechnical units
GANW	Anorthosite (weathered)
GAN	Anorthosite (unweathered)
GABMW and GABW	Gabbro (Moderately weathered and weathered)
GAB	Gabbro (unweathered)
OFXMW and OFXW	Iron Ore (Moderately weathered and weathered)
OFX	Iron Ore (unweathered)
GDO	Dolerite

Most of the test specimens failed along discontinuities, such as foliation and cemented joints. Standard practice would exclude these results from the analysis. However, the hill within the proposed mining/project area has a rock mass that is expected to fail preferentially along these predefined planes of weakness. Therefore, these results are representative of the expected failure mechanics in this rock mass and were included in the analysis. The failures along these discontinuities still result in high UCS values that can sustain the stresses placed on the rock mass.

The laboratory test results are discussed below and attached in Appendix B.

5.2 LABORATORY TESTING RESULTS

5.2.1 Density and strength properties of in situ rock

The rock strength analyses were conducted by fitting a Hoek-Brown failure envelope to the data for each lithological unit. In this method the Hoek-Brown failure envelope reduces to

a straight line where the intercept represents the in-situ rock strength squared (σ_{ci}^2) (Hoek, 2012).

The individual Hoek-Brown failure envelope for each lithological unit tested are presented in Appendix C. The results of the laboratory density tests are summarised in Table 5-2.

Table 5-2 Densities of in situ rock masses

Geotechnical Unit	Density (g/m ³)
GANW	2.68
GAN	2.91
GAB	2.87
GABMW and GABW	2.52
OFX	4.51
OFXMW and OFXW	4.35
GDO	2.97

The Hoek-Brown rock strengths and the statistical analysis of the laboratory UCS results is presented in Table 5-3 and the test results of the base friction angle are shown in

Table 5-4.

Table 5-3 Rock Strength Summary

		Geo Unit	GAB	GABMW and GABW	GAN	GDO	GDO MW	OFX	OFXW and OFXW
Hoek-Brown UCS (MPa)	In situ strength	Mean	242	-	-	-	-	229	-
	Failure on Discontinuities/Discontinuities	Mean	156	50	105	176	161	144	47
Laboratory UCS (MPa)	In situ strength	Min	242	-	-	-	-	229	-
		Mean	246	-	-	-	-	229	-
		Max	250	-	-	-	-	229	-

		Std dev	4	-	-	-	-	0	-
Failure on Discontinuities/Discontinuities		Min	9	10	39	59	60	76	38
		Mean	132	52	63	137	114	126	55
		Max	298	134	86	242	231	167	76
		Std dev	86	46	16	58	68	31	16
Number of samples			15	10	12	17	9	14	6

Table 5-4 Base friction angle results

Borehole no.	Depth (m)	Rock Type	Base Friction Angle
GT002	156.77-157.22	OFX	34°
GT004	37.71-38.08	OFX(W)	35°
GT004	133.60-134.14	GAN	35°

A summary of the elastic material properties is shown in Table 5-5 below.

Table 5-5 Summary of Elastic properties

Young's Elastic Modulus (GPa)						
Geo Unit	Min	Mean - Std Dev	Mean	Mean + Std Dev	Max	Std Dev
GANW	-	-	-	-	-	-
GAN	72	72	78	84	84	6
GAB	72	73	85	96	100	11
GABMW and GABW	-	-	-	-	-	-
OFX	133	136	144	152	150	8
OFXMW and OFXW	-	-	-	-	-	-
GDO	95	97	105	112	111	7
Poisson's Ratio						
Geo Unit	Min	Mean - Std Dev	Mean	Mean + Std Dev	Max	Std Dev
GANW	-	-	-	-	-	-
GAN	0.25	0.25	0.26	0.26	0.26	0.01
GAB	0.24	0.24	0.27	0.29	0.30	0.02
GABMW and GABW	-	-	-	-	-	-
OFX	0.29	0.31	0.35	0.40	0.40	0.05
OFXMW and OFXW	-	-	-	-	-	-
GDO	0.25	0.25	0.27	0.28	0.28	0.01

5.3 ROCK MASS CLASSIFICATION RESULTS

A summary of the RMR and MRMR values calculated is illustrated in Figure 5-2 and summarised in

Table 5-6.

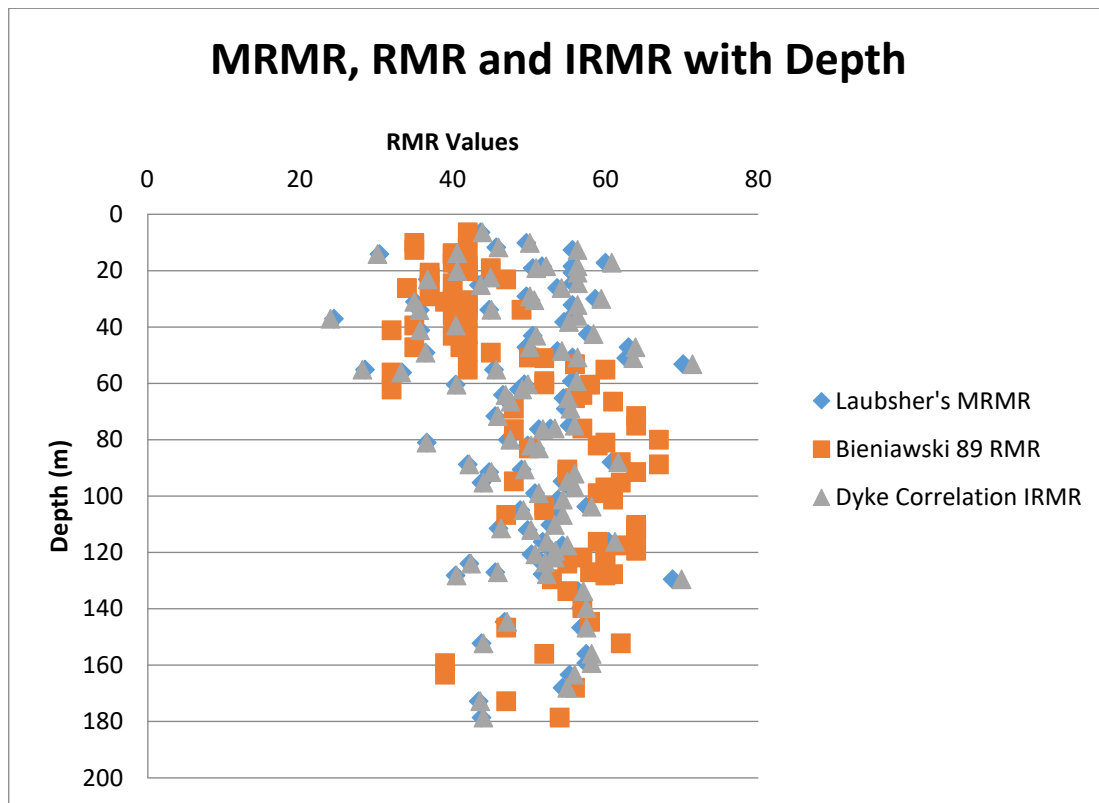


Figure 5-2 Correlation of RMR, MRMR and IRMR with depth

The plotted results of the comparison of the calculated RMR, MRMR and IRMR values shows a “good” of the results indicating a classification of the rock mass as “Fair” to “Good” for all three classification systems.

Table 5-6 Laubscher's (1990) MRMR and Bieniawski (1989) RMR Results

Geotechnical Unit	MRMR (Laubscher 1990)				RMR (Bieniawski 1989)				IRMR (Dyke 2008 Correlation)			
	Min	Mean	Max	Std Dev	Min	Mean	Max	Std Dev	Min	Mean	Max	Std Dev
GANW	24	38	49	7	32	37	49	6	24	38	49	7
GAN	37	48	57	6	48	56	60	5	37	48	58	5
GAB	40	50	69	10	53	57	60	3	40	50	70	9
OFX	42	52	70	6	39	57	67	7	42	53	71	5
OFXM W and OFXW	29	48	60	8	48	56	60	5	29	48	61	7
GDO	55	58	63	3	40	43	48	3	56	59	64	2

A summary of the GSI values for each lithological unit are shown in Table 5-7 below.

Table 5-7: GSI Estimate

Geotechnical Unit	GSI			
	Min	Mean	Max	Std Dev
GANW	11	22	56	13
GAN	41	59	70	10
GAB	53	62	69	6
OFX	13	55	76	15
OFXMW and OFXW	9	23	50	9
GDO	11	19	35	10

A summary of the Mohr-Coulomb strength results from RocData are shown in **Table 5-8** and the RocData outputs are presented in Appendix C.

Table 5-8 Summary of input parameters and results from RocData

Geo. Unit	Unit Weight	UCS (Mpa)	GSI	m_i	D	E (Gpa)	ν	Deep RM (σ_n max=1MPa)		Shallow RM (σ_n max=0.2MPa)	
								c (KPa)	Φ (°)	c (KPa)	Φ (°)
GANW	26.8	105	22	20	0.7	-	-	0.242	39.69	0.081	51.86
GAN	29.1	105	59	11	0.7	78	0.26	0.852	52.82	0.669	60.21
GAB	28.7	156	62	8	0.7	85	0.27	1.539	52.55	1.435	57.48
GABM W and GABW	25.2	50	20	20	0.7	-	-	0.129	24.34	0.045	36.28
OFX	45.1	144	55	12	0.7	144	0.35	0.843	54.31	0.639	61.76
OFXM W and OFXW	43.5	47	23	25	0.7	-	-	0.212	36.08	0.068	48.67
GDO	29.7	176	19	11	0.7	105	0.27	0.328	43.68	0.143	55.14

5.4 SLOPE STABILITY ANALYSIS RESULTS

5.4.1 Structural Data Analysis

The orientation data for each geotechnical domain are illustrated in Figure 5-3 and Figure 5-4 as well as are summarised in Table 5-9.

Table 5-9 Minimum, mean and maximum discontinuity set orientation data

		Set name in DIPS	Minimum Dip (Degrees)	Minimum Dip Direction (Degrees)	Mean Dip (Degrees)	Mean Dip Direction (Degrees)	Maximum Dip (Degrees)	Maximum Dip Direction (Degrees)
Northern Study Area	1	1m (Gabbro banding)/ Anisotropy	43	199	53	213	66	227
	2	2m	63	169	71	180	79	191
	3	3m	04	047	08	337	16	243
	4	4m	57	142	71	150	84	155
	5	5m Anorthosite Foliation	70	246	77	255	83	269
	6	6m	21	045	33	091	50	140
Southern Study Area	1	1m (Gabbro banding)/ Anisotropy	43	275	61	292	81	310
	2	2m	41	332	63	344	83	355
	3	3m	16	164	28	196	42	230
	4	4m	59	000	66	008	74	013
Dykes			-	-	85	315	-	-

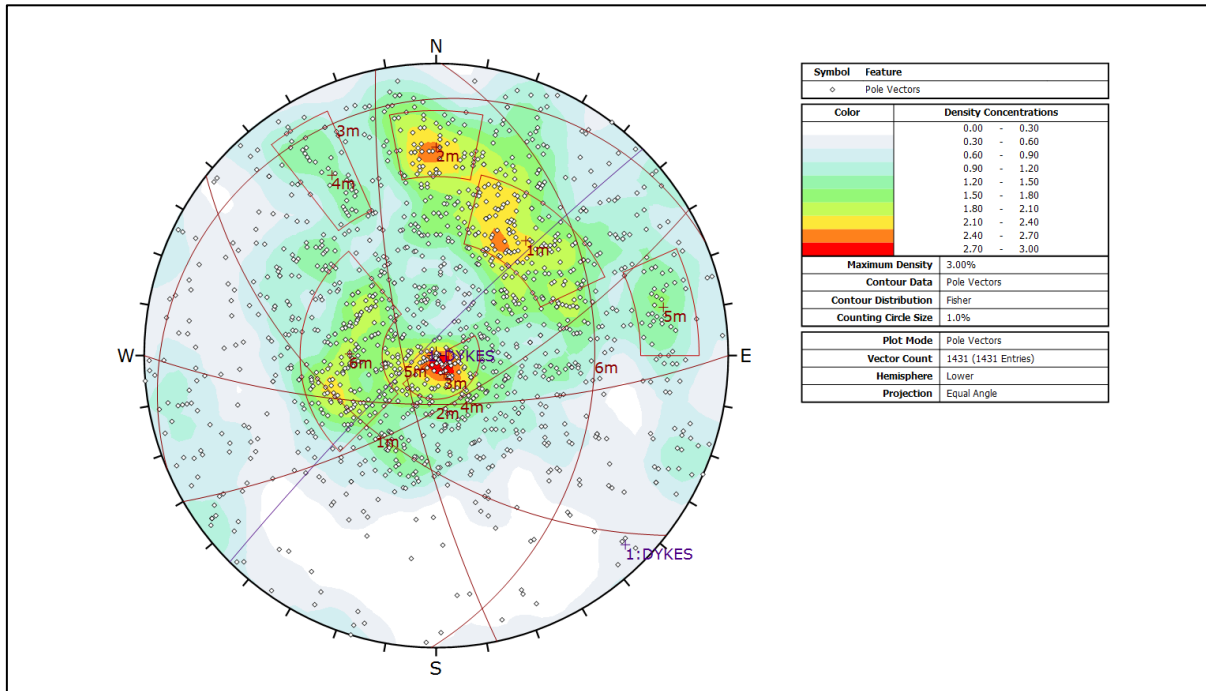


Figure 5-3 Stereographic projection of discontinuities in Northern section of the Study Area

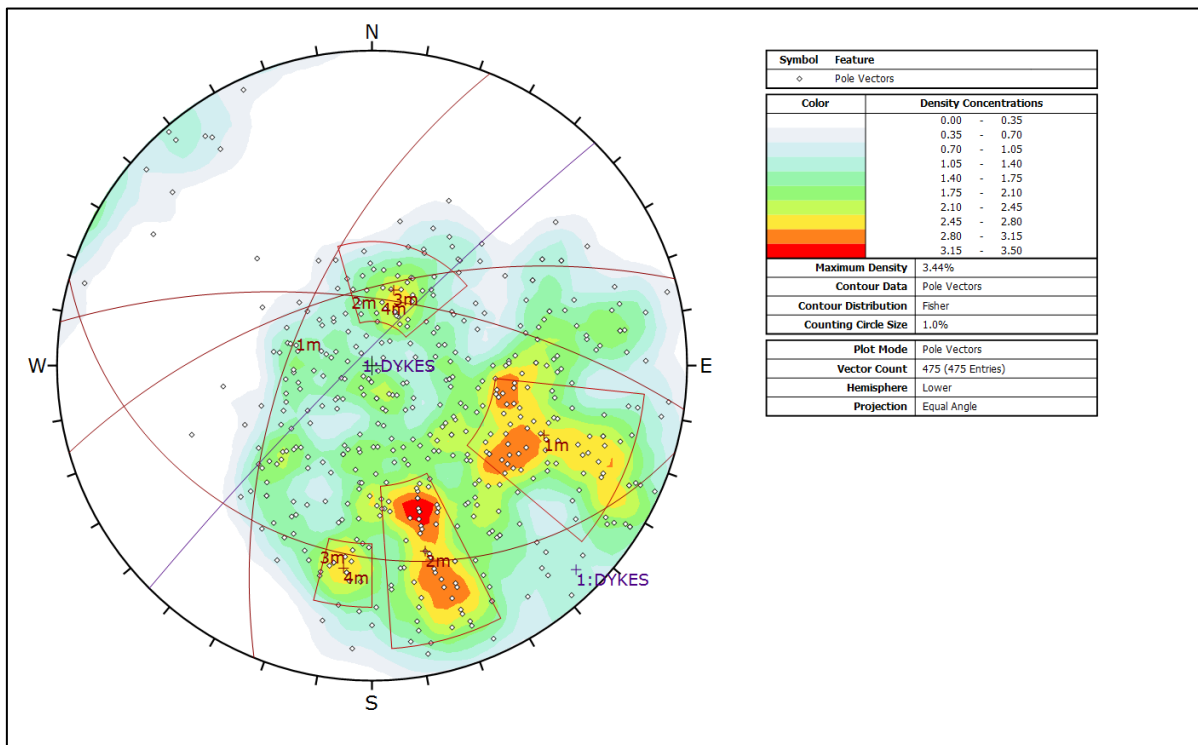


Figure 5-4 Stereographic projection of discontinuities in the Southern section of the Study Area

The dyke structure in the study area has a north westerly dip direction, strike of 235° in relation to the other discontinuities on the stereographic plan. Due to the major fold structure which divides the study area into a northern and southern limb. The poles of the discontinuities in the northern section of the study area plot mainly in the north easterly quadrant of the stereo net and in the southern section of the study area the plot in the south-eastern quadrant of the stereo net. Set 1 in both the northern and southern study area is the Gabbro banding and joints as most joints in this lithology opened along these bands. Set 5 in the northern section of the study area is the foliation orientation noted in the Anorthosite. The Anorthosite foliation orientation was not encountered in the analysed boreholes in the southern study area.

5.4.2 Kinematic Analysis Results

The results of the kinematic analysis graphs illustrate the variation of the PoF in relation to the different bench and stack/inter-ramp angles at different slope orientations. The acceptance criteria applied is as follows:

- Stack/inter-ramp, $\text{PoF} \leq 10$; and
- Bench scale, $\text{PoF} \leq 25$.

These PoF criteria were applied during the kinematic analyses to obtain the following results (Figure 5-5 to Figure 5-8:

- The main mode of failure that exceeded the acceptable criteria threshold is wedge failure in both the Northern and Southern study areas.
- Bench scale wedge failure occurred mainly at 80° to 90° bench angle in the Northern study area at slope directions of 180° to 205° ;
- Stack scale wedge failure occurred only at a 60° stack angles in the Northern study area at slope directions 180° to 205° ;
- Bench scale wedge failure occurred mainly at 80° to 90° bench angles in the Southern study area at a slope direction of 310° ; and
- Stack scale wedge failure occurred only at a 60° stack angle in the Southern study area at slope directions of 310° to 045°

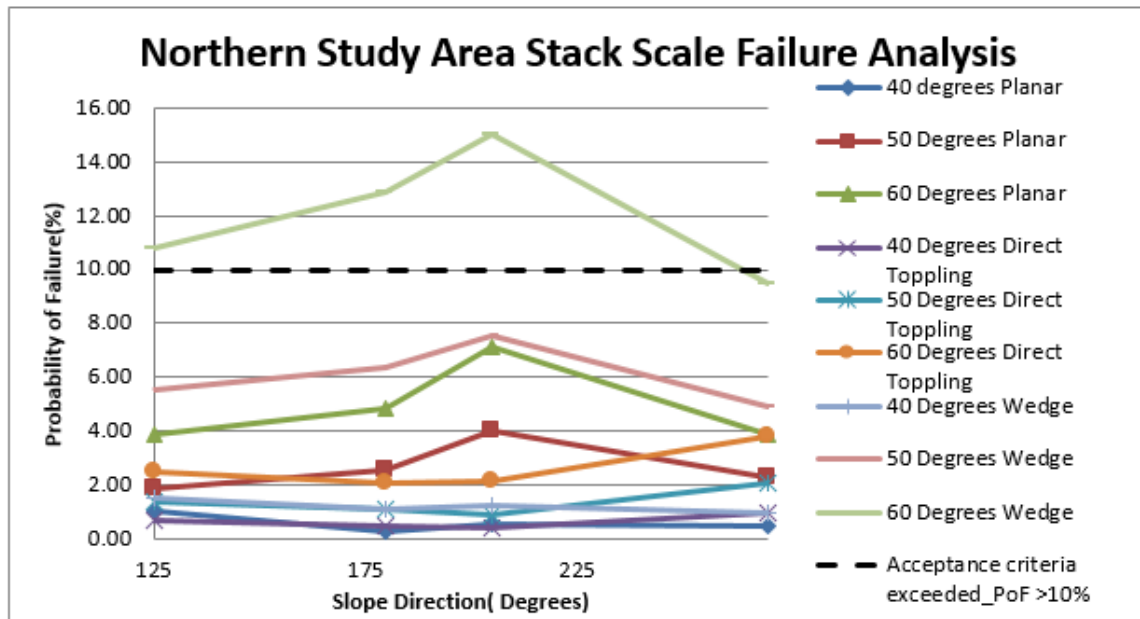


Figure 5-5 Probability of occurrence of stack scale failure in the Northern Study Area

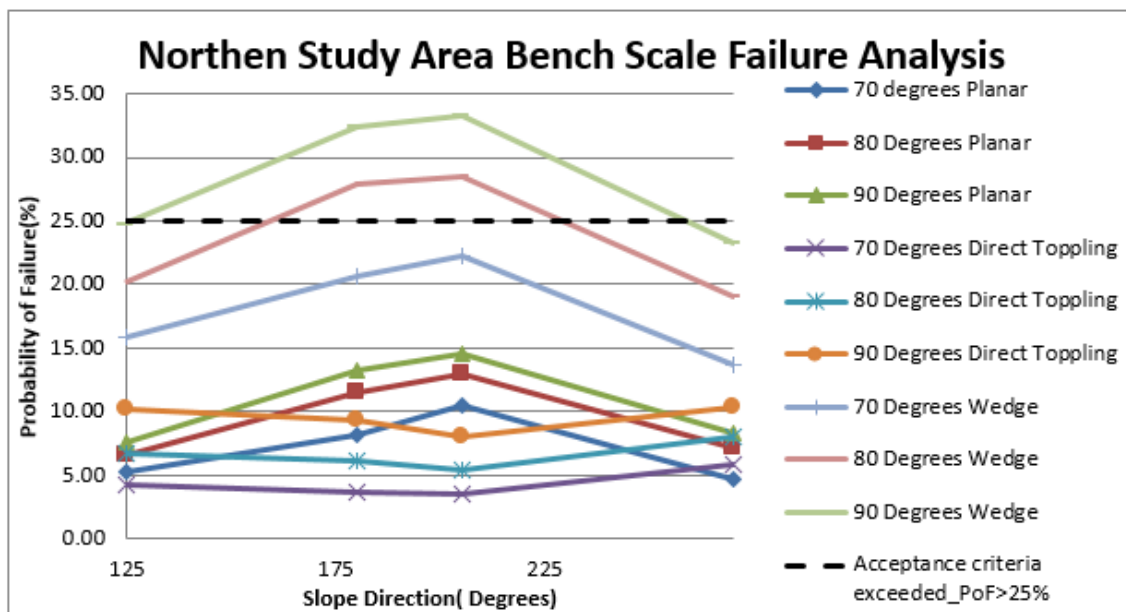


Figure 5-6 Probability of occurrence of bench scale failure in Project area North

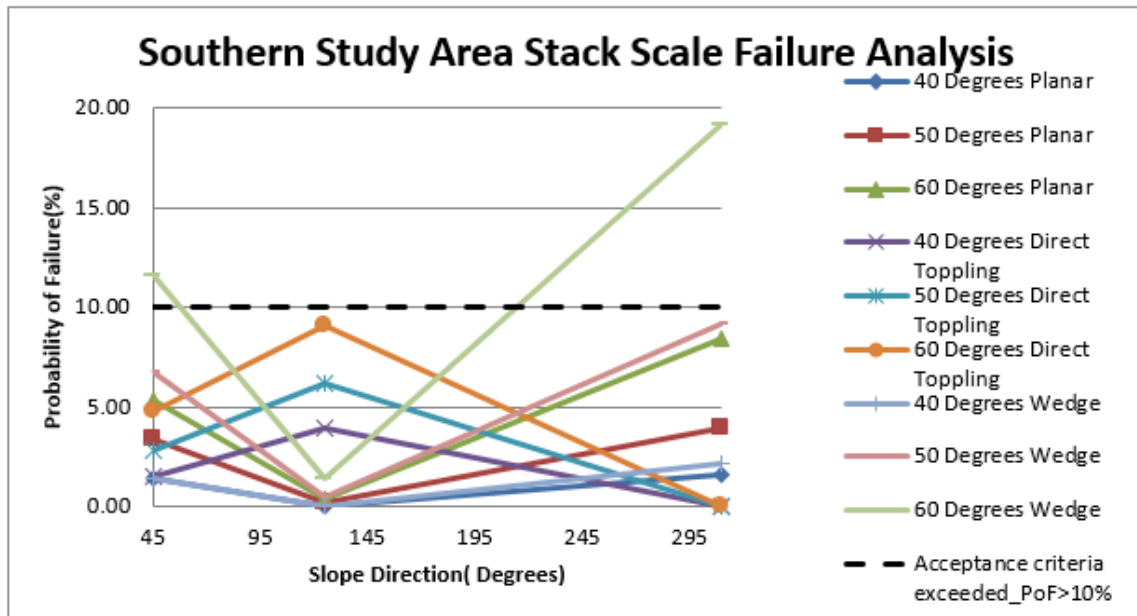


Figure 5-7 Probability of occurrence of stack scale failure in the Southern Study Area

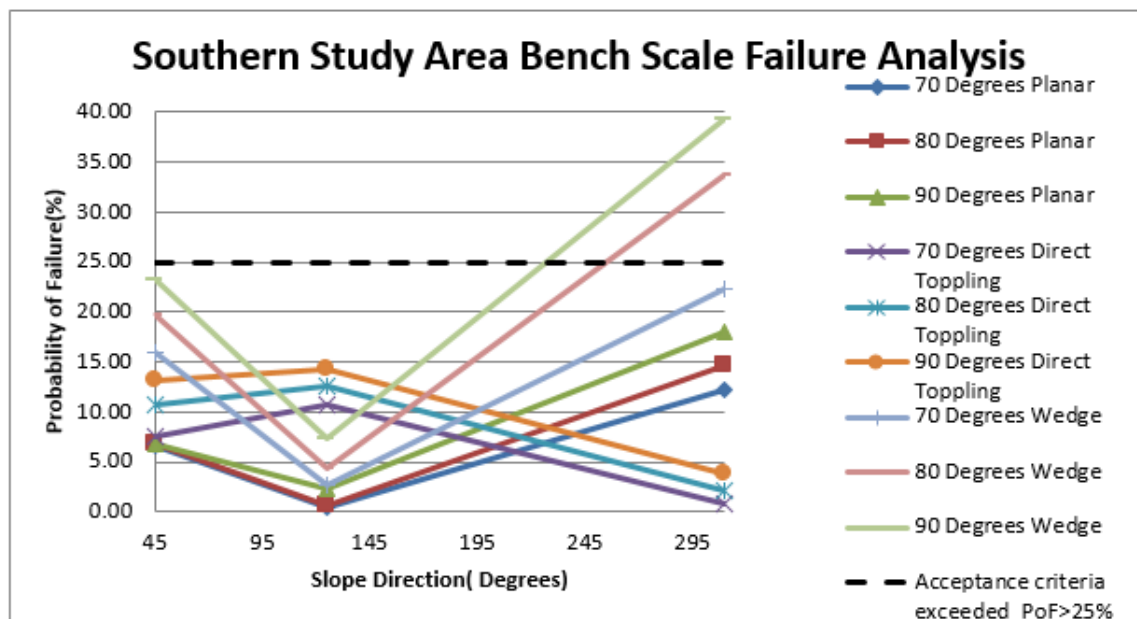


Figure 5-8 Probability of occurrence of bench scale failure in the Southern Study Area

5.4.3 SWEDGE Analysis Results

The SWEDGE analysis results are summarised in Table 5-10 and Table 5-11.

Table 5-10 SWEDGE results Northern Study Area

Northern Study Area	270	Angle	PoF	FoS
		40	0.00	1.57
50	0.73	0.87		
60	1.62	0.74		
70	0.13	0.83		
80	17.00	0.23		
90	22.00	0.02		

Table 5-11 SWEDGE results Southern Study Area

Southern Study Area	310	Angle	PoF	FoS
		40	0.00	1.17
50	1.80	0.89		
60	14.00	0.58		
70	21.00	0.45		
80	27.00	0.25		
90	31.00	0.03		

From this analysis the following was concluded:

- PoF \geq 20 at a 70°, 80° and 90° bench angle in Northern Study Area; and
- PoF \geq 20 at a 90° bench angle in Southern Study Area.

The calculated volume of failed material does not exceed the recommended berm width at a bench face angle of 70°. Utilising the findings of the kinematic and SWEDGE stability analyses a proposed pit geometry is summarised in Table 5-12.

The kinematic and Swedge analyses were used to derive the slope geometry limits that meet the pit design acceptance criteria of acceptable PoF. The geometry of the slopes for each section line analysed in the research area are shown in Table 5-12.

Table 5-12 Slope geometries

Slope			Bench Height (m)	Batter angle (°)	Berm width (m)	Slope/Stack angle		Slope Height (m)	Overall slope angle (°)
Geotechnical domain	Direction	Section				Toe to toe	Crest to toe		
Section A	310	Highly weathered	10	70	7.2	38.4	50	30	44
		Moderately-Unweathered	10	70	2.8	52.4	60	40	
		Moderately-Unweathered (Double bench)	20	70	8.5	52.4	70	40	44
Geotech Berm	-	-	-	-	12.7	-	-	-	-
Section B	270	Highly weathered	10	90	12.7	38.4	50	30	49
		Moderately-Unweathered	10	90	7.7	52.4	60	40	
		Moderately-Unweathered (Double bench)	20	90	14.6	54	70	40	53
Section C	125	Highly weathered	10	90	12.7	38.4	50	30	49
		Moderately-Unweathered	10	90	7.7	52.4	60	40	
		Moderately-Unweathered (Double bench)	20	90	14.6	54	70	40	53
Geotech Berm	-	-	-	-	12.7	-	-	-	-

5.4.4 Limit Equilibrium Analysis Results

The results of this analyses indicate the isotropic models show stable conditions over all slopes with FoS > 1.3. Generated slip surfaces are at a stack scale and not the entire slope, whereas the anisotropic models are stable with FoS > 2.1 in Section A on slip surfaces that cover the entire slope however has FoS=0.3 on bench scale in Section B. Section B has an overall slope direct as that is the same as the anisotropy in this area. The results are summarised in Table 5-13 and the SLIDE outputs are presented in Appendix F.

Table 5-13 Overall slope stability results

Optimised Pit Shell				
Section Line	Isotropic		Anisotropic	
	FoS	PoF	FoS	PoF
A	1.7	< 0.1	2.1	-
B	1.5	< 0.1	0.3	-
C	2.4	< 0.1	-	-

CHAPTER 6 DISCUSSION AND CONCLUSION

The following findings and conclusions are based on the outcomes of the geotechnical investigation and analysis of an orientation bias foliated host rock of an iron ore deposit in Mozambique.

- The applied approach to the case study is as illustrated in Figure 6-1. This flow chart covers the aspect that need to be taken into consideration in completing a comprehensive anisotropic rock mass geotechnical investigation and slope design.

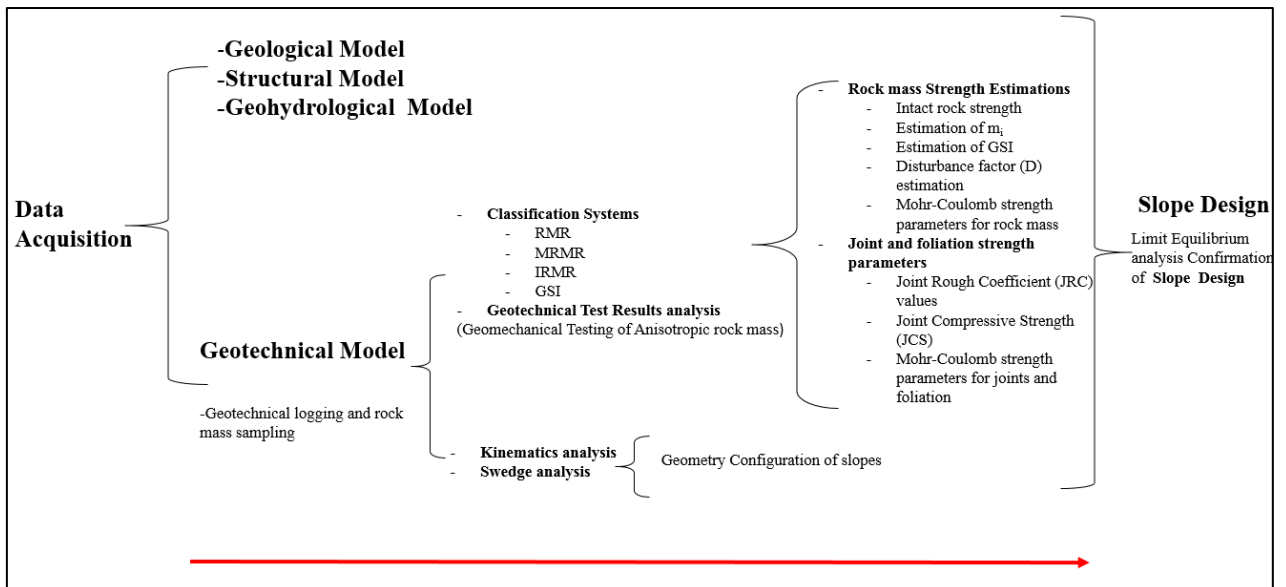


Figure 6-1 Anisotropic rock mass geotechnical investigation and design flow chart.

- The Hoek- Brown envelope plots indicate that there is a scatter in the test results shown for GAB resulting in m_i values that are lower than published values. The small number of data points collected for GABMW and GABW results in an unreliable fit of the linear correlation, however the value selected is in the lower range of published m_i values for gabbro. The scatter in the test results causes the linear correlations of the data to be poor. Interpretation of the data based on the observations during core logging resulted in conservative parameters for the analysis. In situ rock strengths in these ranges are not considered to be critical over the planned slope heights
- Most of the laboratory test specimens failed along discontinuities, such as foliation and cemented joints. Standard practice would exclude these results from the analysis. However, the project area rock mass is expected to fail preferentially along these predefined planes of weakness. Therefore, these results are representative of the expected failure mechanics in this rock mass and were included in the analysis.
- Sampling bias, was accounted for in this study by not discarding the testing samples that field along discontinuities, which is common practice in the industry. Representative samples would include discontinuities which will result in a reduced IRS estimation which would be incorporated in to the designing process.
- Laubscher's (1990) Mining Rock Mass Rating Classification and Bieniawski's (1989) Rock Mass Rating systems indicated that the rock

masses that were geotechnically analysed have ratings ranging from “poor” in the more weathered materials to “Fair” in the unweathered materials.

- The plotted results of the comparison of the calculated RMR, MRMR and IRMR values shows a “good” of the results indicating a classification of the rock mass as “Fair” to “Good” for all three classification systems.
- For foliated rock masses a lower GSI value is needed even if the rock mass does look competent. GSI values for anisotropic rock masses where the alignment of platy minerals originated from alteration or dynamic metamorphosis resulting in the GSI rating declining for the weathered materials in the model.
- The structural data analysis indicated 6 main joint sets in Northern study area and 4 in Southern study area. The main mode of kinematic failure in both Northern study area and Southern study area that exceeded the acceptable criteria thresholds for bench and stack scale analyses was wedge failure. Kinematically, the south section of the project area exhibits stack scale and bench scale failures. However, these failures do not exceed the berm widths. Failures along foliation planes are dependent on the main orientation of the foliation being in the direction of the slope face. It is in these directional scenarios that an anisotropic limit equilibrium analysis is required. The foliation in the in-situ rock mass seems to pre-determine the orientation of an important fracture set (Anttila et al. 1999, Äikäs et al. 2000), and possibly also the preferred orientation of an important set of fracture zones

- The results of the limit equilibrium analyses indicate that the isotropic models show stable conditions in overall slopes analysis with $FoS > 1.3$. The generated slip surfaces are isolated to a stack scale and not the entire slope. The anisotropic models are generally stable, with $FoS > 2.0$ on slip surfaces that covers the entire slope. It is evident that the dip of the foliation plane needs to be greater than that of the foliation strength parameter as well as be daylighting on the slope for failure to occur.
- Sufficient loading of high density rock material on foliated rock masses may also results in failure along the foliation planes even if the joint strength parameters are high (scenario where the pit cut left a large amount of ore behind which was loaded on the gabbro, failure occurred along the weakest plane orientation in the gabbro).
- For anisotropic input parameters to reach an acceptable FoS the slope geometry would have to be modified to have shallower bench face and overall slope angles. This shows that the currently utilised approach is not necessarily the safest method of design approach. It would be a safer design approach if anisotropic models were applied accordingly and the final slope geometries were generated from the outcome of these models and not of those of the assumed homogenous slope parameters which is the current norm

REFERENCES

- Äikäs, K., Anttila, P., Hagros, A., & McEwen, T. (2003). *Host rock Classification Phase 2: Influence of host Rock Properties*.
- Akesson, U. e. (2001). *The Influence of Foliation on the Fragility of Granitic Rocks Assessed with Image analysis and Quantitative Microscopy*. Goteborg University , Department of Earth Sciences.
- Amadei, B. (n.d.). The Influence of Rock Anistrropy on Measurement of Stresses Insitu. 242-251.
- Bieniawski, Z. (1973). Engineering Classification of Jointed Rock Masses. *Transactions of the South Africation Institution of Civil Engineers*, 335-343.
- Chen, C. a. (2001). Measurement of Indirect Tensile Strength of Anisotropic Rocks by Ring Test. *Rock Mechanics and Rock engineering*, 34(4):293-321.
- Contreras, L. (2009). *Cut & Slope Design: Estimation of Rock Mass and Joint Parameters*. Johannesburg: SRK Consulting (Pty) Ltd.
- D.H, J. J. (2000). The MRMR Rock Rating Classification System in Mining Practise. *Mass Miining 2000*, (pp. 413-421). Brisbane.
- Dyke, G. P. (2008). Rock Mass Chracterisation: A Comparison of MRMR and IRMR Classification Systems. *The South African Institue of Mining and Metallurgy*, 217-224.
- Eberhardt, E. (2012). The Hoek- Brown Failure Criterion. *Rock Mech Rock Eng*, 45:981-988.
- Eberhardt, E. e. (1997). Design of tabular excavations in foliated rock: and interated numerical modelling approach. *Geotechnical and Geological Engineering*, 15: 47-85.
- Evans, R. J., Ashwal, I. D., & Hamilton , M. A. (1999). Mafic, anorthositic rocks of the Tete Complex, Mozambique: petrology, age and significance. . *South African Journal of Geology*, 102, no2, 153-166.

REFERENCES

- Goshtasbi, K. A. (2006). Anisotropic Strength behaviour of Slates in the Sirjan- Sanandaj Zone. *The South African Institute of Mining and Metallurgy*, 106:71-76.
- Hoek, E. a. (1988). The Hoek- Brown failure Criterion. *Proceeding of Symposium of 15th Canadian Rock Mechanics* , 31-38.
- Hoek, E. C. (2013). Quantification of the Geological Strength Index Chart. *American Rock Mechanics Association*, 13(672): 1-8.
- Hoek, E. M. (1998). Applicability of the Geological Strength Index (GSI) Classification for Very Weak and Sheared Rock Masses. The Case of the Athens Schist Formation. *Bull. Eng. Geol. Env*, 57:151-160.
- Hoek, Evert. (2012). Blast Damage Factor D, . *Technical Notes for RockNews*.
- Jakubec, J. a. (2000). The MRMR Rock mass rating Classification System in Mining Practice. *Mass Mining*, (pp. 413-421). Brisbane.
- Laubscher, D. (1977). Geomechanics Classification of Jointed Rock Masses- Mining Applications. *Trans. Institution of Mining and Metallurgy*, Section A(86):A1-A8.
- Laubscher, D. (1990). A Geomechanics Classification system for the Rating of Rock Mass in Mine Design. *Journal of the South African Institute of Mining and Metallurgy*, 90(10): 257-473.
- Laubscher, D. a. (1976). The importance of Geomechanics Classification of jointed Rock Masses in Mining Operations. *Proceedings of the Symposium on Exploration for Rock Engineering*, 119-128.
- Maier, W. D., Barnes, S. J., Ashwal, I. D., & Li, C. (2001). A reconnaissance study on magnetic Cu-Ni-PGE sulphide potential of the Tete Complex, Mozambique. *South African Journal of Geology*, V, 104, no 4, 355-363.
- Marinos, P. H. (2006). Variability of the engineering properties of rock masses quantified by geological strength index: the case of ophiolites with special emphasis on tunnelling. *Bull Eng Geol Env*, 65: 129-142.
- Marinos, P. Hoek, E. (2001). Estimating the geotechnical Properties of Heterogeneous Rock Masses such as Flysch. *Bull. Eng. Geol. Env*, 60:85-92.
- Masahiko, O. (2005). geotechnical description and JGS Classification System for Rock Mass. *International Journal of the Japanese Committee for Rock Mechanics*, Volume1:1 7-17.
- Osada, M. e. (2005). Geotechnical Description and JGS Engineering Classification System for Rock Mass. *International Journal of the JCRM* , 7-17.

REFERENCES

- Palmen, J. (2003). Technique to Map Foliation from Boreholes Images, a Case Study of Borehole OL-KR12, Olkiluoto of Eurajoki, W-Finland. 1-8.
- Palmstrom, A. (1995). *RMI: A Rock Mass Characterazation system for Rock Engineering Purposes*. Oslo: Oslo University.
- Poon, C. N. (2009). Enhancing the Collection of Rock Mass Fabric Data for Open Pit Mines. *Proceedings of the 3rd CANUS Rock Mechanics Symposium*, 4015:1-9.
- Poschi, I. a. (2004). Geotechnical Risk in Rock Mass Characterisation- A Concept. *Course on Geotechnical Risks in Rock Tunnelling*, 1-11.
- Read, J. J. (2008). Field Data Collection . In *Guidelines for Open Pit Slope Design* (pp. 15-50). CSIRO.
- Redford, M. a. (2000). Vertical Pit Mining: A Novel Alternative to Open Pit or Underground Methods for Mining of Appropriate Massive Shallow Orebodies. *Mass Mining*, (pp. 859-868). Brisbane.
- Saroglou, H. M. (2003). The Anisotropic Nature of Seleted Metamorphic rocks from Greece. *Technology Roadmap for Rock Mechanics, South African Institute of Mining and Metallurgy*, 1019-1023.
- Shoupletsov, Y. (2003). About Common Principles of Developed Geomechanical Classification and Discrepancies in Estimation of Strength of Rock Masses. *ISRM*, 10631068.
- Singh, J., Ramamurthy, T., & Venkatappa Rao, G. (1989). Strength Anisotropies in Rocks. *Indian Geotechnical journal*, 147-166.
- Singhal, B. a. (2010). Applied Hydrogeology of Fractured Rocks. *Second Edition*, 13-33.
- SRK Consulting (Pty) Ltd. (2014). *Geohydrology Report- Water Department*.
- SRK Consulting (Pty) Ltd. (2015). *Structural Report*.
- Stacey, P. (2008). Fundamentals of Slope Design. In *Guidelines for Open Pit Slope Design* (pp. 1-15). CSIRO.
- Tsidzi, K. E. (1990). The Influence of Foliation on point Load Strength anisotropy of Foliated Rocks. *Engineering Geology, Volume 29, Issue 1*, 49-58.
- Tunono, A. B. (2010). Jwaneneg Open Pit Mine Cut 8 south East Wall Slope Design. *The South African Insitute if Mining and Metallurgy, Diamond Sources to Use*, 85-101.
- Turner, F. a. (1963). *Structural Analysis of Metamorphic Tectonics*. New York: McGraw- Hill.

REFERENCES

- Westerhof, A. P., Tahon, A., Koistinen, T., Lehto, T., & Akerman, C. (2008). Igneous and Tectonic Setting of the Allochthonous Tete Gabbro-Anotijosite Suite, Mozambique. *GTK Consortium Geological Survey in Mozambique, Geological Survey of Finland Special Paper, 48*, 191-210.
- Yasar, E. (2001). Failure and failure Theories for anisotropic Rocks. *Proceedings for the 17th International Mining Congress and Exhibition of Turkey*, 417-424.

APPENDICES

Appendix A: Geotechnical Logs

		Client: BAOBAB RESOURCES		Logged By: STMAT																							
		Project: TENGE		Orientation: 60/59																							
		Project No.: 466974		Borehole Length: 170.51																							
		Borehole No.: GT0004		Date Logged: June 2014																							
Geotechnical Interval	Borehole Depth (m)		Recovery			RQD		Rock	Solid (m)	Matrix (m)	Matrix Type	Weath 1 - 5	Hard 1 - 5	Joint Orientation				Joint Condition				Comments					
	From	To	TCR (m)	SCR (m)	% Rec	(m)	%							1 030	2 3060	3 6090	Total	Micro 1-9	Macro 1-5	Infill 1-10	Alt 1-3						
PQ	0.00	2.89	2.89	1.06	36.68	0.00	0.00	OFX/HCL	0.00	1.06	M5	5	1	-	-	-	-	-	-	-	-	-	-	-	-	-	-
PQ	2.89	8.75	5.86	3.65	62.29	0.00	0.00	OFX/HCL	0.00	3.65	M5	5	1	-	-	-	-	-	-	-	-	-	-	-	-	-	GDO at 2.79m to 3.08m
PQ	8.75	13.31	4.56	3.95	96.62	0.00	0.00	GAN	0.00	3.95	M5	5	1	-	-	-	-	-	-	-	-	-	-	-	-	-	OFX at 11.38m to 12.00m
PQ	13.31	15.10	1.79	1.43	79.89	0.00	0.00	OFX	0.00	1.43	M5	5	1	-	-	-	-	-	-	-	-	-	-	-	-	-	-
PQ	15.10	17.00	1.90	1.46	76.84	0.00	0.00	OFX	0.00	1.46	M5	4/5	1/2	-	-	-	-	-	-	-	-	-	-	-	-	-	-
PQ	17.00	19.21	2.21	1.25	56.56	0.00	0.00	HCL	0.58	0.67	M5	3/4	3	-	-	-	-	-	-	-	-	-	-	-	-	-	-
PQ	19.21	21.53	2.32	1.35	58.19	0.00	0.00	GAN	0.00	1.35	M5	4	1/2	-	-	-	-	-	-	-	-	-	-	-	-	-	-
NQ	21.53	27.00	5.47	5.16	94.33	4.91	89.76	OFX/OFM	4.22	0.94	M5	3	3	0	3	0	3	1	3/2	2	10	1	-	-	-	-	-
NQ	27.00	30.07	3.07	2.55	83.06	2.55	83.06	OFX/OFM	2.20	0.35	M5	3	3	-	-	-	-	-	-	-	-	-	-	-	-	-	-
NQ	30.07	34.05	3.98	3.52	88.44	3.37	84.67	OFX/OFM	1.79	1.73	M5	3	3	1	2	0	3	1	6	2	3	1	-	-	-	-	-
NQ	34.05	35.04	0.99	0.99	100.00	0.99	100.00	GAN	0.00	0.99	M5	3/4	1/2	0	0	0	0	-	-	-	-	-	-	-	-	-	-
NQ	35.04	41.84	6.80	6.34	93.24	6.02	88.53	OFX/OFM	5.00	1.34	M5	3	3	1	3	0	4	5	9	2	4	1	-	-	-	-	-
NQ	41.84	44.68	2.84	1.59	55.99	1.59	55.99	OFX/OFM	1.13	0.46	M5	3	3	0	0	0	0	-	-	-	-	-	-	-	-	-	-
NQ	44.68	50.68	6.00	5.48	91.33	5.05	84.17	GAB	4.35	1.13	M3/5	3	3	6	5	1	12	2	8	2	3/4	1	-	-	-	-	-
NQ	50.68	54.88	4.20	3.81	90.71	3.29	78.33	GAB	2.87	0.94	M3/5	3	3	1	2	12	15	4	3	2	4/3	1	-	-	-	-	-
NQ	54.88	59.00	4.12	3.54	85.92	3.39	82.28	GDO	2.64	0.90	M3	4/3	3/2	2	3	8	13	4	9	2	4/3	1	-	-	-	-	-
NQ	59.00	63.00	4.00	3.23	80.75	2.36	59.00	GAB	2.10	1.13	M5/3	2/3	3/4	2	8	4	14	5	9	2	5/4	1	-	-	-	-	-
NQ	63.00	67.00	4.00	3.75	93.75	3.29	82.25	GAB	3.52	0.23	M6/3	2	4	2	7	8	17	5	6	2	8/3	1	-	-	-	-	-
NQ	67.00	71.68	4.68	4.53	96.79	4.42	94.44	GAB	4.53	0.00	N/A	2	4	1	2	3	6	1	3	2	8/3	1	-	-	-	-	-
NQ	71.68	76.55	4.87	4.54	93.22	4.42	90.76	GAB	4.54	0.00	N/A	1/2	4	1	4	1	6	1	6	2	5/4	1	-	-	-	-	-
NQ	76.55	83.00	6.45	6.15	95.35	6.03	93.49	GAN	6.15	0.00	N/A	2	4	1	4	4	9	2	3	2	3/4	1	-	-	-	-	-
NQ	83.00	88.00	5.00	4.61	92.20	4.23	84.60	GAB	4.50	0.11	M5	2	4	1	4	5	10	2	3	2	3/4	1	-	-	-	-	-
NQ	88.00	92.51	4.51	4.17	92.46	3.86	85.59	GAB	3.92	0.25	M5	2	4	1	6	1	8	2	6	2	3/4	1	-	-	-	-	-
NQ	92.51	98.51	6.00	5.97	94.01	5.97	99.50	GAB	5.97	0.00	N/A	2	4	0	2	1	3	1	9	2	5/3	1	-	-	-	-	-
NQ	98.51	101.51	3.00	2.94	98.00	2.94	98.00	GAB	2.94	0.00	N/A	2	4	0	1	1	2	1	3	2	3	1	-	-	-	-	-
NQ	101.51	107.51	6.00	5.74	95.67	5.18	86.33	GAB	5.50	0.24	M6	2	4	0	5	2	7	1	9	2	10	1	-	-	-	-	-
NQ	107.51	111.00	3.49	3.24	92.84	3.10	88.83	GAB	3.24	0.00	N/A	2	4	0	6	6	12	4	3	2	3/10	1	-	-	-	-	-
NQ	111.00	116.51	5.51	5.14	93.28	4.86	88.20	GDO	4.76	0.38	M6	1	4	1	7	2	10	2	9	2	3/10	1	-	-	-	-	-
NQ	116.51	120.00	3.49	3.11	89.11	2.91	83.38	GAB	2.64	0.47	M6	2	4	1	2	3	6	2	6	2	8/5/3	1	-	-	-	-	-
NQ	120.00	125.00	5.00	4.81	96.20	4.61	92.20	GAB	4.81	0.00	N/A	2	4	0	0	4	4	1	6	2	8/5/3	1	-	-	-	-	-
NQ	125.00	130.00	5.00	4.62	92.40	4.45	89.00	GAN	4.38	0.24	M6	2	4	0	4	8	12	3	8	2	8/4	1	-	-	-	-	-
NQ	130.00	135.00	5.00	4.94	98.80	4.90	98.00	GAN	4.88	0.06	M5	2	4	0	3	1	4	1	8	2	5/8	1	-	-	-	-	-
NQ	135.00	140.51	5.51	5.46	99.09	5.46	99.09	GAB	5.46	0.00	N/A	2	4	0	3	0	3	1	9	2	6/5	1	-	-	-	-	-
NQ	140.51	146.51	6.00	5.85	97.50	5.76	96.00	GAN	5.85	0.00	N/A	2	4	0	2	0	2	0	9	2	8/4	1	-	-	-	-	-
NQ	146.51	149.51	3.00	2.84	94.67	2.89	89.67	GAB	2.84	0.00	N/A	2	4	0	2	0	2	1	6	2	10/3	1	-	-	-	-	-
NQ	149.51	155.51	6.00	6.09	101.50	5.91	98.50	GAB	5.93	0.16	M6	2	4	2	3	1	6	1	8	2	10/3	1	-	-	-	-	-
NQ	155.51	161.51	6.00	5.84	97.33	5.70	95.00	GAB	5.84	0.00	N/A	2	4	0	5	4	9	2	9	2	8/7/3	1	-	-	-	-	-
NQ	161.51	164.51	3.00	2.81	93.67	2.81	93.67	GAB	2.45	0.36	M5	2	4	0	2	0	2	1	6	2	7/6	1	-	-	-	-	-
NQ	164.51	170.51	6.00	5.92	98.67	5.82	97.00	GAB	5.75	0.17	M5	2	4	2	4	1	7	1	8	2	7/6	1	-	-	-	-	-

E.O.H

Appendix B: Laboratory Results

Issued by:

ROCKLAB

(ROCK MECHANICS & EXCAVATION LABORATORIES)
230 ALBERTUS STREET
LA MONTAGNE
PRETORIA
SOUTH AFRICA
TEL: +27 12 813 4910
FAX: +27 12 481 3812
E-MAIL: CHENJ@ROCKLAB.CO.ZA

RESULTS OF ROCK PROPERTIES TESTS

Sampling Site: Baobao Resources, Mozambique

BY
DR J. F. CHEN

Submitted to:
SRK CONSULTING (PTY) LTD

28 August 2014

CONTENTS

TABLE 1	-	RESULTS OF UNIAXIAL COMPRESSIVE STRENGTH TESTS
TABLE 2	-	RESULTS OF UNIAXIAL COMPRESSIVE STRENGTH TESTS WITH ELASTIC MODULUS & POISSON RATIO MEASUREMENTS BY MEANS OF STRAIN GAUGES
TABLE 3	-	RESULTS OF BRAZILIAN TENSILE STRENGTH TESTS
TABLE 4	-	RESULTS OF TRIAXIAL COMPRESSIVE STRENGTH TESTS
TABLE 5	-	RESULTS OF ROCK BASIC FRICTION ANGLE MEASUREMENTS
APPENDIX 1		DIAGRAM OF STRESS VIS STRAIN FOR UCM TESTS
APPENDIX 1		DIAGRAM OF STRESS VIS DISPLACEMENTS FOR ROCK BASIC FRICTION ANGLE MEASUREMENTS
APPENDIX 3		FAILURE CODES OF ROCK COMPRESSION TESTS

TABLE 1 RESULTS OF UNIAXIAL COMPRESSION STRENGTH TESTS



Client: SRK Consulting

Site : Baobab Resources, Mozambique

2014/8/28

SPECIMEN PARTICULARS						SPECIMEN DIMENSIONS					SPECIMEN TEST RESULTS			
Rocklab Specimen No	BH ID	Sample No	Depth From	Depth To	Rock Type	Diameter	Height	Ratio of Height to diameter	Mass	Density	Failure Load	Strength (UCS)	Failure Code	Note
5845-			m	m		mm	mm		g	g/cm ³	kN	MPa		
UCS-02	GT001	GT0001GDO(MW)	61.51	61.65	GDO(MW)	60.96	132.27	2.2	1138.8	2.95	249.2	85.4	4B	
UCS-08A	GT001	GT0001GDO(UW)	137.09	137.68	GDO(UW)	44.97	129.27	2.9	604.3	2.94	166.6	104.9	0B	
UCS-08B						44.99	125.92	2.8	585.0	2.92	318.0	200.0	1B	
UCS-09	GT001	GT0001GDO(MW)	61.74	61.88	GDO(MW)	47.97	95.70	2.0	500.2	2.89	103.4	57.2	0B	
UCS-10	GT001	GT0001GDO(MW)	62.49	62.64	GDO(MW)	61.09	122.31	2.0	1107.0	3.09	678.4	231.5	2B	
UCS-11	GT001	GT0001GDO(MW)	71.20	71.33	GDO(MW)	47.69	101.02	2.1	515.3	2.86	143.8	80.5	5B	
UCS-16	GT001	GT0001GAB(MW)	54.16	54.30	GAB(MW)	47.68	96.16	2.0	455.1	2.65	128.8	72.1	0B	
UCS-17	GT001	GT0001GAB(MW)	49.88	50.03	GAB(MW)	28.59	39.72	1.4	62.4	2.45	11.8	18.4	0B	
UCS-18	GT001	GT0001GAB(MW)	39.08	39.26	GAB(MW)									1
UCS-20A						45.10	123.98	2.7	638.2	3.22	214.8	134.4	5B	
UCS-20B	GT001	GT0001GAB(UW)	212.67	212.98	GAB(UW)	45.08	124.95	2.8	618.8	3.10	212.9	133.4	0B	
UCS-21	GT001	GT0001GAB(UW)	127.06	127.30	GAB(UW)	45.00	130.98	2.9	638.5	3.07	474.7	298.5	2B	
UCS-25	GT001	GT0001GDO(UW)	151.33	151.57	GDO(UW)	45.03	130.12	2.9	614.3	2.96	260.9	163.8	5B	
UCS-26	GT001	GT0001GDO(UW)	155.95	156.24	GDO(UW)	45.00	115.97	2.6	544.9	2.95	221.5	139.3	5B	
UCS-27	GT001	GT0001GDO(UW)	157.11	157.41	GDO(UW)	45.00	129.69	2.9	602.0	2.92	214.4	134.8	5B	
UCS-28	GT002	GT0002OFX(MW)	118.81	119.15	OFX(MW)	44.92	130.31	2.9	968.7	4.69	193.5	122.1	3B	
UCS-29	GT002	GT0002OFX(UW)	120.33	120.52	OFX(UW)	44.92	129.45	2.9	961.9	4.69	260.1	164.1	3B	
UCS-30	GT002	GT0002OFX(UW)	125.23	125.47	OFX(UW)	44.98	129.19	2.9	953.4	4.64	179.9	113.2	4B	
UCS-32	GT002	GT0002OFX(UW)	135.21	135.52	OFX(UW)	44.93	130.11	2.9	960.2	4.65	222.3	140.2	3B	
UCS-34	GT002	GT0002OFX(UW)	153.31	153.55	OFX(UW)	45.08	129.66	2.9	934.3	4.51	178.5	111.8	4B	
UCS-36	GT002	GT0002OFX(UW)	104.57	104.91	OFX(UW)	44.94	129.46	2.9	914.9	4.46	362.7	228.6	YA	
UCS-41	GT002	GT0002GAN(SW)	26.20	26.52	GAN(SW)	60.94	165.89	2.7	1359.9	2.81	296.2	101.6	3B	
UCS-45	GT003	GT0001GDO(UW)	146.78	147.01	GDO(UW)									1
UCS-56	GT003	GT0003GAB(MW)	29.71	29.88	GAB(MW)	60.95	120.33	2.0	861.8	2.45	28.8	9.9	0B	
UCS-57	GT003	GT0003GAB(MW)	33.29	33.49	GAB(MW)	60.88	116.36	1.9	880.0	2.60	76.4	26.3	0B	
UCS-59	GT003	GT0003GAB(UW)	189.22	189.45	GAB(UW)	44.92	130.09	2.9	583.2	2.83	383.4	241.9	YA	
UCS-60	GT003	GT0003GAB(UW)	216.75	217.05	GAB(UW)	44.97	130.60	2.9	602.1	2.90	347.2	218.6	YA	
UCS-61	GT003	GT0003GAB(UW)	39.08	39.26	GAB(UW)	60.58	131.50	2.2	910.1	2.40	24.7	8.6	3B	

UCS-62	GT003	GT0003GDO(UW)	155.95	156.24	GDO(UW)										1
UCS-64	GT004	GT0004OFX(W)	35.75	36.02	OFX(W)	60.97	165.65	2.7	2110.2	4.36	145.8	49.9	0B		
UCS-65	GT004	GT0004OFX(W)	42.97	43.19	OFX(W)									1	
UCS-66	GT004	GT0004OFX(W)	39.07	39.25	OFX(W)	61.07	118.59	1.9	1494.3	4.30	111.6	38.1	2B		
UCS-67	GT004	GT0004OFX(W)	37.23	39.95	OFX(W)	60.57	127.08	2.1	1595.0	4.36	218.6	75.9	2B		
UCS-68	GT004	GT0004OFX(W)	25.36	25.80	OFX(W)									1	
UCS-70	GT004	GT0004GDO(MW)	57.58	57.98	GDO(MW)	60.85	160.98	2.6	1443.2	3.08	173.8	59.8	3B		
UCS-72	GT004	GT0004GDO(UW)	111.19	111.39	GDO(UW)	44.95	128.21	2.9	612.9	3.01	93.3	58.8	5B		
UCS-73	GT004	GT0004GDO(UW)	112.27	112.52	GDO(UW)	44.96	130.81	2.9	636.7	3.07	378.1	238.1	YB		
UCS-74	GT004	GT0004GDO(UW)	113.25	113.51	GDO(UW)	44.93	130.39	2.9	633.7	3.07	384.5	242.5	3B		
UCS-80	GT004	GT0004GAN(MW)	19.23	19.37	GAN(MW)	60.74	97.27	1.6	721.2	2.56	15.8	5.5	0B		
UCS-82	GT004	GT0004GAN(UW)	130.10	130.34	GAN(UW)	44.82	130.53	2.9	554.3	2.69	61.1	38.7	4B		
UCS-83	GT004	GT0004GAN(UW)	130.83	131.00	GAN(UW)	28.62	60.37	2.1	102.2	2.63	33.0	51.2	2B		
UCS-84	GT004	GT0004GAN(UW)	126.90	127.11	GAN(UW)	44.90	125.56	2.8	625.8	3.15	135.8	85.8	4B		
UCS-85	GT004	GT0004GAN(UW)	127.55	127.76	GAN(UW)	44.81	130.64	2.9	600.5	2.91	111.2	70.5	1B		
UCS-89	GT004	GT0004GAB(UW)	168.84	169.20	GAB(UW)	44.87	130.15	2.9	617.8	3.00	274.7	173.7	2B		
UCS-90	GT004	GT0004GAB(UW)	146.62	147.03	GAB(UW)	44.68	130.91	2.9	598.8	2.92	132.2	84.3	6B		
UCS-91	GT004	GT0004GAB(UW)	140.69	140.95	GAB(UW)	44.83	115.27	2.6	545.5	3.00	393.9	249.5	YA		
UCS-93	GT004	GT0004GDO(UW)	146.68	147.01	GDO(UW)									1	
UCS-95	GT004	GT0004OFX(UW)	28.15	28.47	OFX(UW)	60.90	163.45	2.7	2155.1	4.53	222.7	76.5	1B		
UCS-98	GT001	GT0001GDO(UW)	146.68	147.01	GDO(UW)	45.02	126.58	2.8	587.6	2.92	113.6	71.4	4B		

Note: All tests were conducted according to the ISRM's Specification.

1 - No suitable specimen could be prepared for the test.

TABLE 2 RESULTS OF UNIAXIAL COMPRESSIVE STRENGTH TESTS WITH MODULUS & POISSON'S RATIO MEASUREMENTS BY MEANS OF STRAIN GAUGES



Client: SRK Consulting

Sampling Site: Baobab Resources, Mozambique

2014-08-028

SPECIMEN PARTICULARS						SPECIMEN DIMENSIONS					SPECIMEN TEST RESULTS								
Rocklab Specimen No	BH Number	Sample Number	Depth From ,, (m)	Depth to .. (m)	Rock Type	Diameter mm	Height mm	Ratio of Height to Diameter	Mass g	Density g/cm ³	Failure Load kN	Strength (UCS) MPa	Tangent Elastic Modulus @ 50% UCS GPa	Secant Elastic Modulus @ 50% UCS GPa	Poisson's Ratio Tangent @ 50% UCS	Poisson's Ratio Secant @ 50% UCS	Linear Axial Strain at Failure mm/mm	Failure Code	Note
UCM-12	GT001	GT0001GDO(UW)	133.80	134.01	GDO(UW)	44.99	126.1	2.8	584.8	2.92	187.9	118.2	94.7	95.7	0.25	0.24	0.001259	0B	
UCM-19	GT001	GT0001GAB(UW)	206.67	207.00	GAB(UW)	45.07	126.9	2.8	573.5	2.83	143.9	90.2	81.5	81.3	0.30	0.26	0.001132	2B	
UCM-22	GT001	GT0001GAB(UW)	84.04	84.29	GAB(UW)	44.85	97.0	2.2	434.7	2.84	136.2	86.2	72.4	73.7	0.24	0.23	0.001284	0B	
UCM-23	GT001	GT0001GDO(UW)	143.79	144.00	GDO(UW)	44.99	125.5	2.8	587.6	2.95	371.3	233.6	111.0	110.0	0.28	0.28	0.002213	2B	
UCM-31	GT002	GT0002OFX(UW)	127.13	127.41	OFX(UW)	44.97	126.4	2.8	919.3	4.58	259.4	163.3	133.0	136.0	0.40	0.39	0.001322	2B	
UCM-33	GT002	GT0002OFX(UW)	152.08	152.57	OFX(UW)	45.05	127.1	2.8	940.1	4.64	168.9	106.0	150.0	155.0	0.29	0.27	0.000721	3B	
UCM-35	GT002	GT0002OFX(UW)	92.57	92.82	OFX(UW)	44.93	125.8	2.8	920.1	4.61	264.7	167.0	150.0	152.0	0.37	0.37	0.001124	3B	
UCM-46	GT003	GT0003GDO(UW)	195.53	195.80	GDO(UW)	44.90	127.0	2.8	621.3	3.09	167.8	106.0	108.0	112.0	0.27	0.28	0.000960	5B	
UCM-48	GT003	GT0003GAN(UW)	61.56	61.85	GAN(UW)														1
UCM-58	GT003	GT0003GAB(UW)	175.10	175.33	GAB(UW)	44.93	125.9	2.8	565.2	2.83	108.2	68.2	100.0	101.0	0.27	0.27	0.000677	0B	
UCM-81	GT004	GT0004GAN(UW)	131.51	131.89	GAN(UW)	44.89	126.6	2.8	555.9	2.77	99.0	62.6	83.8	80.6	0.26	0.24	0.000769	5B	
UCM-86	GT004	GT0004GAN(UW)	129.85	130.09	GAN(UW)	44.87	75.6	1.7	337.3	2.82	107.8	68.2	71.8	71.4	0.25	0.25	0.000974	4B	

Note: All tests were conducted according to the ISRM's specifications.

1 - No suitable specimen could be prepared for the test.

TABLE 3 RESULTS OF BRAZILIAN TENSILE STRENGTH TESTS



Client : SRK Consulting

Sampling Site: Baobab Resources, Mozambique

14-08-2014

SPECIMEN PARTICULARS						SPECIMEN DIMENSIONS				SPECIMEN TEST RESULTS		
Rocklab Specimen No	BH Number	Sample Number	Depth From	Depth To	Rock Type	Diameter	Height	Mass	Density	Failure Load	Tensile Strength	Note
5845-			m	m		mm	mm	g	g/cm ³	kN	MPa	
UTB-01	GT001	GT0001GDO(MW)	61.34	61.51	GDO(MW)	60.69	30.54	261.86	2.96	50.23	17.25	
UTB-03	GT001	GT0001GDO(MW)	63.19	66.89	GDO(MW)	61.11	30.43	256.41	2.87	36.17	12.38	
UTB-13	GT001	GT0001GDO(UW)	125.32	125.57	GDO(UW)	45.09	22.60	111.41	3.09	38.80	24.24	
UTB-15	GT001	GT0001GAB(MW)	53.96	54.12	GAB(MW)							
UTB-24	GT001	GT0001GAB(UW)	200.67	200.97	GAB(UW)	45.12	22.61	99.69	2.76	26.45	16.51	
UTB-43	GT002	GT00002GDO(UW)	120.01	120.33	OFX(UW)	44.97	22.80	164.35	4.54	15.58	9.67	
UTB-44	GT002	GT0002GDO(UW)	108.97	109.39	OFX(UW)	45.00	22.50	163.16	4.56	19.1	12.01	
UTB-49	GT003	GT0003GAN(UW)	75.04	75.43	GAN(UW)	61.08	30.90	269.68	2.98	52.1	17.56	
UTB-50	GT003	GT0003GAN(UW)	62.67	62.98	GAN(UW)	61.03	30.54	283.45	3.17	25.7	8.78	
UTB-53	GT003	GT0003GAB(MW)	22.15	22.32	GAB(MW)							
UTB-54	GT003	GT0003GAB(MW)	40.71	40.88	GAB(MW)	60.24	30.70	203.89	2.33	2.7	0.94	
UTB-55	GT003	GT0003GAB(UW)	162.53	162.76	GAB(UW)	45.00	22.75	101.20	2.80	14.9	9.25	
UTB-67	GT004	GT0004OFX(W)	37.23	39.95	OFX(W)	61.03	30.66	361.20	4.03	8.0	2.72	Cracks
UTB-69	GT004	GT0004OFX	37.52	37.70	OFX	60.94	30.52	306.40	3.44	7.4	2.55	Cracks
UTB-71	GT004	GT0004GDO(MW)	59.43	59.57	GDO(MW)	60.90	30.75	256.19	2.86	50.2	17.07	
UTB-75	GT004	GT0004GDO(UW)	111.94	112.15	GDO(UW)	44.99	23.06	106.50	2.91	27.9	17.13	
UTB-76	GT004	GT0004GDO(UW)	117.11	117.33	GDO(UW)	44.88	22.82	105.40	2.92	26.2	16.26	
UTB-87	GT004	GT0004GAN(UW)	150.81	151.04	GAN(UW)	44.75	22.73	98.30	2.75	16.2	10.14	
UTB-96A						61.12	30.93	381.86	4.21	3.9	1.32	Cracks
UTB-96B	GT004	GT0004OFX(W)	39.70	39.95	OFX(W)	61.13	30.68	375.47	4.17	2.9	0.99	
UTB-97A						60.81	31.09	366.78	4.06	34.2	11.53	
UTB-97B	GT002	GT0002OFX(W)	25.36	25.80	OFX(W)	60.81	30.96	407.36	4.53	38.6	13.04	

Note: Tests were conducted according to the ISRM's specification

1 - No suitable specimen could be prepared for the test.

TABLE 4 RESULTS OF TRIAXIAL COMPRESSIVE STRENGTH TESTS



Client: SRK Consulting

Sampling Site: Baobab Resources, Mozambique

22-08-2014

SPECIMEN PARTICULARS						SPECIMEN DIMENSIONS					SPECIMEN TEST RESULTS				
Rocklab Specimen No	Sample ID	BH ID	Depth From ... m	Depth to ... m	Rock Type	Diameter mm	Height mm	Ratio of Height to Diameter	Mass g	Density g/cm ³	Confining Pressure σ_3 MPa	Failure Load P kN	Strength (TCS) σ_1 MPa	Failure Mode	Notes
TCS-04A	GT001	GT0001GDO(SW)	66.29	66.89	GDO(SW)	61.08	124.8	2.0	1075.5	2.94	5.0	686.0	234.1	5B	
TCS-04B						61.09	107.2	1.8	919.1	2.93	10.0	719.2	245.4	1B	
TCS-04C						61.09	113.5	1.9	964.3	2.90	20.0	980.3	334.5	2B	
TCS-04D						61.08	113.4	1.9	976.6	2.94	30.0	1299.7	443.6	YA	
TCS-04E						36.53	73.3	2.0	226.0	2.94	15.0	323.5	308.7	5B	
TCS-04F						28.73	59.9	2.1	226.0	5.82	25.0	275.0	424.2	XA	
TCS-05A	GT001	GT0001GDO(LW)	70.27	70.76	GDO(LW)	61.07	115.7	1.9	1054.1	3.11	10.0	880.2	300.5	0B	
TCS-05B						47.65	80.7	1.7	446.9	3.11	20.0	635.4	356.3	4B	
TCS-05C						36.52	60.5	1.7	186.6	2.95	30.0	540.6	516.1	XA	
TCS-06A	GT001	GT0001GDO(LW)	70.85	70.99	GDO(LW)	61.09	123.5	2.0	1129.6	3.12	5.0	616.5	210.3	0B	
TCS-06B						61.10	124.1	2.0	1139.8	3.13	15.0	1006.9	343.4	2B	
TCS-06C						28.76	66.6	2.3	135.0	3.12	25.0	351.8	541.6	YA	
TCS-07A	GT001	GT0001GDO(LW)	132.58	133.20	GDO(LW)	45.03	89.1	2.0	422.3	2.98	5.0	301.6	189.4	XA	
TCS-07B						45.04	88.9	2.0	420.9	2.97	10.0	197.4	123.9	4B	
TCS-07C						45.01	86.0	1.9	393.1	2.87	15.0	308.5	193.9	5B	
TCS-07D						45.00	88.9	2.0	414.0	2.93	20.0	472.5	297.1	0B	
TCS-07E						45.02	81.1	1.8	387.5	3.00	30.0	498.8	313.3	XA	
TCS-14A	GT001	GT0001GAB(MW)	195.63	196.31	GAB(MW)	45.06	99.8	2.2	447.9	2.82	5.0	251.6	157.7	3B	
TCS-14B						45.07	99.5	2.2	447.4	2.82	10.0	291.9	182.9	2B	
TCS-14C						45.07	99.9	2.2	446.1	2.80	20.0	299.9	188.0	2B	
TCS-14D						45.05	99.3	2.2	440.0	2.78	30.0	461.3	289.4	2B	
TCS-14E						28.70	61.2	2.1	111.1	2.81	15.0	207.1	320.2	XA	
TCS-38A	GT002	GT0002OFX(LW)	96.62	97.26	OFX(LW)	44.90	89.2	2.0	634.6	4.49	5.0	383.7	242.3	XA	
TCS-38B						44.94	89.9	2.0	629.5	4.41	10.0	441.6	278.4	XA	
TCS-38C						44.91	86.5	1.9	628.7	4.59	15.0	417.1	263.3	XA	
TCS-38D						44.90	89.5	2.0	652.3	4.60	20.0	511.5	323.1	XA	
TCS-38E						44.90	88.7	2.0	647.5	4.61	25.0	543.6	343.3	XA	
TCS-38F						44.91	88.9	2.0	639.1	4.54	30.0	561.0	354.2	XA	
TCS-39A	GT002	GT0002OFX(LW)	106.89	107.54	OFX(LW)	44.89	88.9	2.0	628.6	4.47	5.0	385.4	243.5	XA	
TCS-39B						44.90	88.7	2.0	638.0	4.54	10.0	421.2	266.0	4B	
TCS-39C						44.82	100.7	2.2	676.2	4.26	20.0	539.5	341.9	XA	
TCS-39D						44.84	100.3	2.2	666.6	4.21	30.0	562.0	355.9	4B	
TCS-39E						29.68	61.5	2.1	159.2	3.74	25.0	228.3	330.0	XA	

TCS-40A	GT002	GT0002OFX(LW)	136.45	137.10	OFX(LW)	45.00	88.7	2.0	653.7	4.63	5.0	280.8	176.5	XA
TCS-40B						44.99	88.9	2.0	659.0	4.66	10.0	339.3	213.4	3B
TCS-40C						44.98	88.4	2.0	642.9	4.58	15.0	435.1	273.8	XA
TCS-40D						45.01	88.6	2.0	596.8	4.23	20.0	434.7	273.2	XA
TCS-40E						45.01	88.6	2.0	600.1	4.26	30.0	473.1	297.3	XA
TCS-42A	GT002	GT0002GDO(LW)	83.57	84.34	OFX(LW)	44.95	95.3	2.1	696.9	4.61	5.0	154.5	97.3	4B
TCS-42B						44.94	83.0	1.8	605.5	4.60	10.0	343.8	216.7	3B
TCS-42C						44.95	95.8	2.1	690.5	4.54	15.0	462.8	291.6	0B
TCS-42D						44.89	87.8	2.0	631.0	4.54	20.0	587.8	371.4	XA
TCS-42E						44.96	87.8	2.0	628.7	4.51	25.0	568.9	358.3	XA
TCS-42F						44.95	87.2	1.9	618.8	4.47	30.0	536.5	338.1	7B
TCS-42G						44.98	89.2	2.0	617.6	4.36	20.0	504.0	317.2	XA
TCS-47A	GT003	GT0003GAN(LW)	61.88	62.47	GAN(LW)	47.66	84.5	1.8	430.0	2.85	5.0	265.8	149.0	3B
TCS-47B						47.68	91.7	1.9	543.2	3.32	10.0	295.0	165.2	3B
TCS-47C						47.68	91.3	1.9	477.9	2.93	20.0	373.2	209.0	4B
TCS-47D						47.72	95.9	2.0	536.2	3.13	30.0	495.0	276.8	4B
TCS-51A	GT003	GT0003GAB(MW)	41.76	42.25	GAB(MW)	28.74	41.7	1.5	84.0	3.10	5.0	149.0	229.7	XA
TCS-51B						59.86	119.1	2.0	796.5	2.38	10.0	149.0	52.9	3B
TCS-51C						60.49	78.1	1.3	543.4	2.42	20.0	277.8	96.7	0B
TCS-52A	GT003	GT0003GAB(LW)	193.71	194.48	GAB(LW)	44.91	100.4	2.2	453.7	2.85	5.0	248.2	156.7	4B
TCS-52B						44.94	100.7	2.2	455.2	2.85	10.0	453.6	286.0	4B
TCS-52C						44.91	83.5	1.9	376.8	2.85	15.0	479.1	302.4	XA
TCS-52D						44.92	100.2	2.2	478.9	3.01	20.0	379.8	239.6	6B
TCS-52E						44.89	100.0	2.2	479.5	3.03	30.0	189.3	119.6	3B
TCS-52F						28.72	54.5	1.9	100.1	2.83	20.0	269.0	415.2	XA
TCS-52G						28.71	60.4	2.1	118.5	3.03	30.0	292.8	452.3	XA
TCS-78A						GT004	GT0004GAN(LW)	132.72	133.41	GAN(LW)	44.85	88.1	2.0	388.6
TCS-78B	44.85	89.1	2.0	384.7	2.73						20.0	240.5	152.2	5B
TCS-78C	44.94	100.4	2.2	457.3	2.87						30.0	242.9	153.2	5B
TCS-78D	28.70	60.0	2.1	111.6	2.87						15.0	128.8	199.0	6B
TCS-79A	GT004	GT0004GAN(LW)	125.71	126.47	GAN(LW)	44.90	87.0	1.9	414.0	3.00	5.0	330.1	208.5	5B
TCS-79B						44.90	81.3	1.8	387.6	3.01	10.0	332.3	209.9	7B
TCS-79C						44.95	93.2	2.1	457.1	3.09	15.0	478.7	301.7	3B
TCS-79D						44.89	93.4	2.1	456.4	3.09	20.0	350.0	221.1	4B
TCS-79E						44.74	91.1	2.0	447.4	3.12	25.0	484.7	308.3	4B
TCS-79F						44.81	90.7	2.0	444.3	3.11	30.0	524.5	332.6	XA
TCS-88A						GT004	GT0004GAB(LW)	167.04	167.66	GAB(LW)	44.94	89.0	2.0	421.4
TCS-88B	44.92	89.1	2.0	420.3	2.98						10.0	481.7	304.0	XA
TCS-88C	44.92	99.0	2.2	459.5	2.93						20.0	523.9	330.6	XA
TCS-88D	44.91	100.7	2.2	473.1	2.97						30.0	483.4	305.2	0B
TCS-92A	GT004	GT0004GAN(LW)	132.72	133.41	GAN(LW)	44.91	101.1	2.3	452.0	2.82	10.0	381.8	241.0	XA
TCS-92B						44.88	100.3	2.2	449.1	2.83	20.0	262.2	165.8	5B
TCS-92C						28.71	59.5	2.1	110.7	2.87	30.0	220.6	340.8	XA

Note: All tests were conducted according to the ISRM's Specification.

TABLE 5 RESULTS OF BASE FRICTION ANGLE TESTS OF ROCKS BASED ON DIRECT SHEAR TESTS ON SAW-CUT ROCK SURFACE



Client: SRK Consulting

Sampling Site: Baobab Resources

14-08-2014

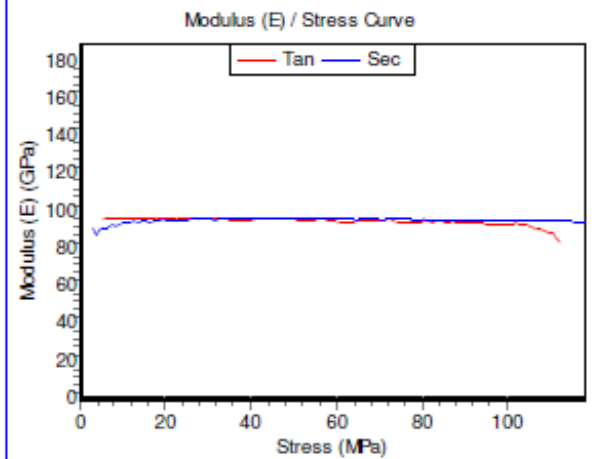
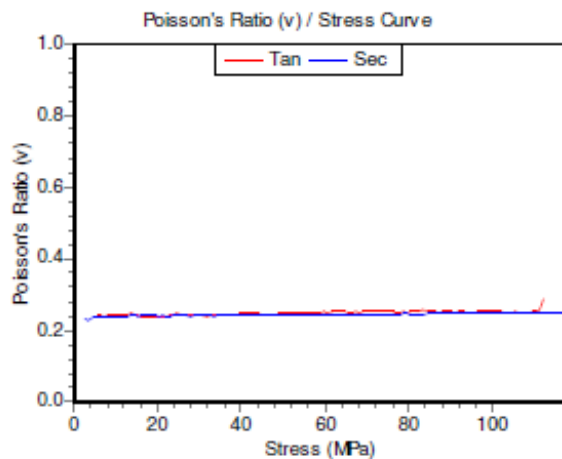
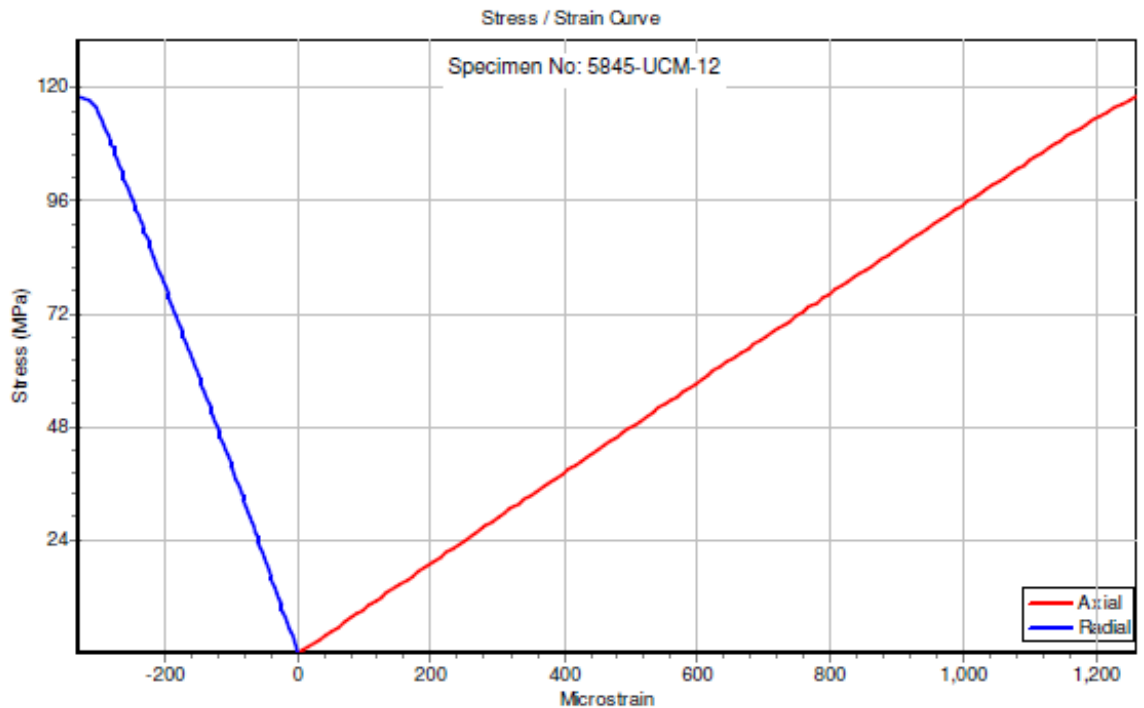
ROCKLAB Specimen No	Borehole No	Sample No	Depth (m)	Rock Type	Shear Area (mm²)	Shear Cycle No	Hor. Force (kN)	Vert. Force (kN)	Dil. Angle (°)	Normal Stress (MPa)	Shear Stress (MPa)	Angle or App. Angle (°)	Base Friction Angle (°)	Note
BFA-37	GT002	GT0002OFX(UW)	156.77 - 157.22	OFX(UW)	1317 1312 1295	1 2 3	0.68 1.26 2.01	1.00 2.00 3.00	-0.4 -1.2 -0.6	0.76 1.50 2.30	0.52 0.99 1.58	34.4 33.4 34.5	34.0	
BFA-63	GT004	GT0004OFX(W)	37.71 - 38.08	OFX(W)	2407 2381 2373	1 2 3	1.06 1.83 2.54	1.00 2.00 3.00	0.8 1.3 0.4	0.42 0.86 1.27	0.43 0.75 1.06	45.8 41.1 39.8	37.0	
BFA-77	GT004	GT0004GAN(UW)	133.60 - 134.14	GAN(UW)	1253 1249 1240	1 2 3	1.04 1.75 2.57	1.00 2.00 3.00	-0.4 0.0 0.1	0.79 1.60 2.42	0.83 1.40 2.07	46.5 41.2 40.5	37.0	

Note: The tests were conducted using ROCKLAB servo-controlled direct rock shear testing equipment. They were conducted according to the ASTM standard D5607-95.

UNIAXIAL COMPRESSION TEST

2014/8/13 7:45:11

WITH ELASTIC MODULUS AND POISSON'S RATIO MEASUREMENTS BY MEANS OF STRAIN GAUGES



Failure Load: 187.9 kN

Peak Strength: 118.2 MPa

Axial Strain at Failure: 1259 microstrain

% Strength	Strength (MPa)	E Tan (GPa)	E Sec (GPa)	ν Tan	ν Sec
10	11.8	96.8	94.6	0.245	0.240
20	23.6	96.9	95.2	0.244	0.241
30	35.5	95.1	95.7	0.244	0.241
40	47.3	96	95.5	0.242	0.242
50	59.1	94.7	95.7	0.251	0.244
60	70.9	95.5	95.5	0.251	0.245
70	82.7	94.6	95.4	0.255	0.245
80	94.6	93.3	95.2	0.249	0.247
90	106	90	95.1	0.248	0.247

ROCKLAB

A division of Sollab
(PTY) LTD
Reg. No. 71/00112/07

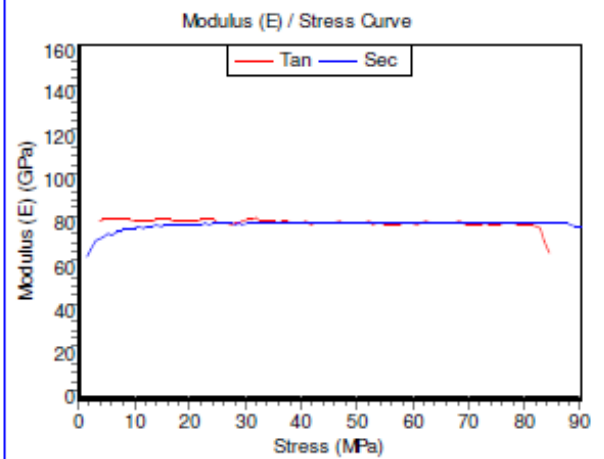
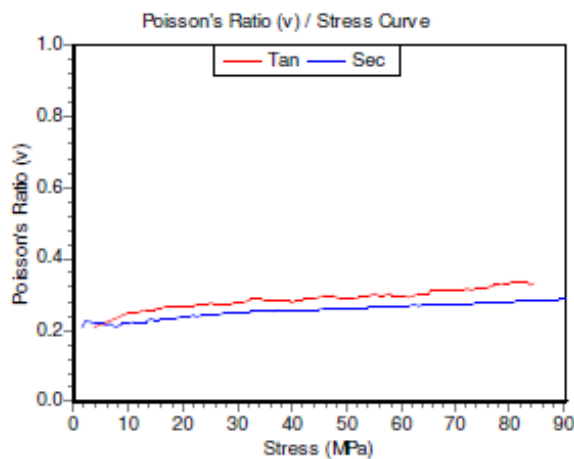
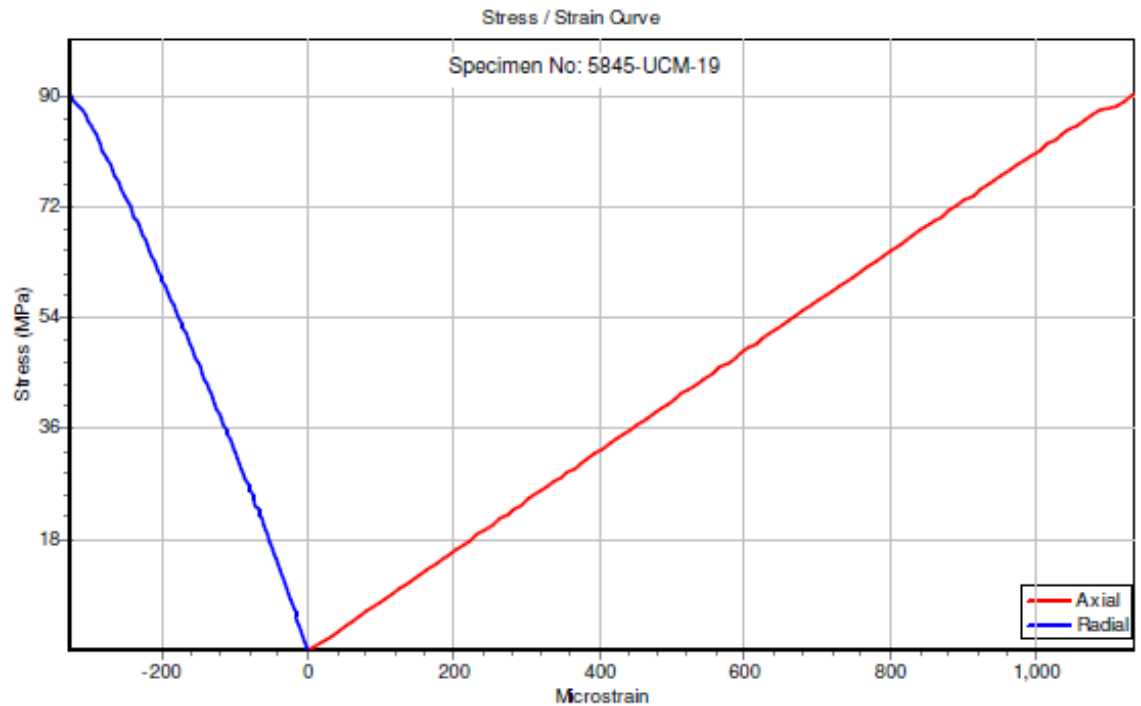
230 Albertus Street
La Montagne
Tel (012) 481-3894
Fax (012) 481-3812

P O Box 72928
Lynnwood Ridge
0040
email: chen@rocklab.co.za

UNIAXIAL COMPRESSION TEST

2014/9/13 7:46:01

WITH ELASTIC MODULUS AND POISSON'S RATIO MEASUREMENTS BY MEANS OF STRAIN GAUGES



Failure Load: 143.9 kN

Peak Strength: 90.21 MPa

Axial Strain at Failure: 1132 microstrain

% Strength	Strength (MPa)	E Tan (GPa)	E Sec (GPa)	ν Tan	ν Sec
10	9.02	82.5	78.8	0.244	0.220
20	18	81.8	80.6	0.267	0.235
30	27.1	80.3	81	0.271	0.247
40	36.1	81.7	81.3	0.281	0.254
50	45.1	81.5	81.3	0.296	0.260
60	54.1	81.4	81.3	0.295	0.265
70	63.1	81	81.2	0.301	0.269
80	72.2	80.5	81.1	0.316	0.274
90	81.2	80	81.1	0.338	0.280

ROCKLAB

A division of Sollab
(PTY) LTD
Reg. No. 71/00112/07

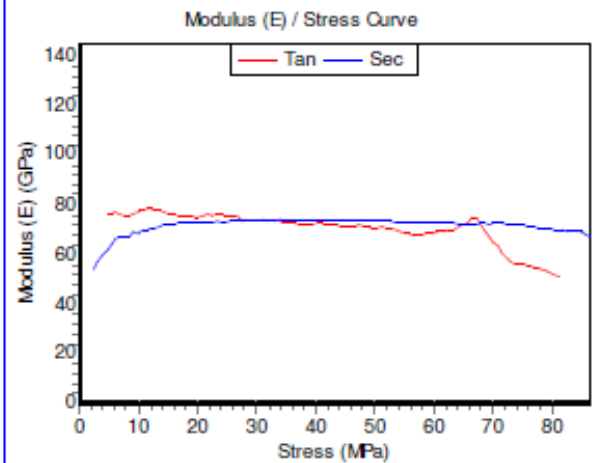
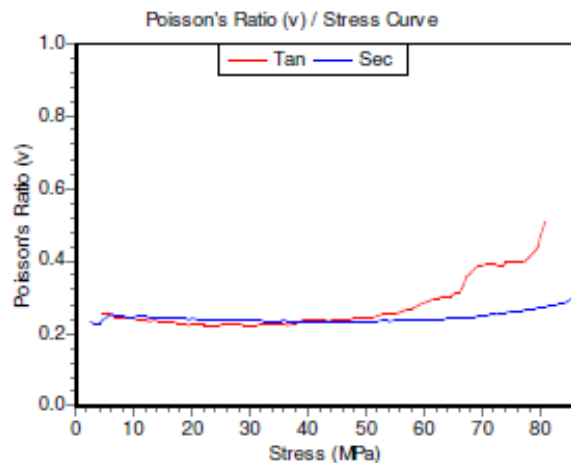
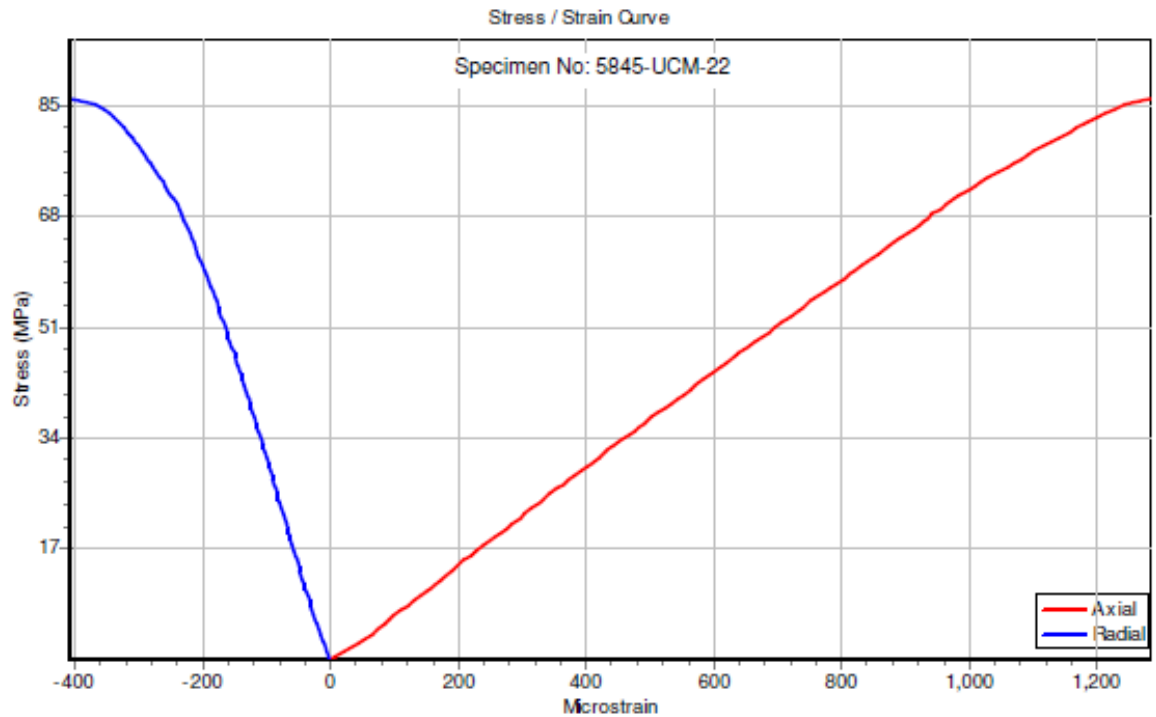
230 Albertus Street
La Montagne
Tel (012) 481-3894
Fax (012) 481-3812

P O Box 72928
Lynnwood Ridge
0040
email: chen@rocklab.co.za

UNIAXIAL COMPRESSION TEST

2014/8/13 7:46:44

WITH ELASTIC MODULUS AND POISSON'S RATIO MEASUREMENTS BY MEANS OF STRAIN GAUGES



Failure Load: 136.2 kN

Peak Strength: 86.22 MPa

Axial Strain at Failure: 1284 microstrain

% Strength	Strength (MPa)	E Tan (GPa)	E Sec (GPa)	ν Tan	ν Sec
10	8.62	76.4	69.2	0.244	0.244
20	17.2	75.7	72.6	0.228	0.243
30	25.9	75.8	73.8	0.229	0.237
40	34.5	73.1	73.7	0.228	0.235
50	43.1	72.4	73.7	0.235	0.234
60	51.7	70.6	73.3	0.249	0.235
70	60.4	69.5	72.7	0.287	0.239
80	69	67.3	72.5	0.384	0.247
90	77.6	54	70.9	0.411	0.267

ROCKLAB

A division of Sollab
(PTY) LTD
Reg. No. 71/00112/07

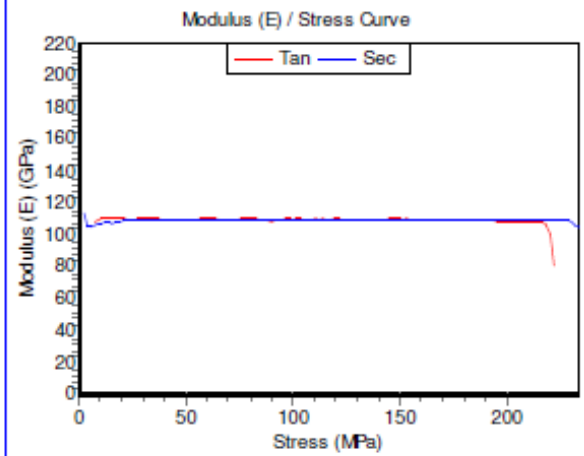
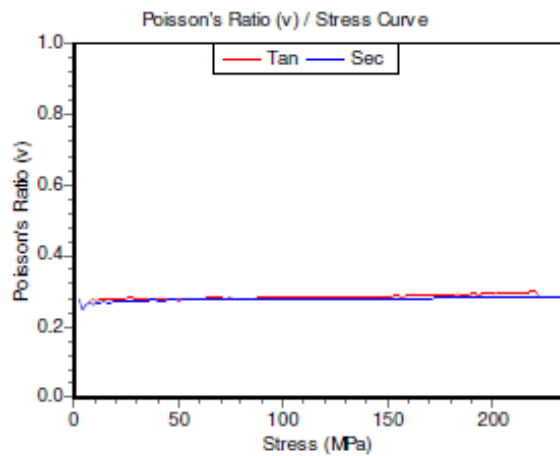
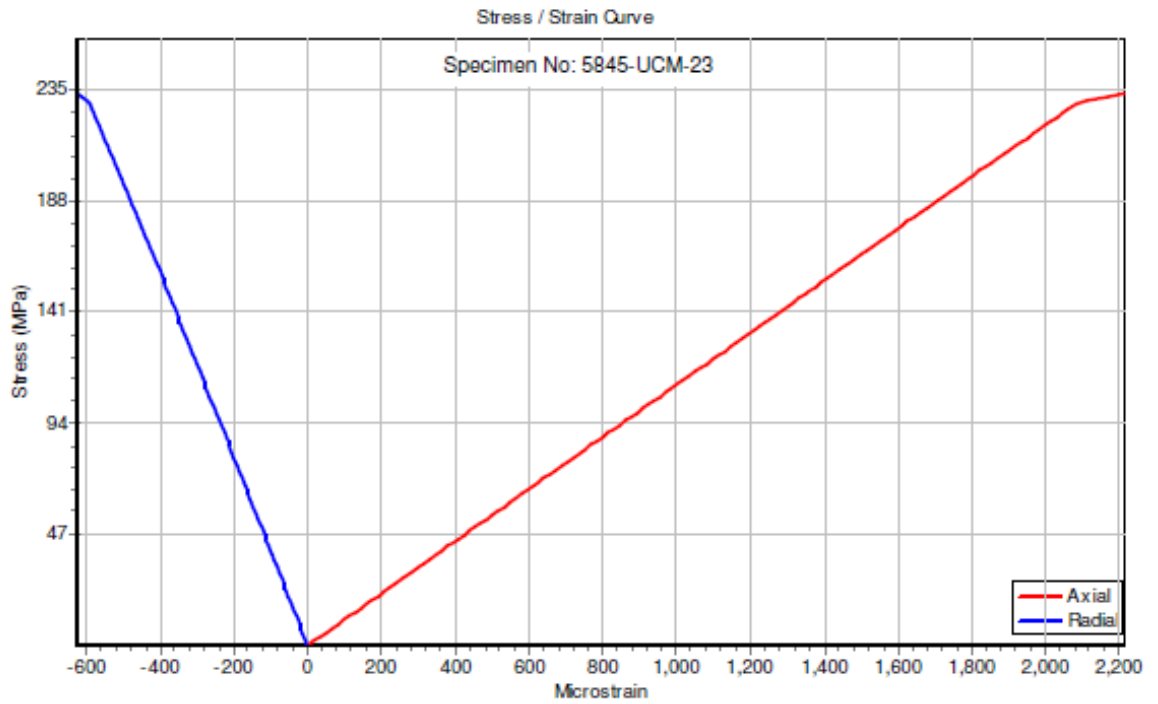
230 Albertus Street
La Montagne
Tel (012) 481-3894
Fax (012) 481-3812

P O Box 72928
Lynnwood Ridge
0040
email: chen@rocklab.co.za

UNIAXIAL COMPRESSION TEST

2014/8/13 7:49:25

WITH ELASTIC MODULUS AND POISSON'S RATIO MEASUREMENTS BY MEANS OF STRAIN GAUGES



Failure Load: 371.3 kN Peak Strength: 233.6 MPa Axial Strain at Failure: 2213 microstrain

% Strength	Strength (MPa)	E Tan (GPa)	E Sec (GPa)	ν Tan	ν Sec
10	23.4	111	110	0.279	0.272
20	46.7	110	110	0.278	0.275
30	70.1	110	110	0.280	0.276
40	93.4	110	110	0.281	0.276
50	117	111	110	0.283	0.278
60	140	110	110	0.283	0.279
70	164	110	110	0.286	0.279
80	187	110	110	0.289	0.280
90	210	109	110	0.296	0.281

ROCKLAB

A division of Sollab
(PTY) LTD

Reg. No. 71/00112/07

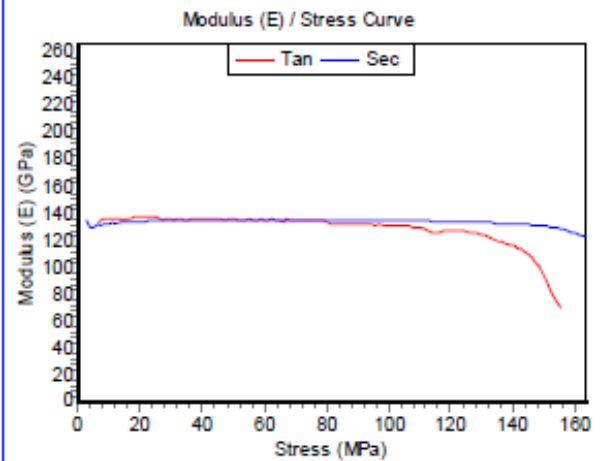
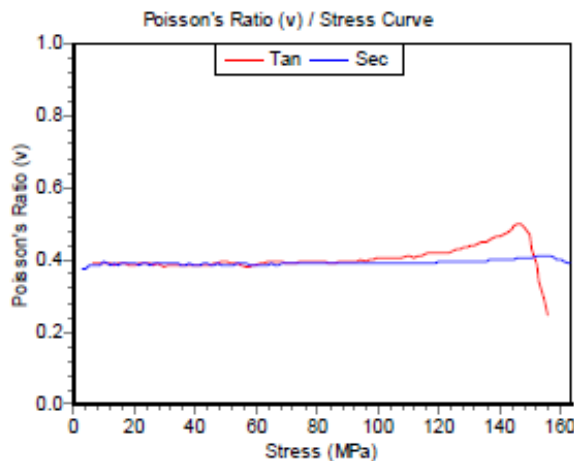
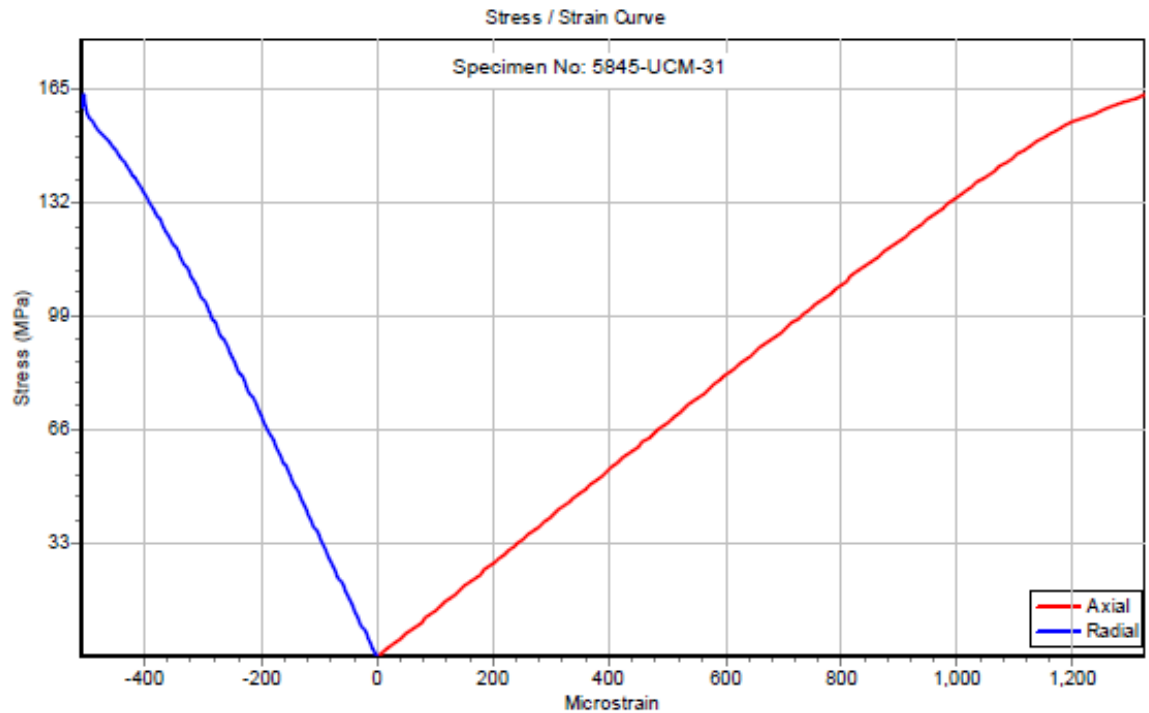
230 Albertus Street
La Montagne
Tel (012) 481-3894
Fax (012) 481-3812

P O Box 72928
Lynnwood Ridge
0040
email: chenj@rocklab.co.za

UNIAXIAL COMPRESSION TEST

8/12/2014 3:36:22 PM

WITH ELASTIC MODULUS AND POISSON'S RATIO MEASUREMENTS BY MEANS OF STRAIN GAUGES



Failure Load: 259.4 kN Peak Strength: 163.3 MPa Axial Strain at Failure: 1322 microstrain

% Strength	Strength (MPa)	E Tan (GPa)	E Sec (GPa)	ν Tan	ν Sec
10	16.3	137	135	0.390	0.392
20	32.7	137	136	0.384	0.389
30	49	136	136	0.394	0.387
40	65.3	135	136	0.394	0.388
50	81.7	133	136	0.395	0.390
60	98	132	135	0.402	0.391
70	114	126	135	0.416	0.393
80	131	123	134	0.443	0.397
90	147	104	132	0.500	0.404

ROCKLAB

A division of Sollab
(PTY) LTD
Reg. No. 71/00112/07

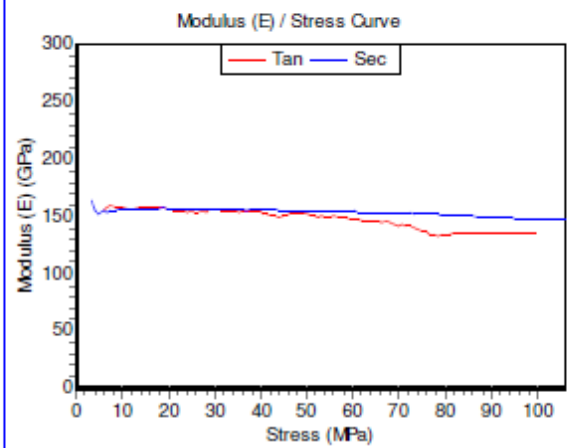
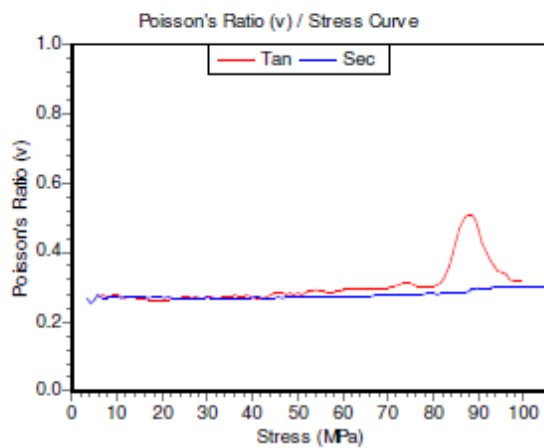
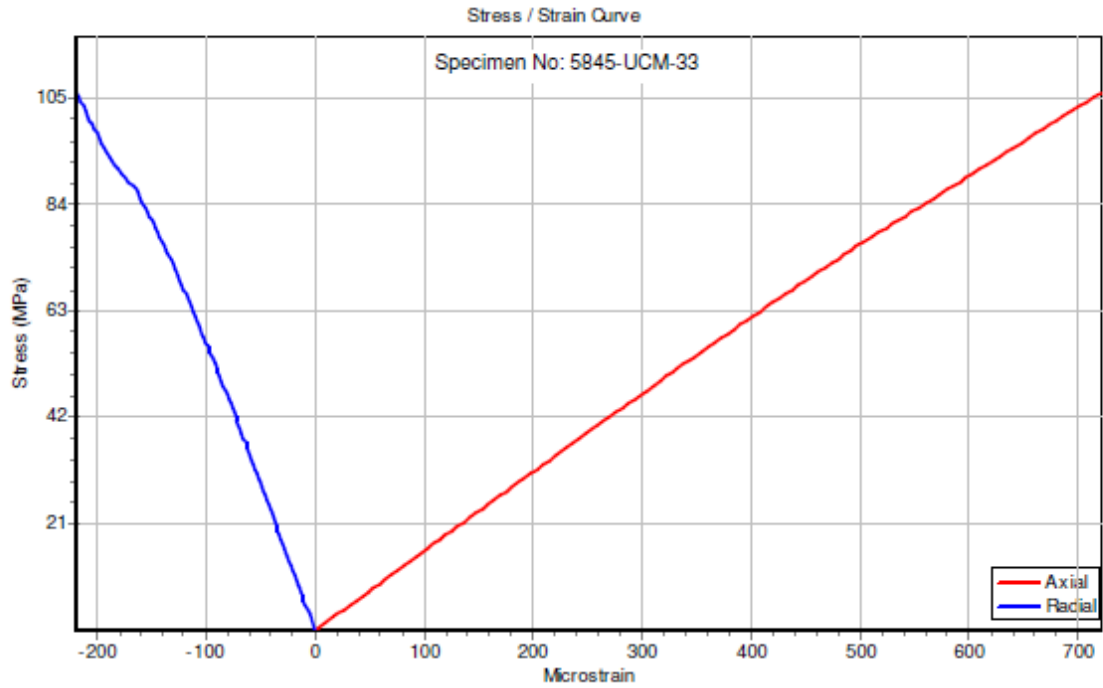
230 Albertus Street
La Montagne
Tel (012) 481-3894
Fax (012) 481-3812

P O Box 72928
Lynnwood Ridge
0040
email: chenj@rocklab.co.za

UNIAXIAL COMPRESSION TEST

2014/8/13 7:52:42

WITH ELASTIC MODULUS AND POISSON'S RATIO MEASUREMENTS BY MEANS OF STRAIN GAUGES



Failure Load: 168.9 kN Peak Strength: 106 MPa Axial Strain at Failure: 721 microstrain

% Strength	Strength (MPa)	E Tan (GPa)	E Sec (GPa)	ν Tan	ν Sec
10	10.6	157	156	0.273	0.267
20	21.2	155	157	0.264	0.271
30	31.8	155	157	0.266	0.269
40	42.4	150	156	0.270	0.269
50	53	150	155	0.289	0.271
60	63.6	147	154	0.294	0.274
70	74.2	138	152	0.314	0.278
80	84.8	136	150	0.434	0.282
90	95.4	136	148	0.335	0.302

ROCKLAB

A division of Sollab
(PTY) LTD

Reg. No. 71/00112/07

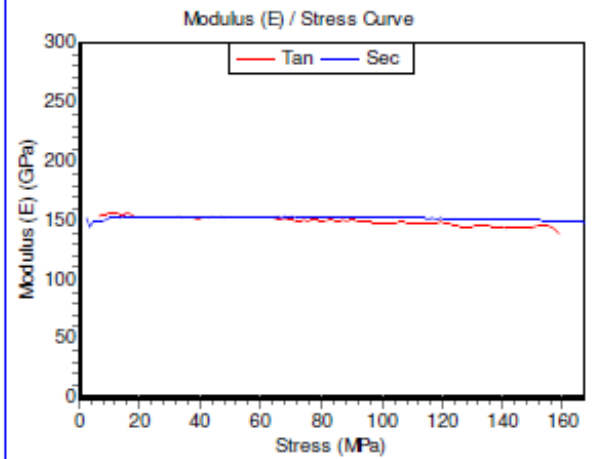
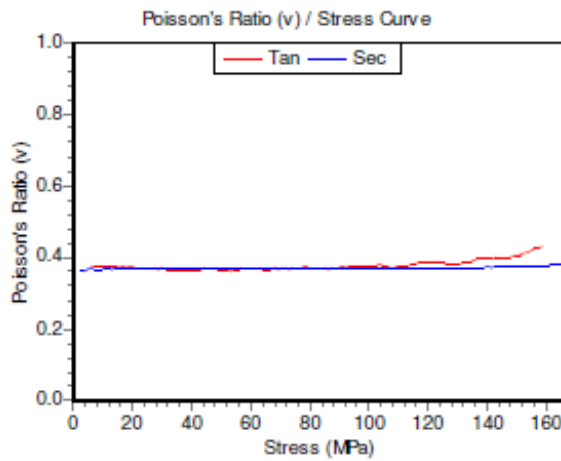
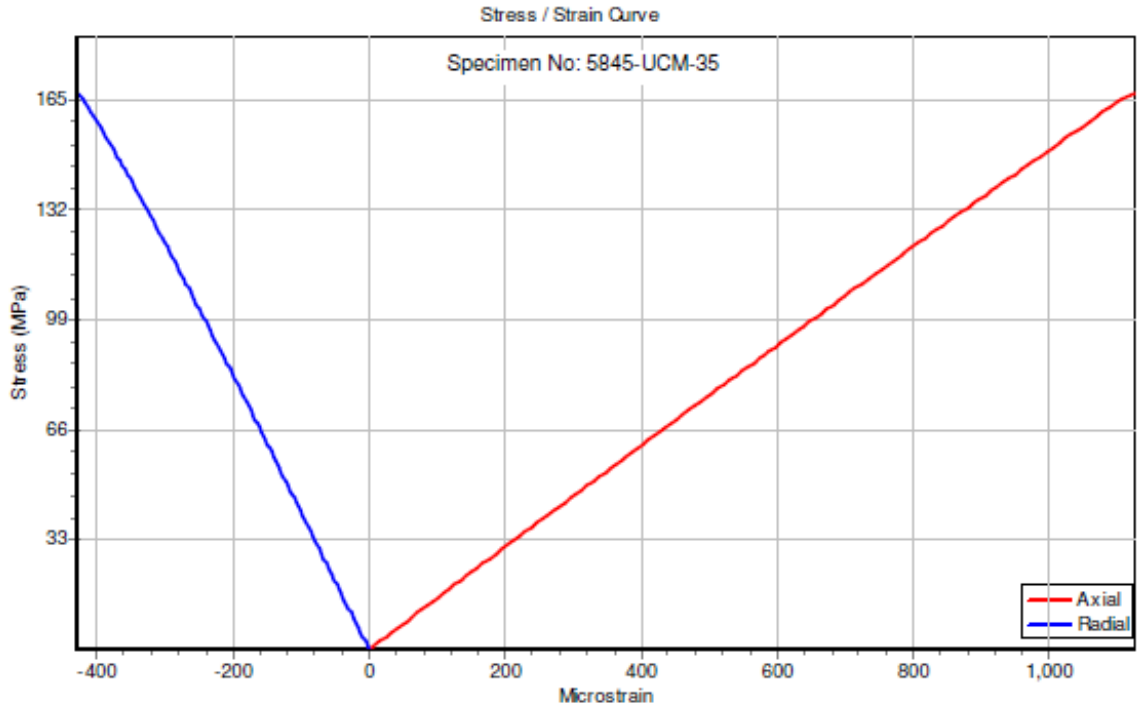
230 Albertus Street
La Montagne
Tel (012) 481-3894
Fax (012) 481-3812

P O Box 72928
Lynnwood Ridge
0040
email: chen@rocklab.co.za

UNIAXIAL COMPRESSION TEST

2014/8/13 7:50:10

WITH ELASTIC MODULUS AND POISSON'S RATIO MEASUREMENTS BY MEANS OF STRAIN GAUGES



Failure Load: 264.7 kN Peak Strength: 167 MPa Axial Strain at Failure: 1124 microstrain

% Strength	Strength (MPa)	E Tan (GPa)	E Sec (GPa)	ν Tan	ν Sec
10	16.7	155	154	0.374	0.370
20	33.4	153	154	0.367	0.371
30	50.1	152	153	0.367	0.370
40	66.8	152	153	0.369	0.370
50	83.5	150	152	0.369	0.370
60	100	148	152	0.377	0.370
70	117	148	151	0.388	0.371
80	134	146	151	0.386	0.372
90	150	145	150	0.406	0.375

ROCKLAB

A division of Soillab
(PTY) LTD
Reg. No. 71/00112/07

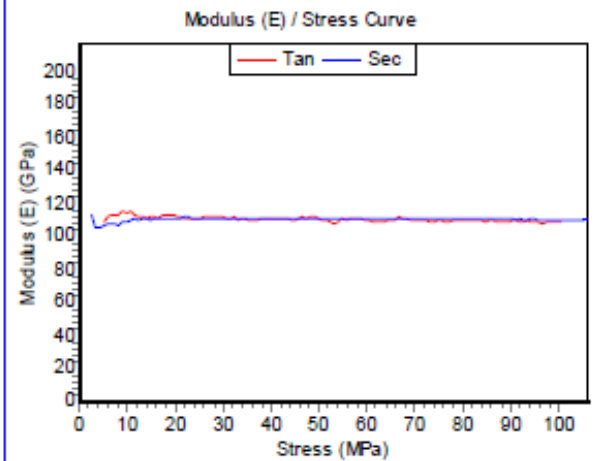
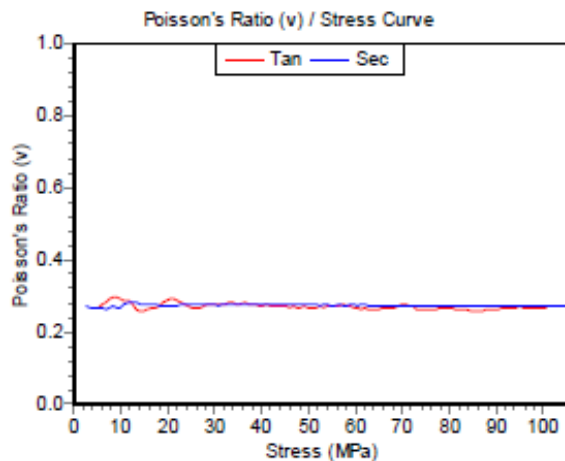
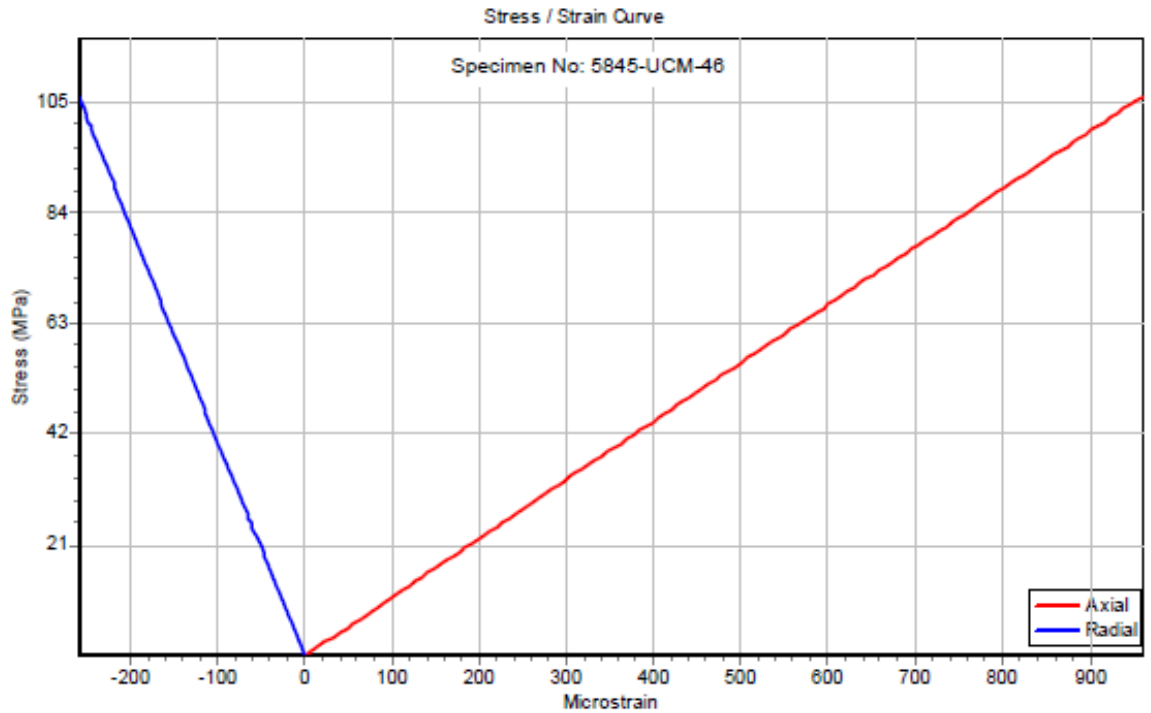
230 Albertus Street
La Montagne
Tel (012) 481-3894
Fax (012) 481-3812

P O Box 72928
Lynnwood Ridge
0040
email: chenj@rocklab.co.za

UNIAXIAL COMPRESSION TEST

8/12/2014 3:40:56 PM

WITH ELASTIC MODULUS AND POISSON'S RATIO MEASUREMENTS BY MEANS OF STRAIN GAUGES



Failure Load: 167.8 kN Peak Strength: 106 MPa Axial Strain at Failure: 960 microstrain

% Strength	Strength (MPa)	E Tan (GPa)	E Sec (GPa)	ν Tan	ν Sec
10	10.6	115	110	0.289	0.275
20	21.2	111	112	0.289	0.274
30	31.8	112	111	0.278	0.276
40	42.4	111	112	0.271	0.276
50	53	108	112	0.268	0.275
60	63.6	110	111	0.264	0.274
70	74.2	110	111	0.264	0.273
80	84.8	110	111	0.259	0.272
90	95.4	109	111	0.267	0.271

ROCKLAB

A division of Soillab
(PTY) LTD
Reg. No. 71/00112/07

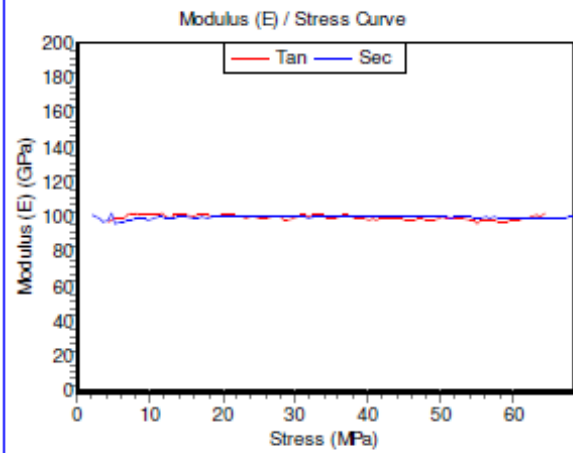
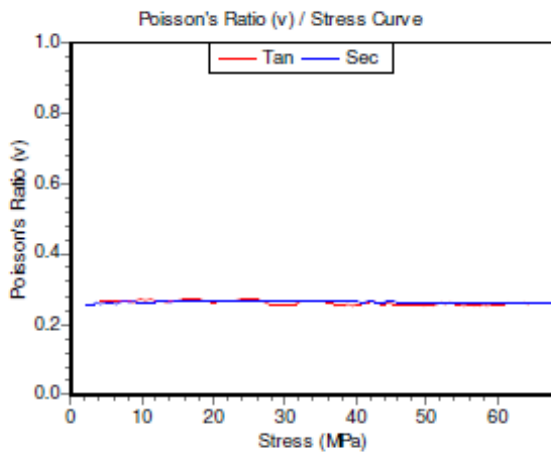
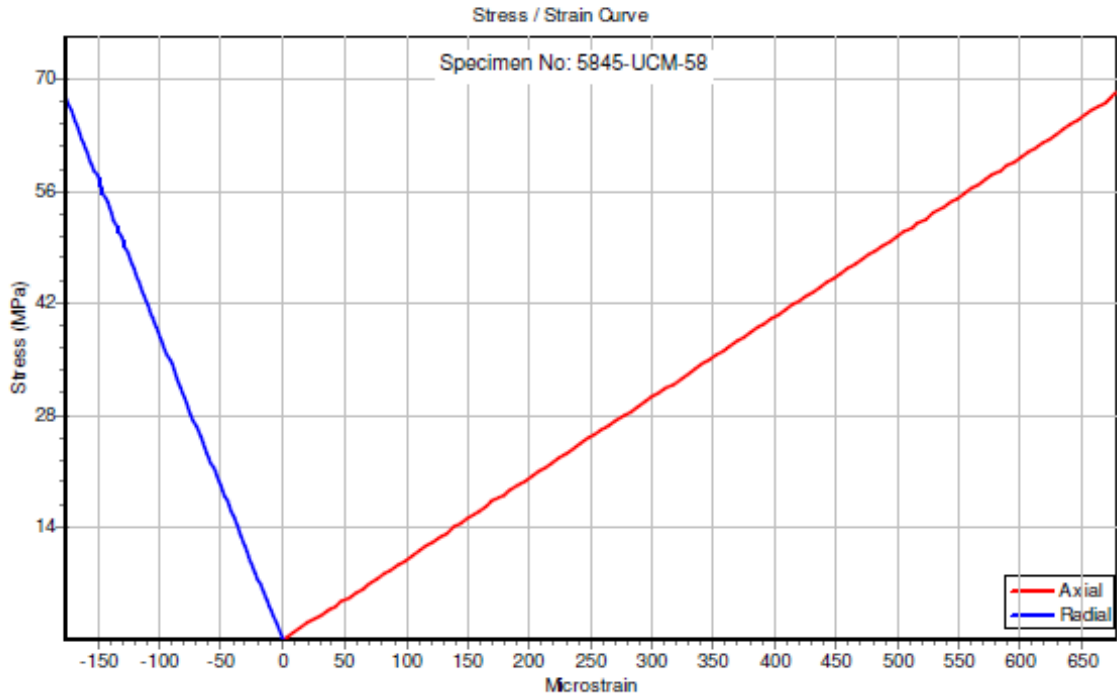
230 Albertus Street
La Montagne
Tel (012) 481-3894
Fax (012) 481-3812

P O Box 72926
Lynnwood Ridge
0040
email: chenj@rocklab.co.za

UNIAXIAL COMPRESSION TEST

2014/8/13 7:50:42

WITH ELASTIC MODULUS AND POISSON'S RATIO MEASUREMENTS BY MEANS OF STRAIN GAUGES



Failure Load: 108.2 kN Peak Strength: 68.23 MPa Axial Strain at Failure: 677 microstrain

% Strength	Strength (MPa)	E Tan (GPa)	E Sec (GPa)	ν Tan	ν Sec
10	6.82	102	99.3	0.268	0.264
20	13.6	102	101	0.265	0.264
30	20.5	102	101	0.266	0.266
40	27.3	101	101	0.263	0.267
50	34.1	100	101	0.268	0.265
60	40.9	99.4	101	0.262	0.264
70	47.8	98.5	101	0.256	0.264
80	54.6	97.5	101	0.254	0.263
90	61.4	99.7	100	0.262	0.262

ROCKLAB

A division of Sollab
(PTY) LTD
Reg. No. 71/00112/07

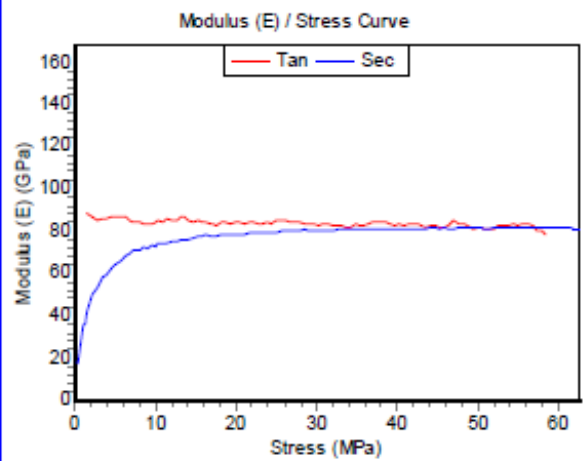
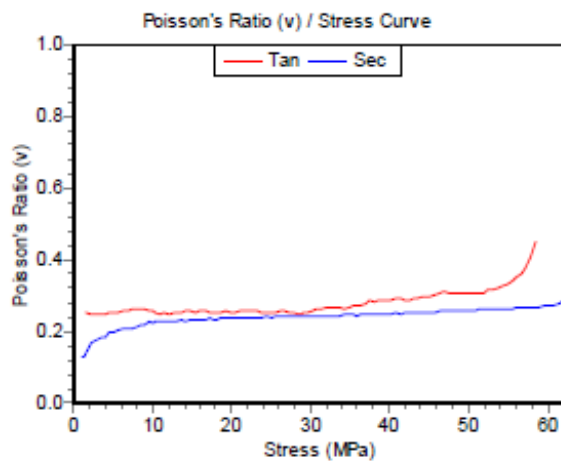
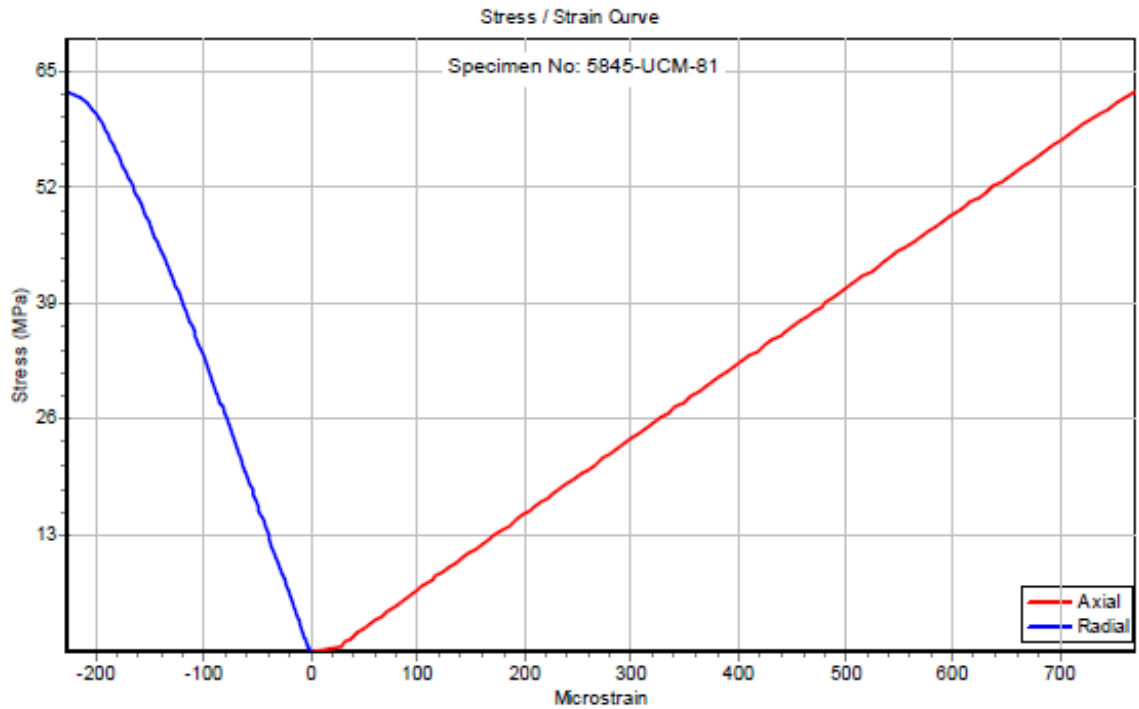
230 Albertus Street
La Montagne
Tel (012) 481-3894
Fax (012) 481-3812

P O Box 72928
Lynnwood Ridge
0040
email: chen@rocklab.co.za

UNIAXIAL COMPRESSION TEST

8/12/2014 3:43:52 PM

WITH ELASTIC MODULUS AND POISSON'S RATIO MEASUREMENTS BY MEANS OF STRAIN GAUGES



Failure Load: 99 kN

Peak Strength: 62.55 MPa

Axial Strain at Failure: 769 microstrain

% Strength	Strength (MPa)	E Tan (GPa)	E Sec (GPa)	ν Tan	ν Sec
10	6.25	86.8	68.5	0.259	0.209
20	12.5	85.4	75.4	0.252	0.228
30	18.8	83.8	78.8	0.255	0.238
40	25	85.1	79.7	0.254	0.240
50	31.3	83.8	80.6	0.264	0.243
60	37.5	84	81	0.285	0.247
70	43.8	82.8	81.5	0.297	0.253
80	50	82.1	81.9	0.308	0.259
90	56.3	82.7	81.8	0.362	0.265

ROCKLAB

A division of Sollab
(PTY) LTD

Reg. No. 71/00112/07

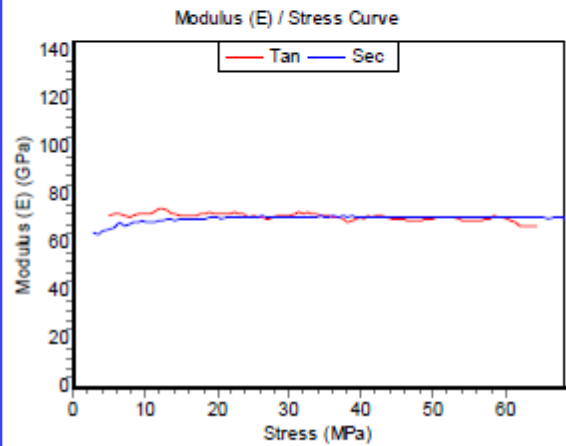
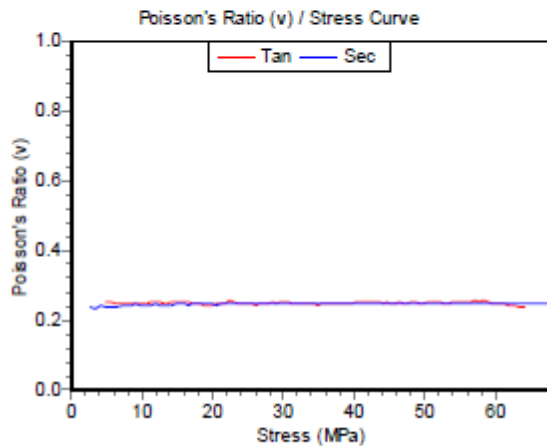
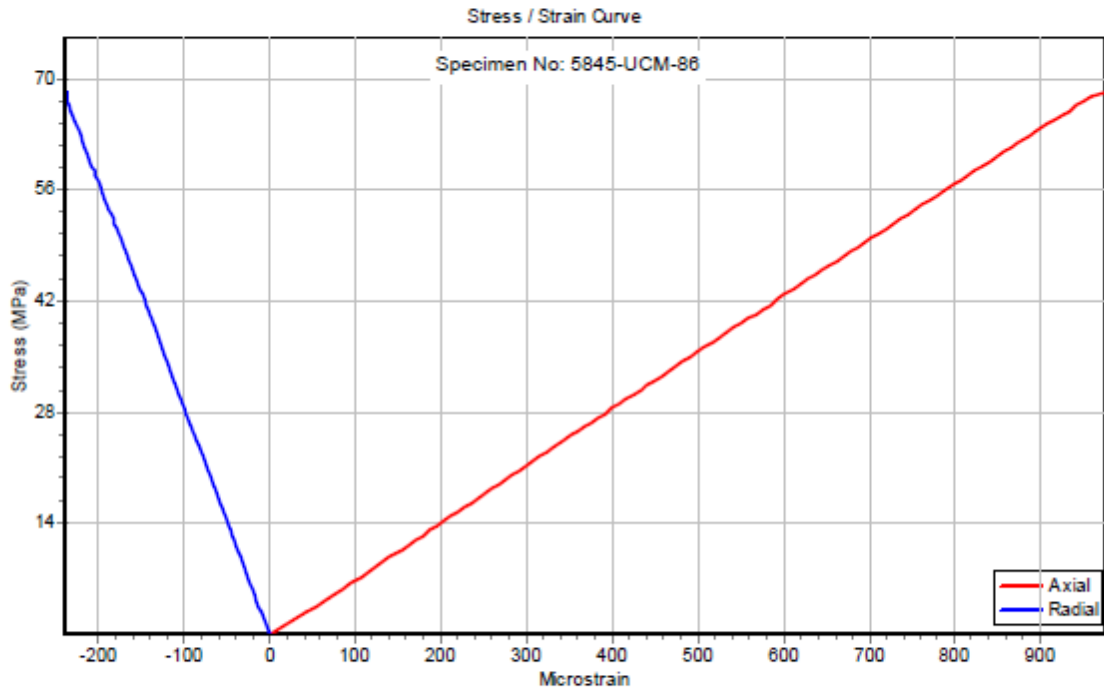
230 Albertus Street
La Montagne
Tel (012) 461-3894
Fax (012) 461-3812

P O Box 72928
Lynnwood Ridge
0040
email: chenj@rocklab.co.za

UNIAXIAL COMPRESSION TEST

8/12/2014 3:44:11 PM

WITH ELASTIC MODULUS AND POISSON'S RATIO MEASUREMENTS BY MEANS OF STRAIN GAUGES



Failure Load: 107.8 kN Peak Strength: 68.15 MPa Axial Strain at Failure: 974 microstrain

% Strength	Strength (MPa)	E Tan (GPa)	E Sec (GPa)	ν Tan	ν Sec
10	6.82	71.8	67.5	0.250	0.245
20	13.6	72.5	70.1	0.249	0.245
30	20.4	72.2	70.5	0.247	0.245
40	27.3	70.3	71	0.249	0.247
50	34.1	71.8	71.4	0.247	0.247
60	40.9	71.3	71.1	0.251	0.248
70	47.7	69.6	71.1	0.252	0.248
80	54.5	69.8	71	0.251	0.249
90	61.3	68.9	70.9	0.247	0.249

ROCKLAB

A division of Sollab
(PTY) LTD
Reg. No. 71/00112/07

230 Albertus Street
La Montagne
Tel (012) 481-3894
Fax (012) 481-3812

P O Box 72928
Lynnwood Ridge
0040
email: chenj@rocklab.co.za

APPENDIX 2

**GRAPHS OF BASIC FRICTION ANGLE TESTS BASED
ON DIRECT SHAER TESTS ON ROCK SAW-CUTTING SURFACE
USING ROCKLAB'S SERVO-CONTROLLED
COMPUTERIZED DIRECT SHEAR TESTER**

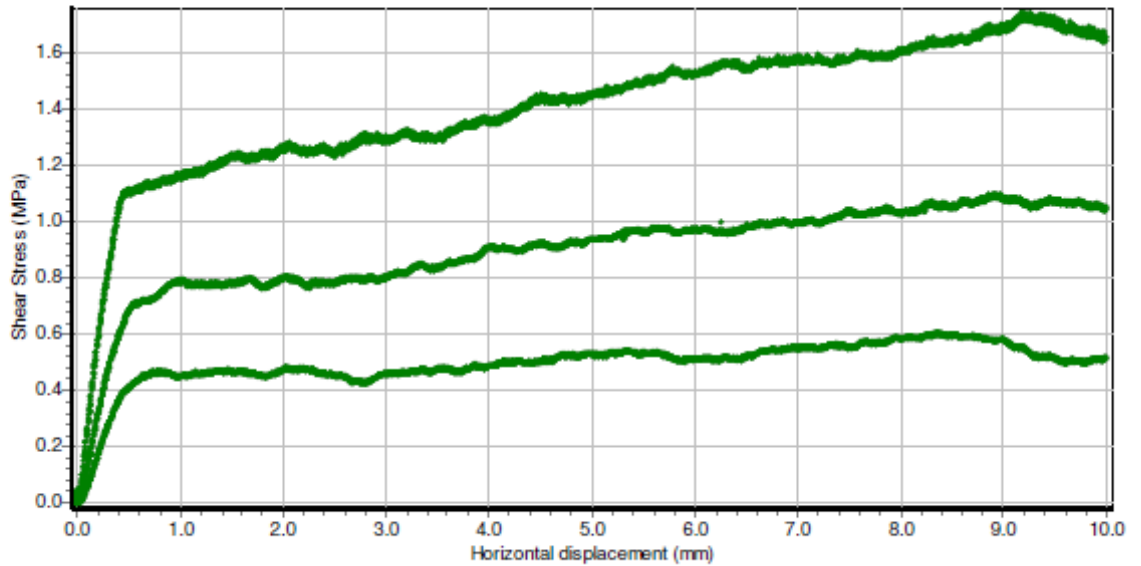
GCTS SHEAR TEST

2014/8/8 9:07:44

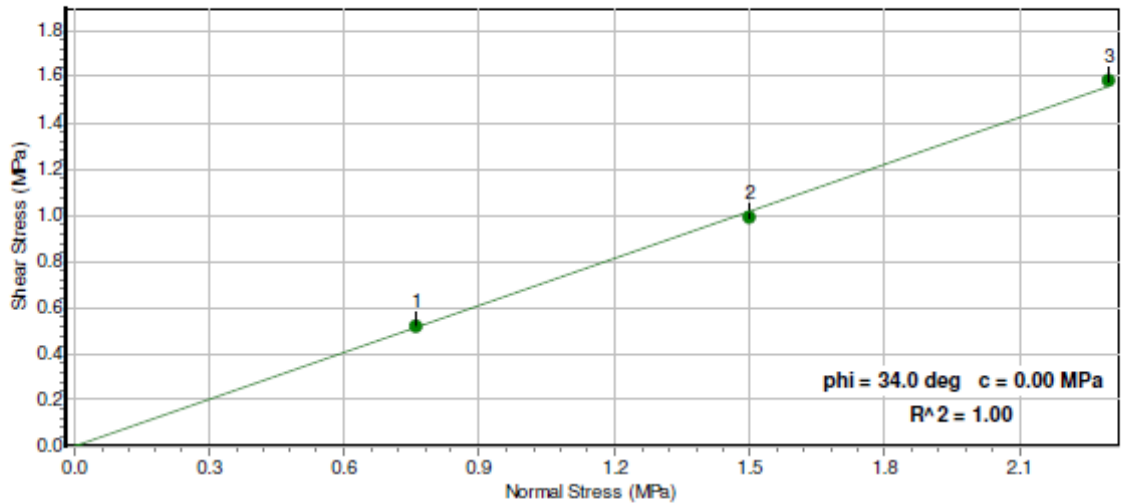
ON AN A SAW CUT JOINT - BASIC FRICTION

5845-bfa-37-a, 5845-bfa-37-b, 5845-bfa-37-c

Stress vs Displacement Curve



Shear Stress / Normal Stress



Selected Points

No	Horiz. Displ. (mm)	Vertical Load (kN)	Horizontal Load (kN)	Dilatancy Angle (deg)	Contact Area (mm ²)	Normal Stress (MPa)	Shear Stress (MPa)	App. Friction Angle (deg)
1	6.14	1.00	0.68	-0.4	1317	0.76	0.52	34.4
2	6.26	2.00	1.26	-1.2	1312	1.50	0.99	33.4
3	6.63	3.00	2.01	-0.6	1295	2.30	1.58	34.5

ROCKLAB

A division of Sollab
(PTY) LTD
Reg. No. 71/00112/07

230 Albertus Street
La Montagne
Tel (012) 481-3894
Fax (012) 481-3812

P O Box 72928
Lynnwood Ridge
0040
email: chenj@rocklab.co.za

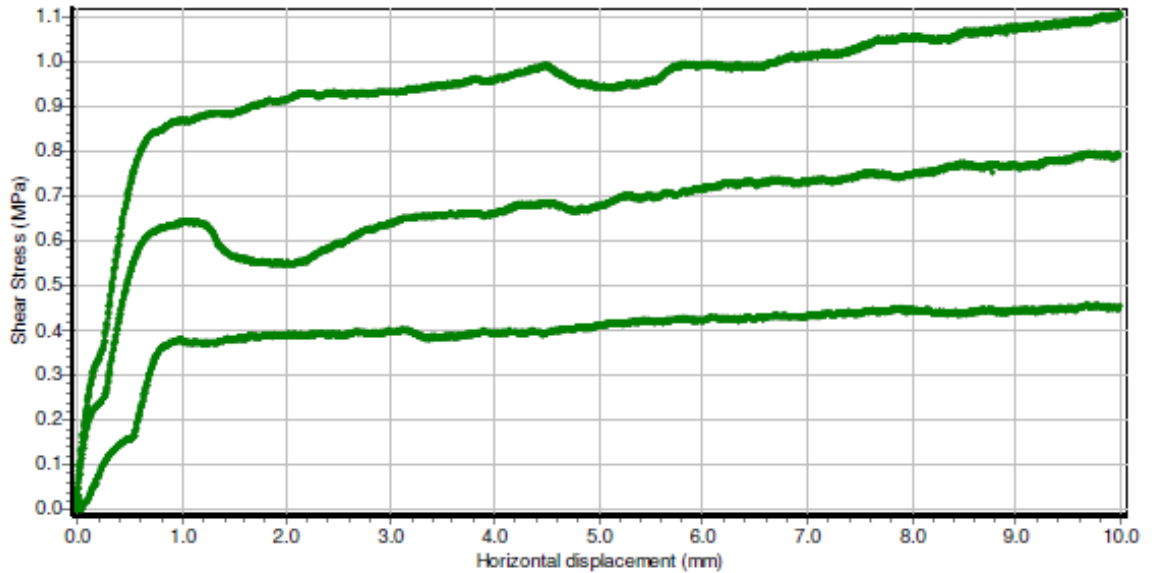
GCTS SHEAR TEST

2014/8/8 9:11:18

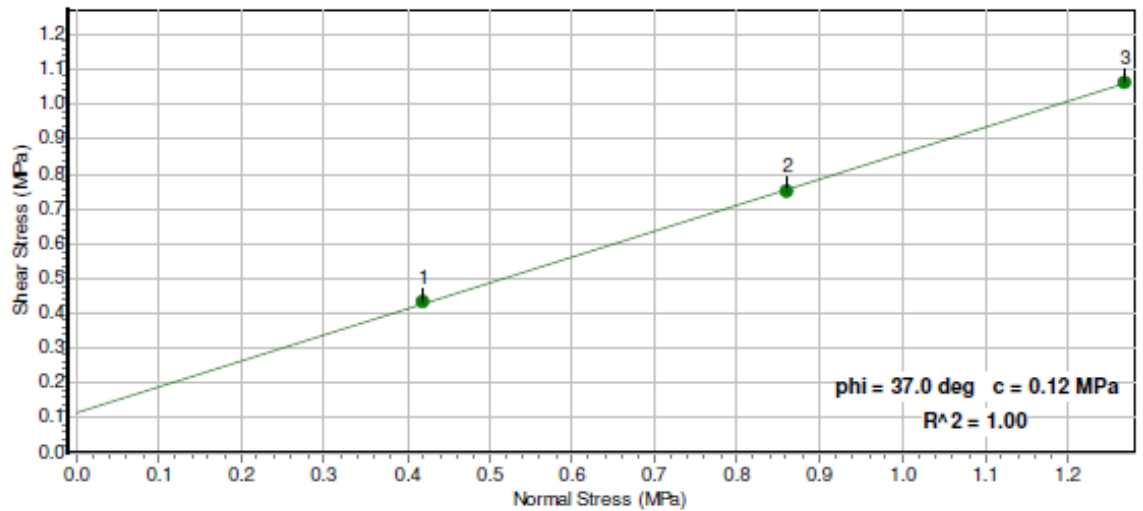
ON AN A SAW CUT JOINT - BASIC FRICTION

5845-bfa-63-a, 5845-bfa-63-b, 5845-bfa-63-c

Stress vs Displacement Curve



Shear Stress / Normal Stress



Selected Points

No	Horiz. Displ. (mm)	Vertical Load (kN)	Horizontal Load (kN)	Dilatancy Angle (deg)	Contact Area (mm ²)	Normal Stress (MPa)	Shear Stress (MPa)	App. Friction Angle (deg)
1	8.35	1.00	1.06	0.8	2407	0.42	0.43	45.8
2	8.78	2.00	1.83	1.3	2381	0.86	0.75	41.1
3	8.91	3.00	2.54	0.4	2373	1.27	1.06	39.8

ROCKLAB

A division of Sollab
(PTY) LTD
Reg. No. 71/00112/07

230 Albertus Street
La Montagne
Tel (012) 481-3894
Fax (012) 481-3812

P O Box 72928
Lynnwood Ridge
0040
email: chen@rocklab.co.za

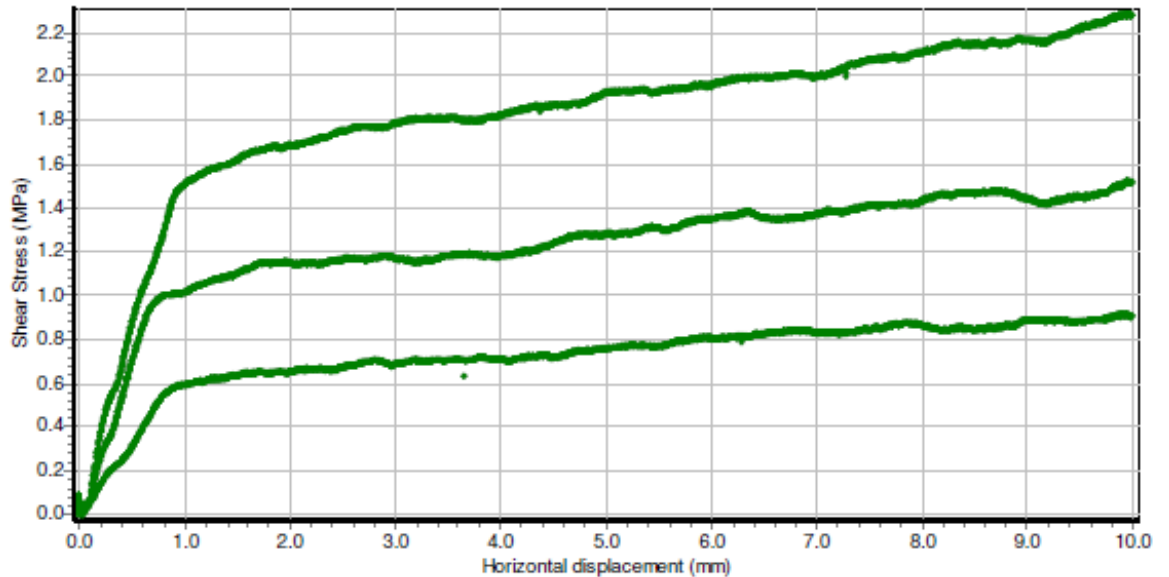
GCTS SHEAR TEST

2014/8/14 16:00:31

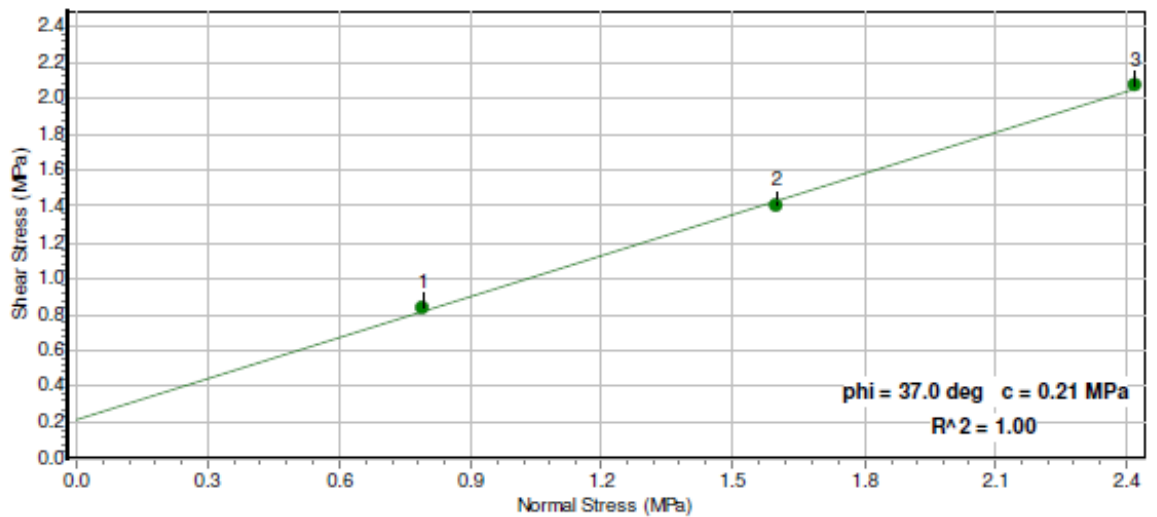
ON AN A SAW CUT JOINT - BASIC FRICTION

5845-bfa-77b-a, 5845-bfa-77b-b, 5845-bfa-77b-c

Stress vs Displacement Curve



Shear Stress / Normal Stress



Selected Points

No	Horiz. Displ. (mm)	Vertical Load (kN)	Horizontal Load (kN)	Dilatancy Angle (deg)	Contact Area (mm ²)	Normal Stress (MPa)	Shear Stress (MPa)	App. Friction Angle (deg)
1	7.33	1.00	1.04	-0.4	1253	0.79	0.83	46.5
2	7.43	2.00	1.75	0.0	1249	1.60	1.40	41.2
3	7.64	3.00	2.57	0.1	1240	2.42	2.07	40.5

ROCKLAB

A division of Soilab
(PTY) LTD
Reg. No. 71/00112/07

230 Albertus Street
La Montagne
Tel (012) 481-3894
Fax (012) 481-3812

P O Box 72928
Lynnwood Ridge
0040
email: chenj@rocklab.co.za

APPENDIX 3

CLASSIFICATION OF ROCK SPECIMEN FAILURE MODE INFLUENCED / NOT INFLUENCED BY DISCONTINUITIES DURING COMPRESSION TESTING

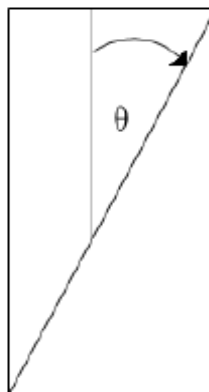
FAILURE NOT INFLUENCED BY DISCONTINUITIES (INTACT)

TYPE CODE	DESCRIPTION OF SUB CODES	
	A	B
X	SLIDING SHEAR FAILURE	COMPLETE CONE DEVELOPMENT
Y	SPLITTING	BREAKING INTO A LOT OF PIECES

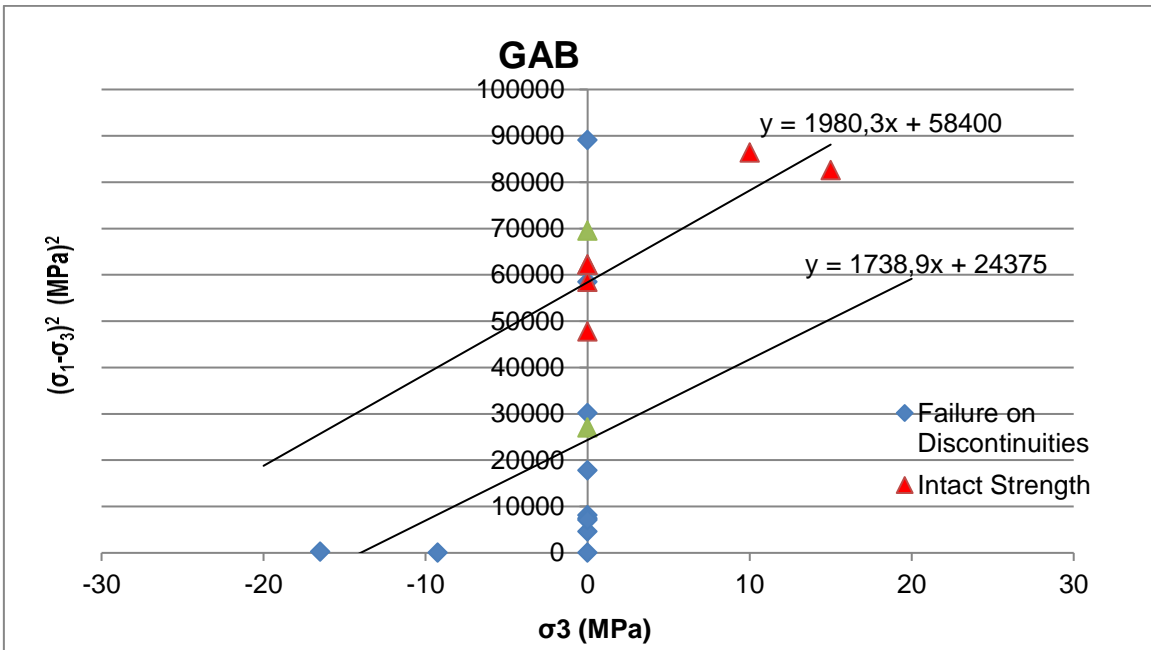
FAILURE INFLUENCED BY DISCONTINUITIES

TYPE CODE	DESCRIPTION OF SUB CODES	
	A	B
	PARTIAL FAILURE ON DISCONTINUITY	FAILURE COMPLETELY ON DISCONTINUITY
1	AT 0-10° TO AXIS	AT 0-10° TO AXIS
2	AT 11-20° TO AXIS	AT 11-20° TO AXIS
3	AT 21-30° TO AXIS	AT 21-30° TO AXIS
4	AT 31-40° TO AXIS	AT 31-40° TO AXIS
5	AT 41-50° TO AXIS	AT 41-50° TO AXIS
6	AT 51-70° TO AXIS	AT 51-70° TO AXIS
7	AT 71-90° TO AXIS	AT 71-90° TO AXIS
0	Multiple Discontinuities	Multiple Discontinuities

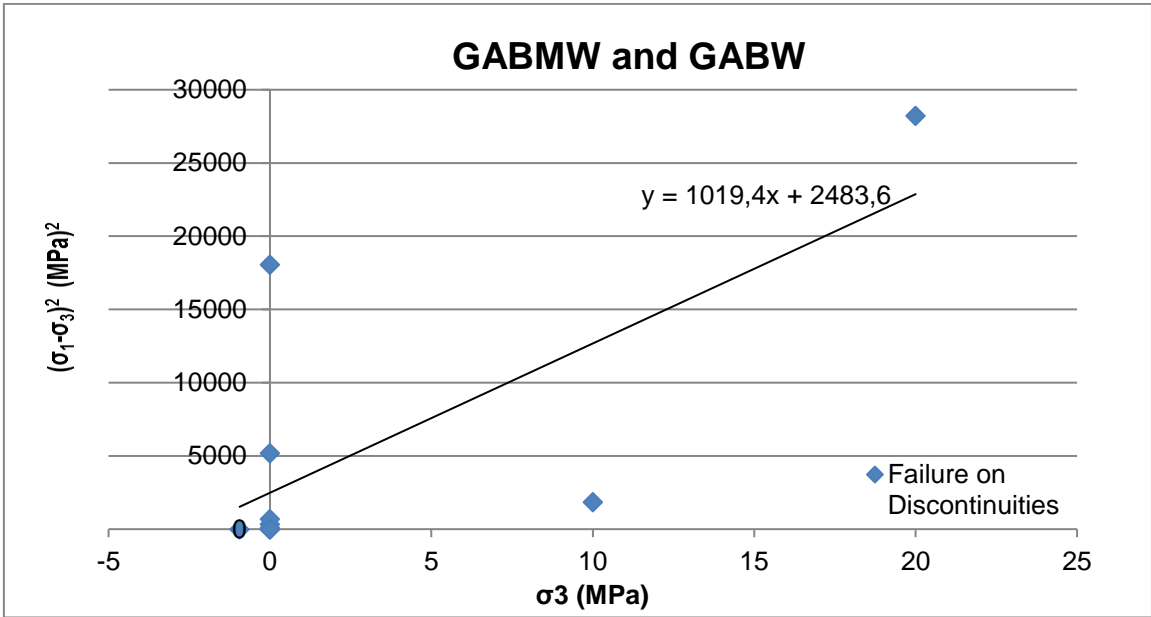
Example: Failure Type3B: Failure completely on a discontinuity with an orientation of between 21° and 30° to the specimen axis.



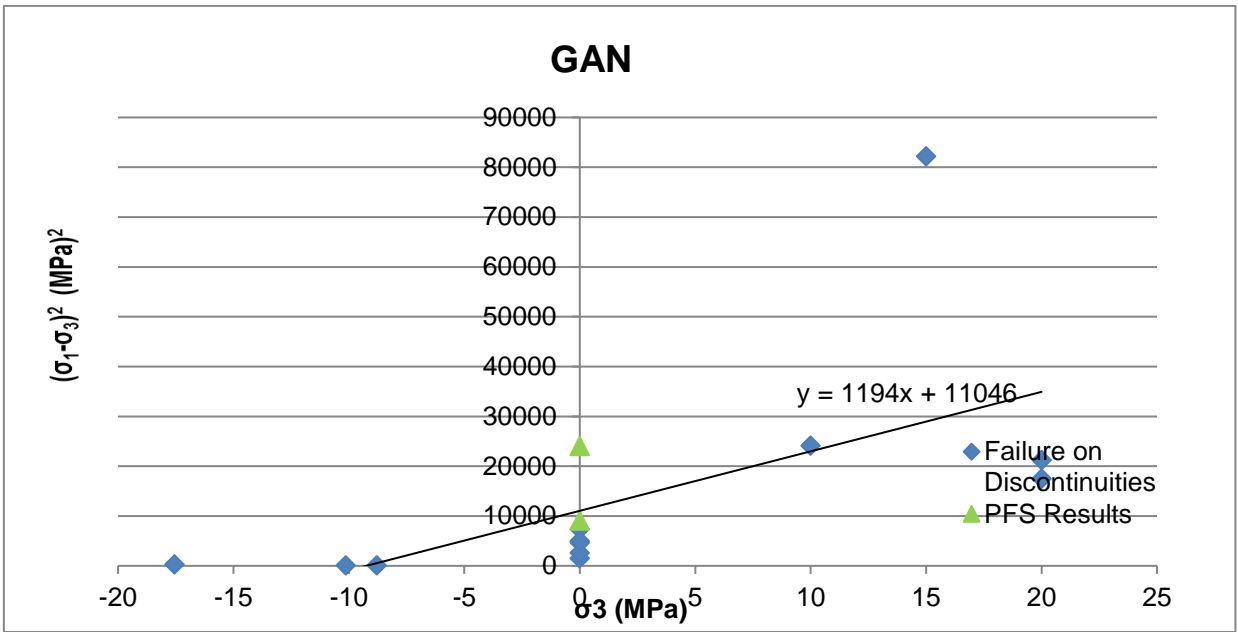
Appendix C: Hoek Brown Plots



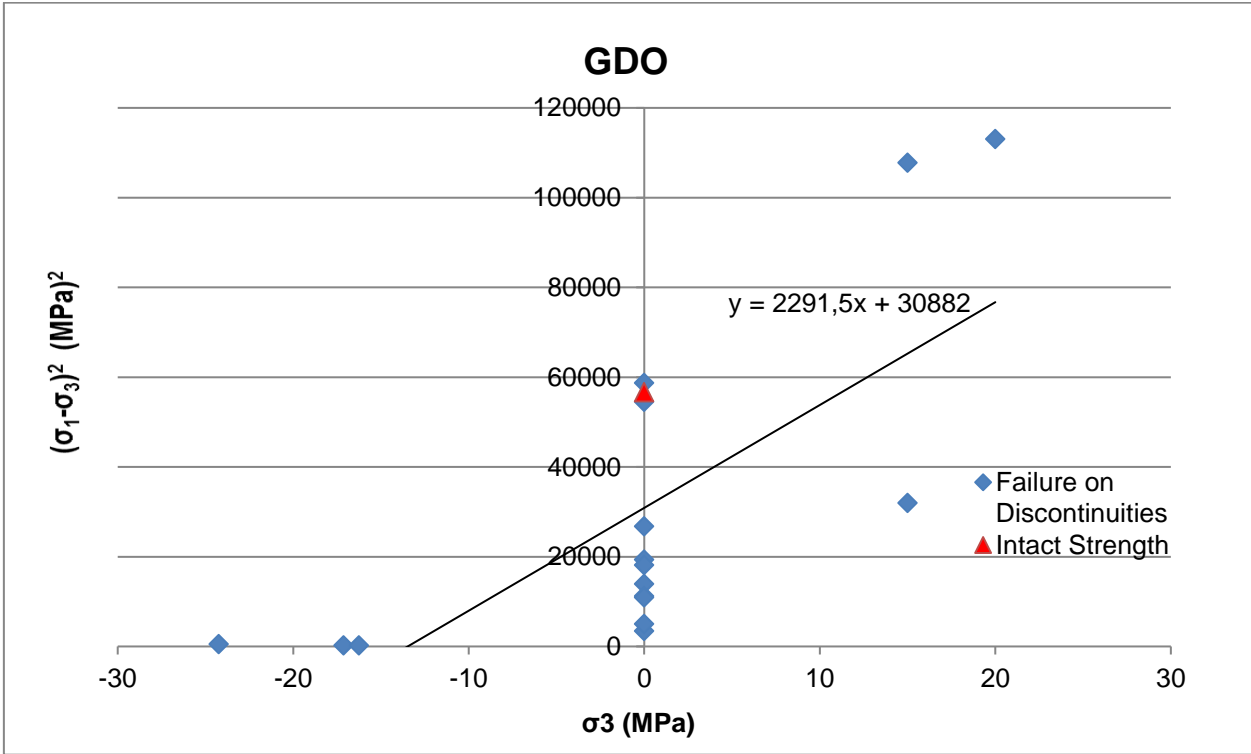
Graph showing the rock strengths results based on laboratory tests for GABUW



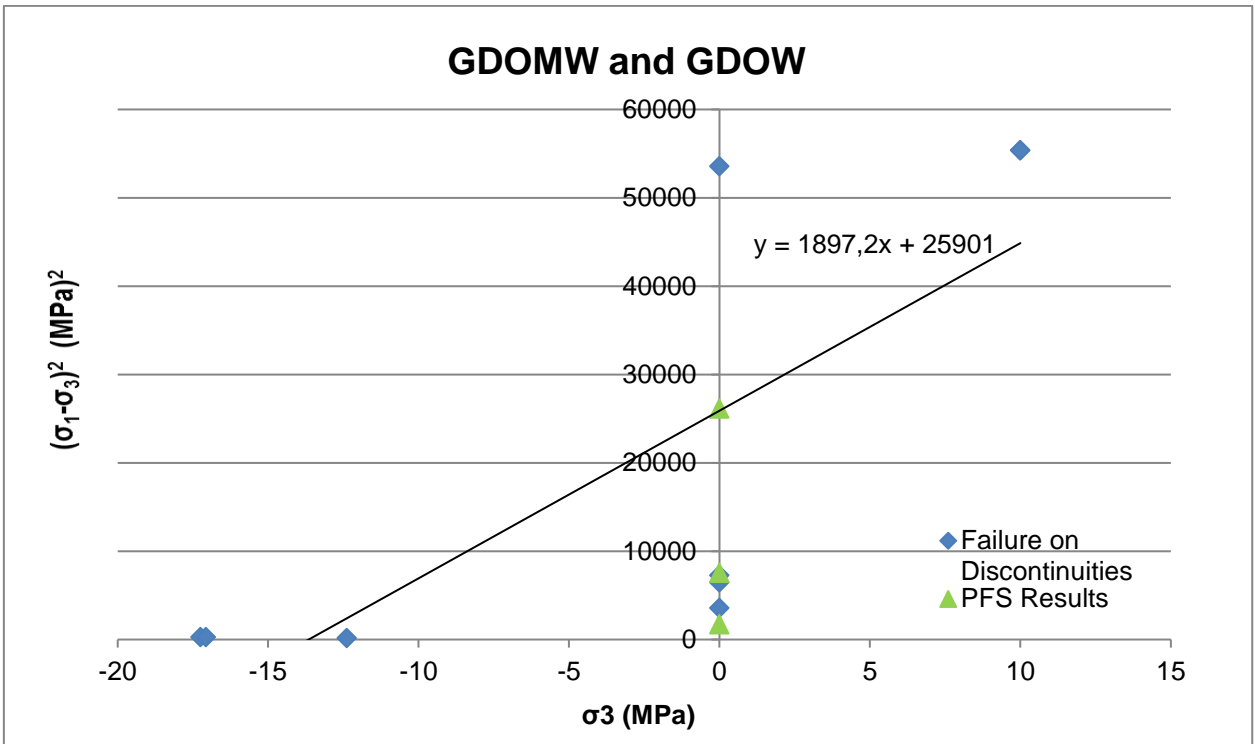
Graph showing the rock strengths results based on laboratory tests for GABMW and GABW



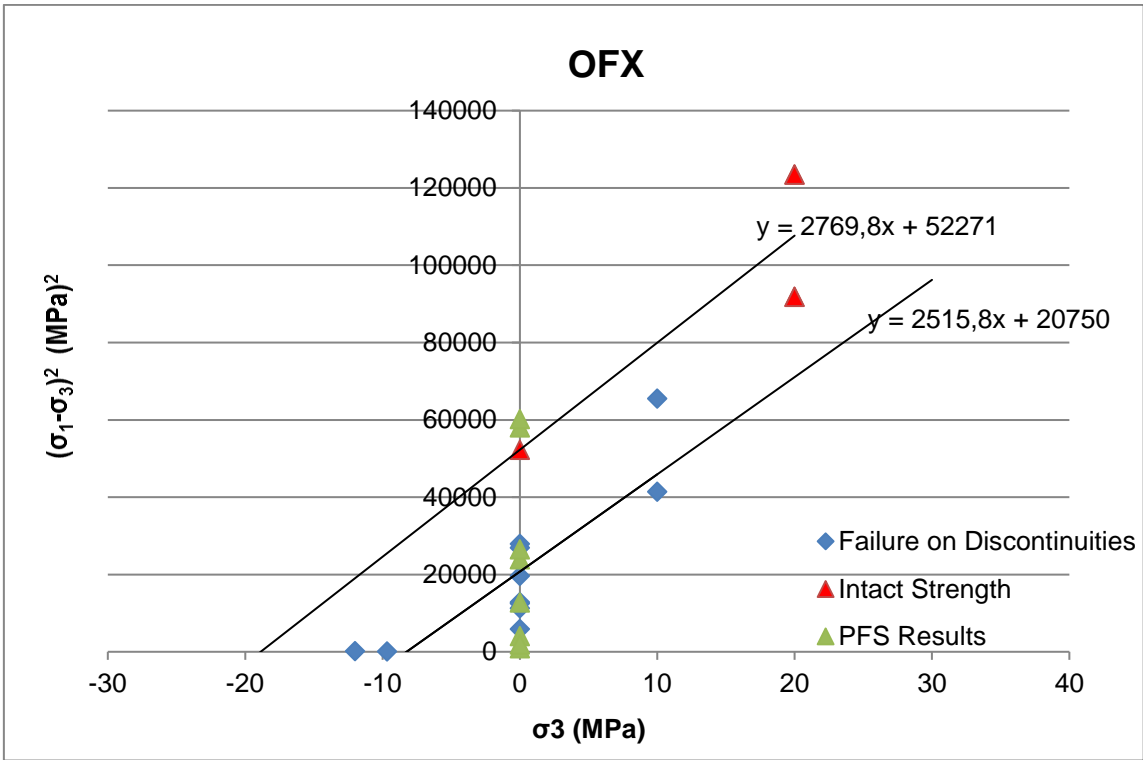
Graph showing the rock strengths results based on laboratory tests for GAN



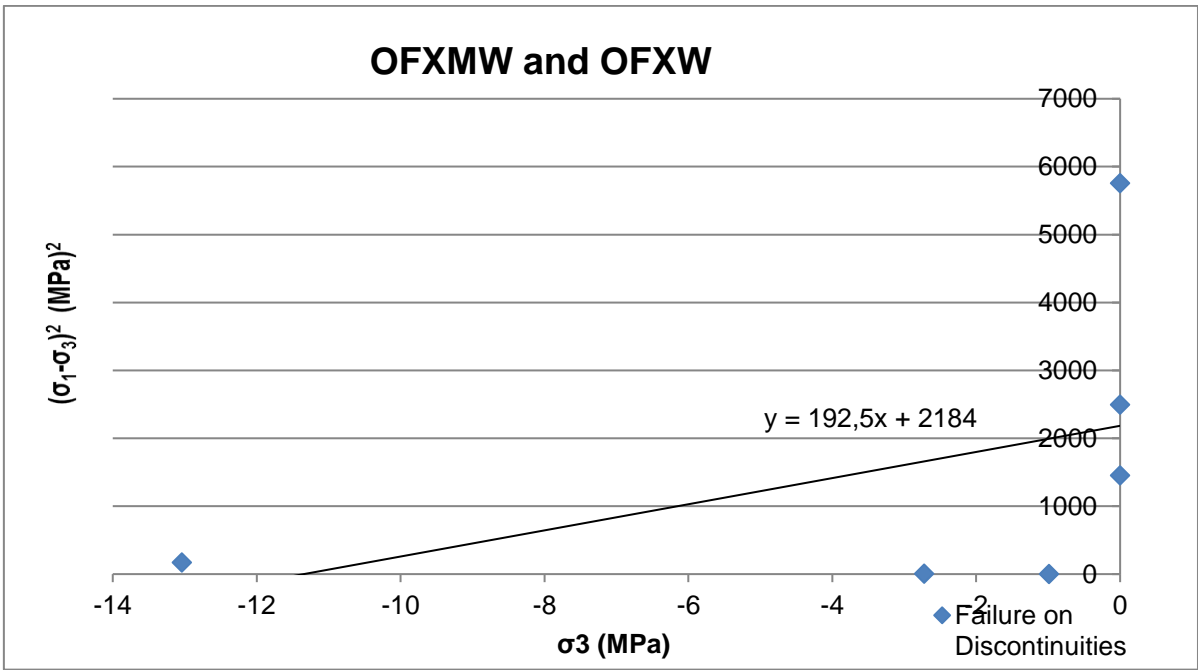
Graph showing the rock strengths results based on laboratory tests for GDO



Graph showing the rock strengths results based on laboratory tests for GDOMW and GDOW

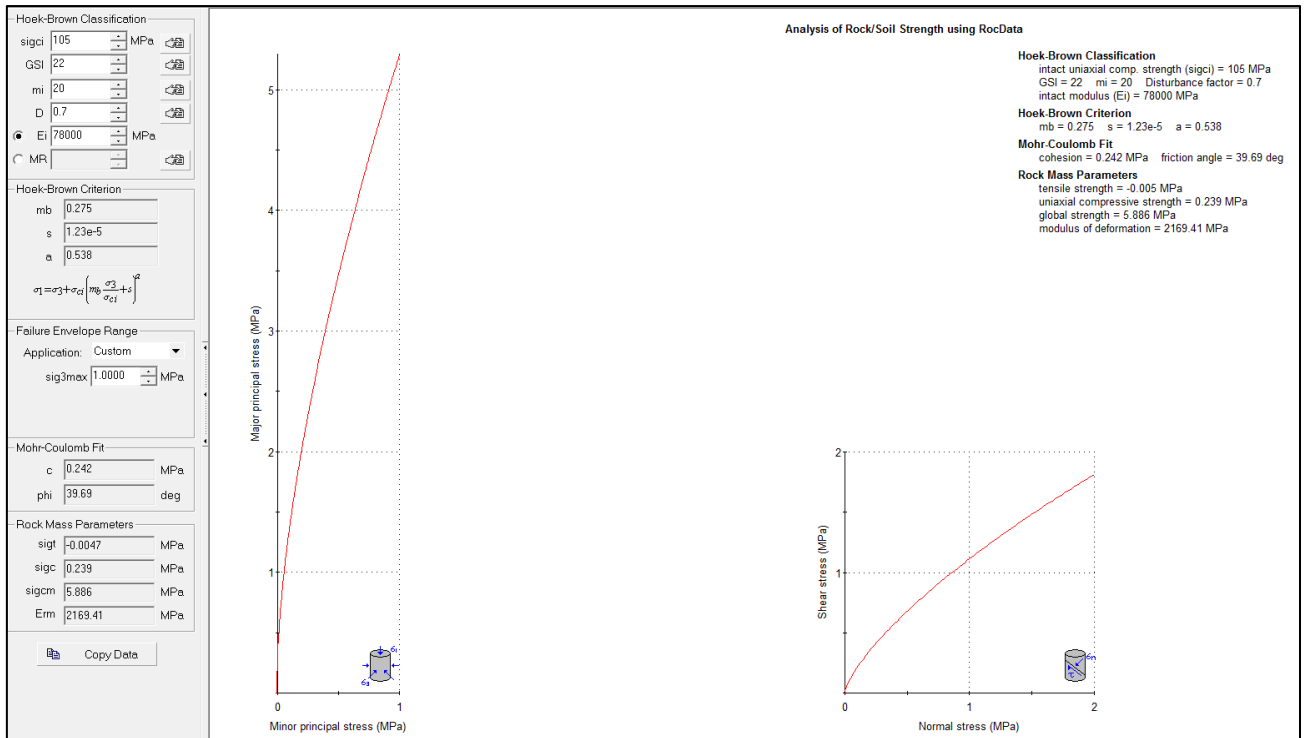


Graph showing the rock strengths results based on laboratory tests for OFX

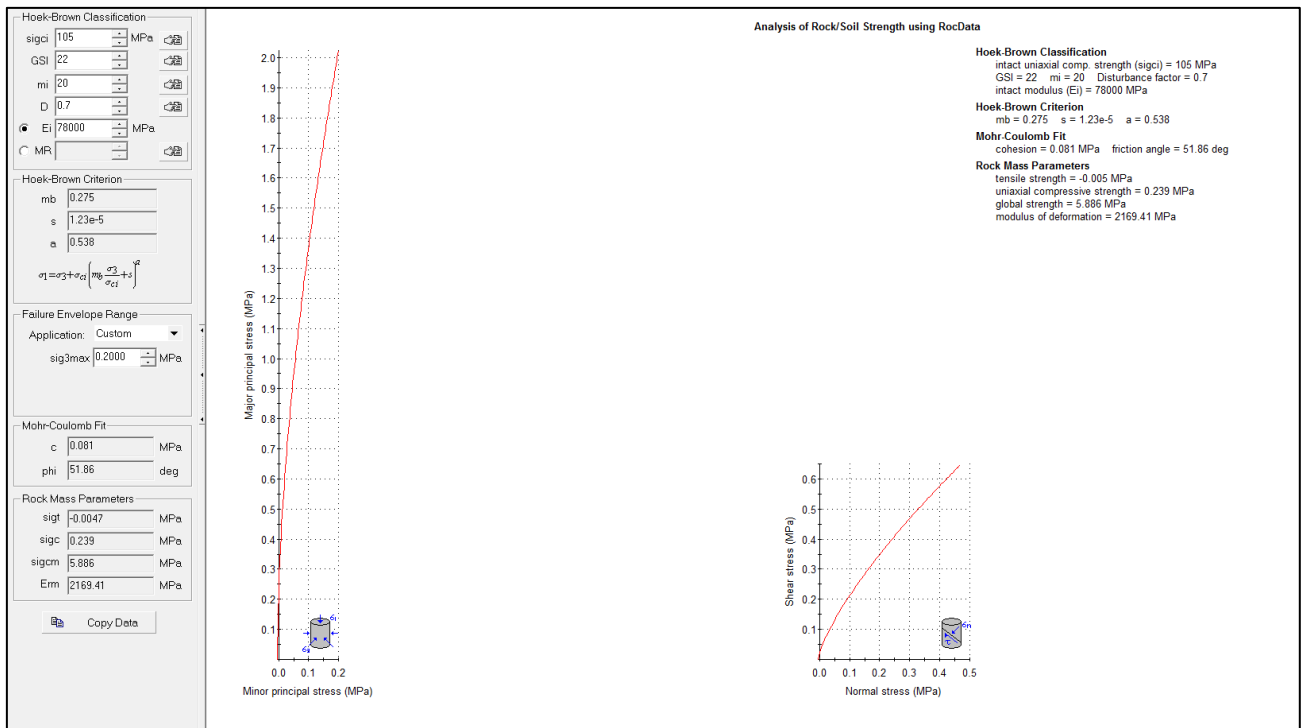


Graph showing the rock strengths results based on laboratory tests for OFX

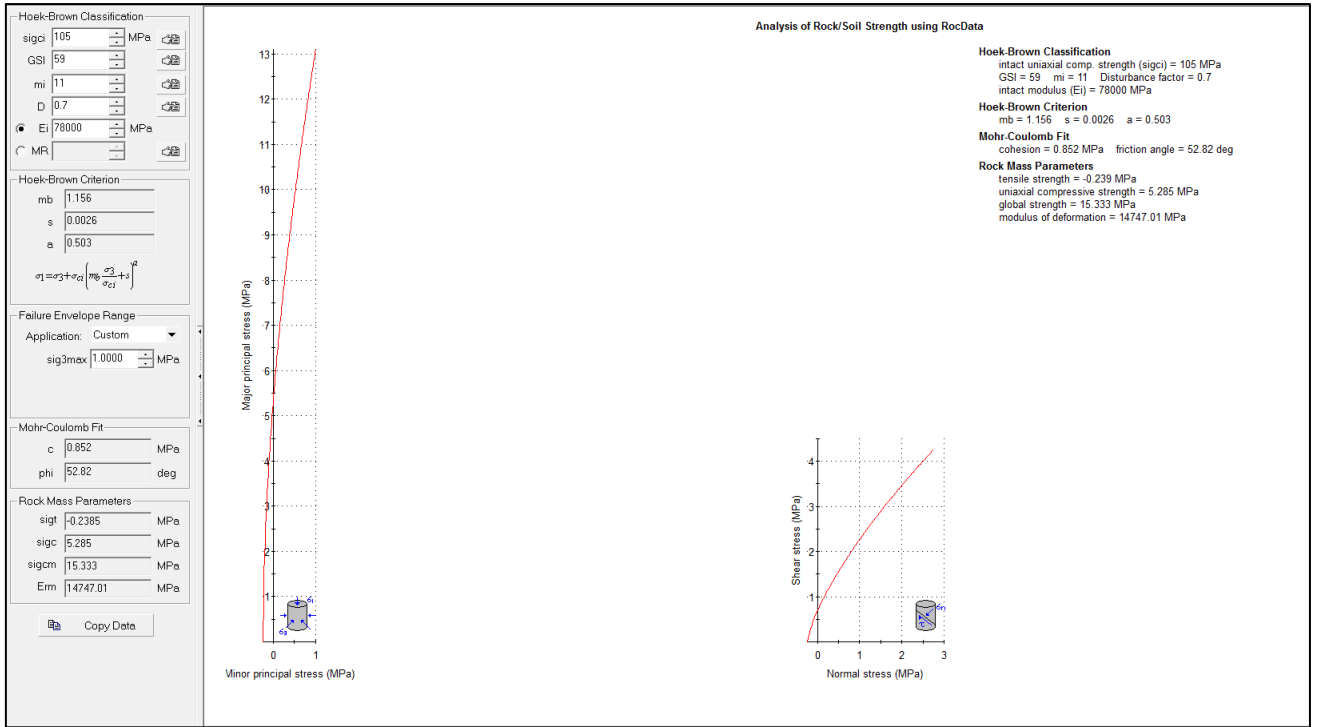
Appendix D: RocData



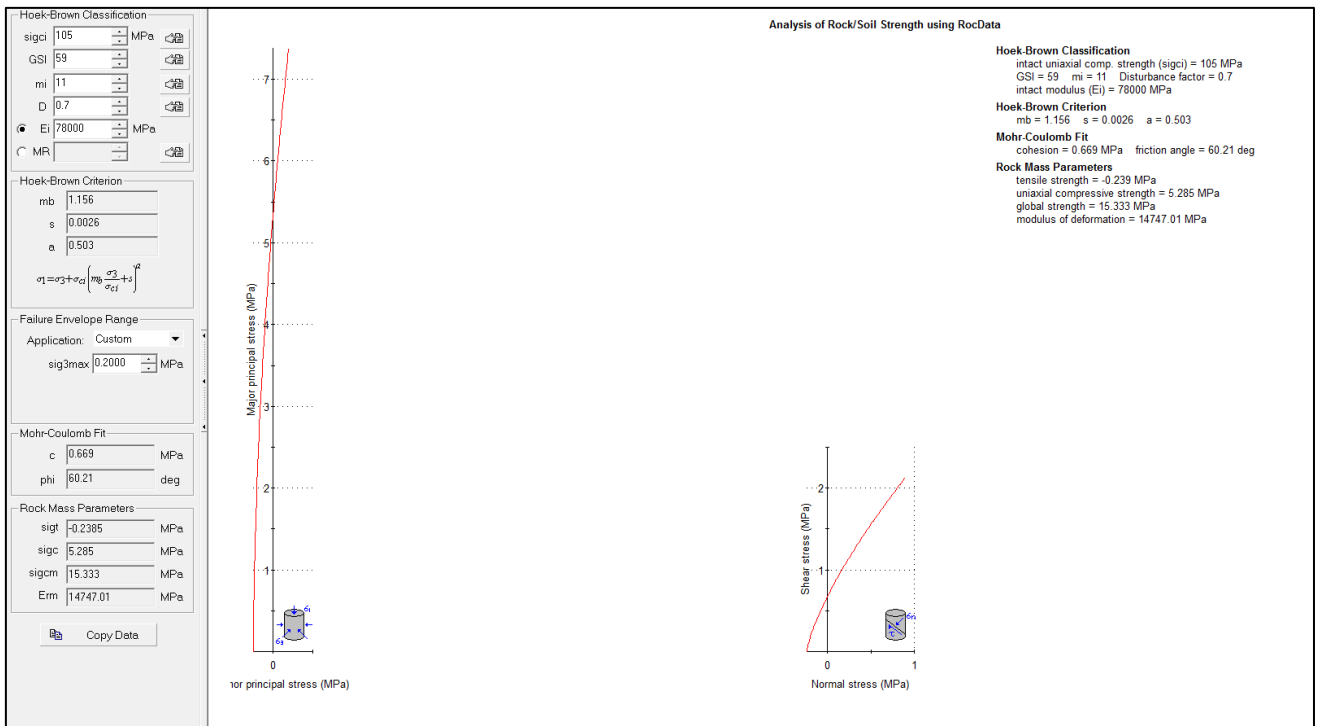
GANW_Deep Rock Mass



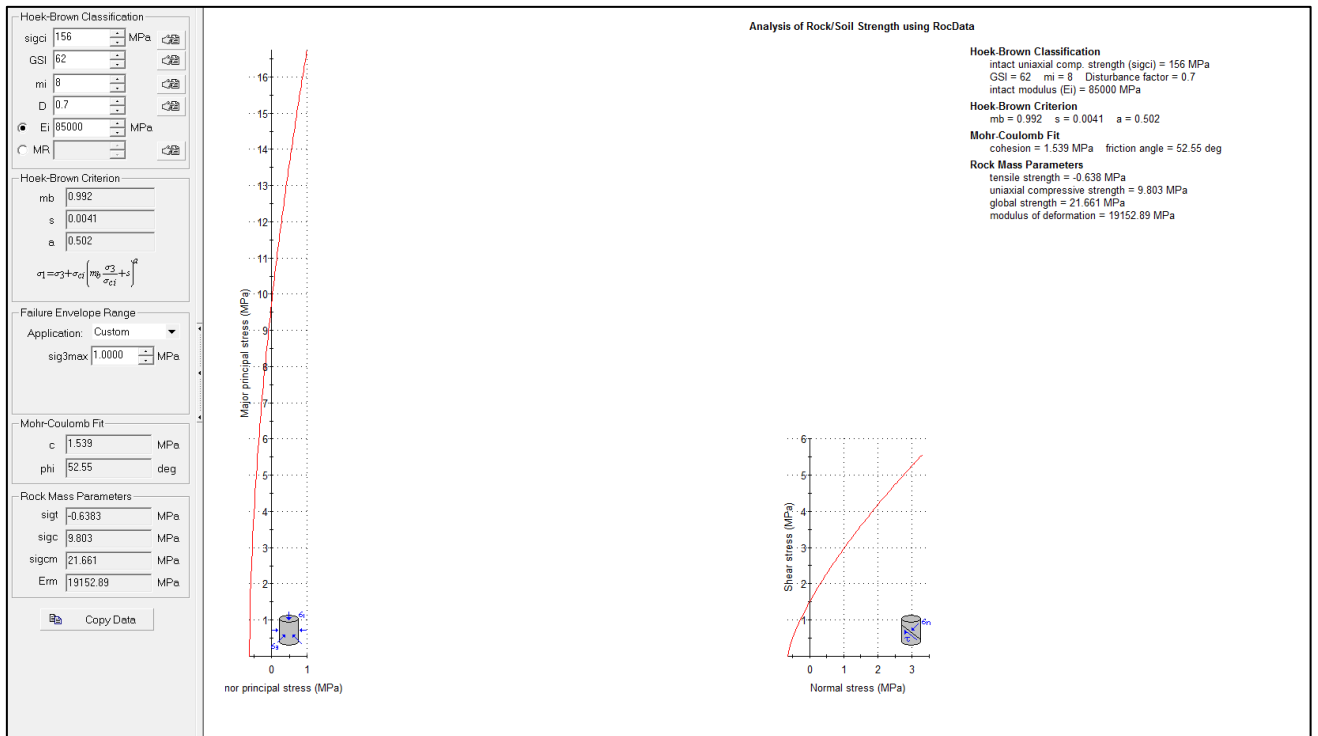
GANW_Shallow Rock Mass



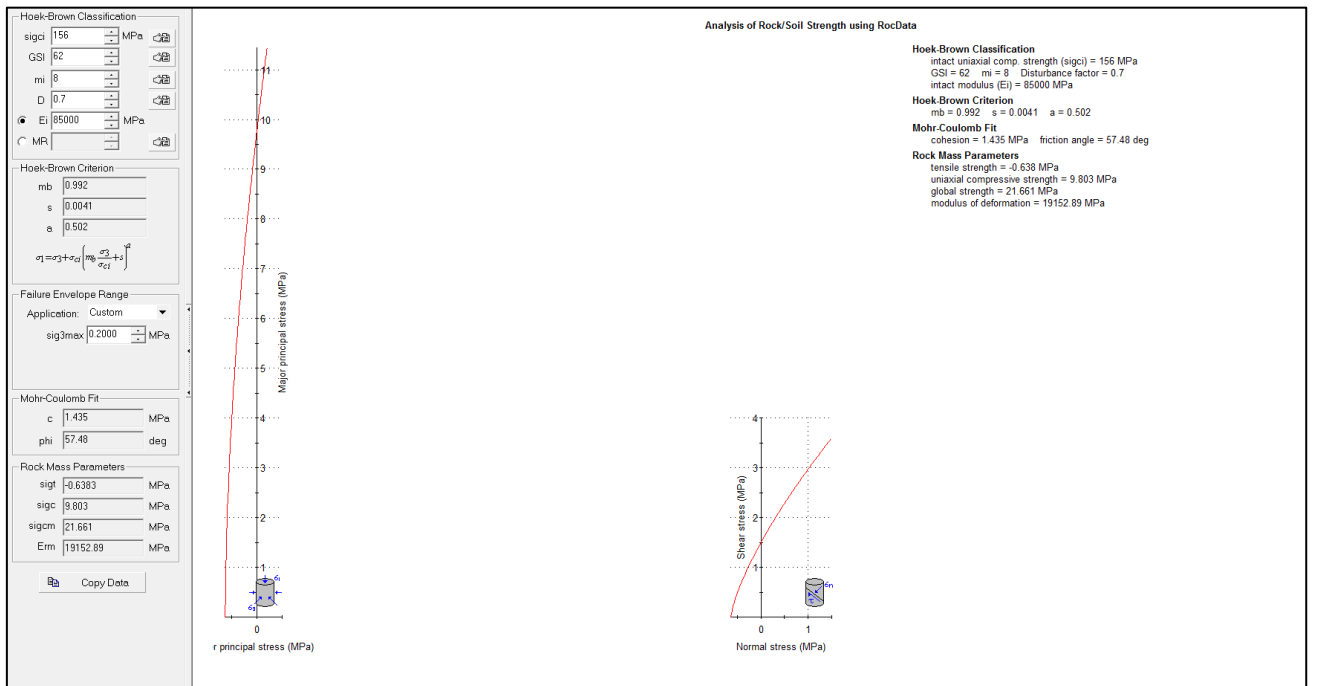
GAN_Deep Rock mass



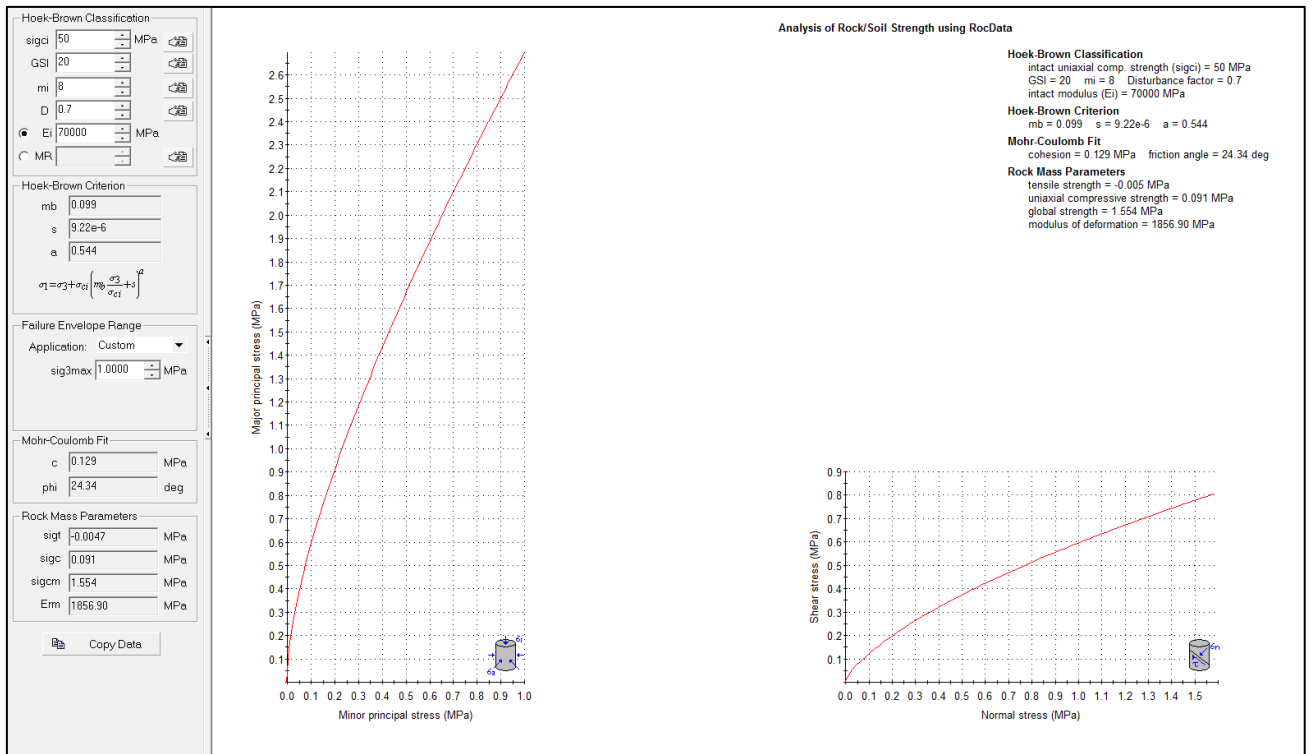
GAN_Shallow Rock Mass



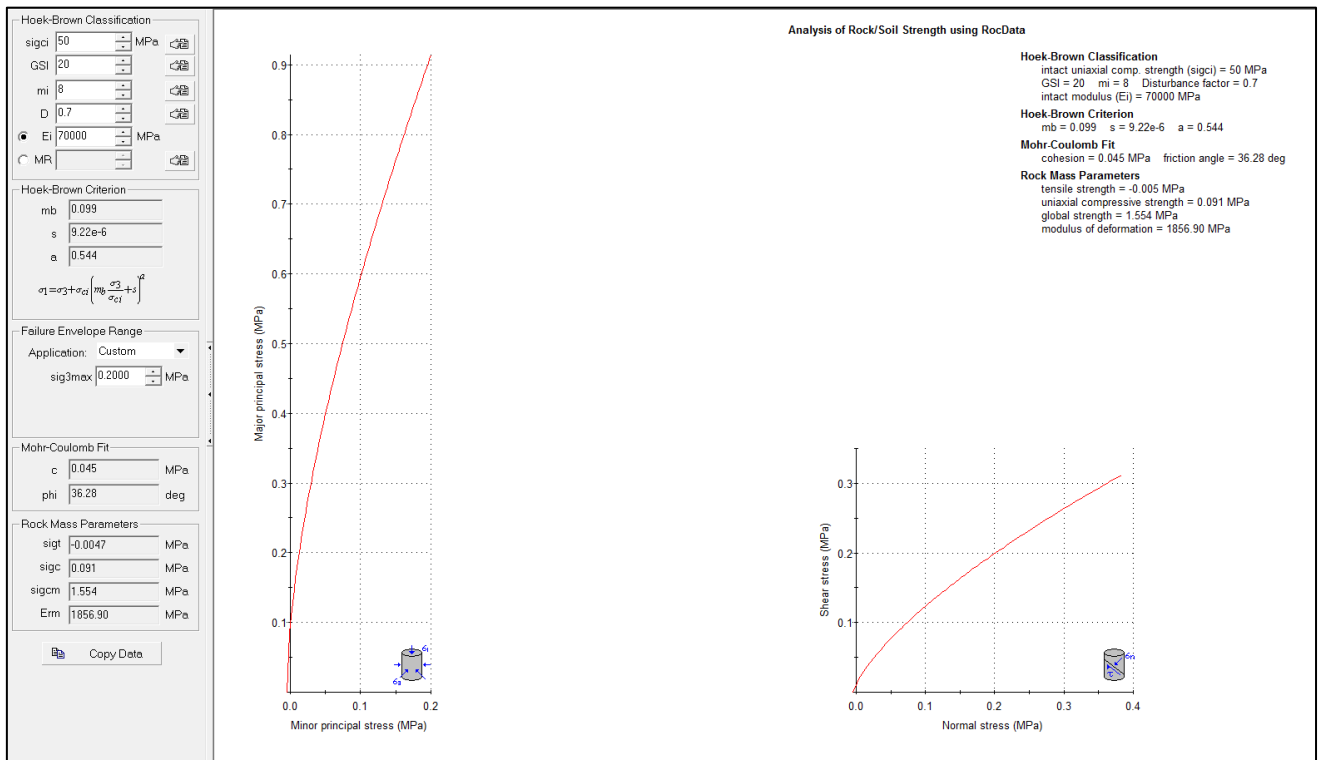
GAB_Deep Rock Mass



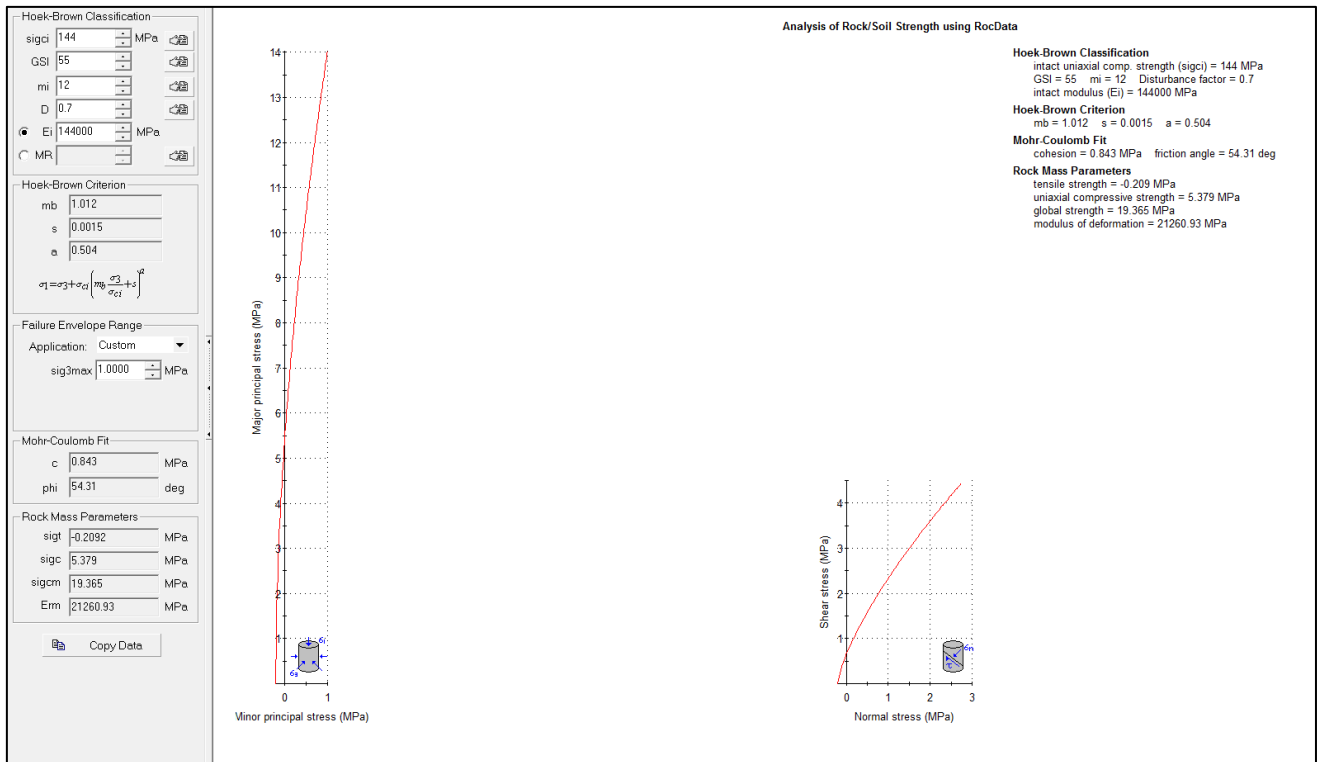
GAB_Shallow Rock Mass



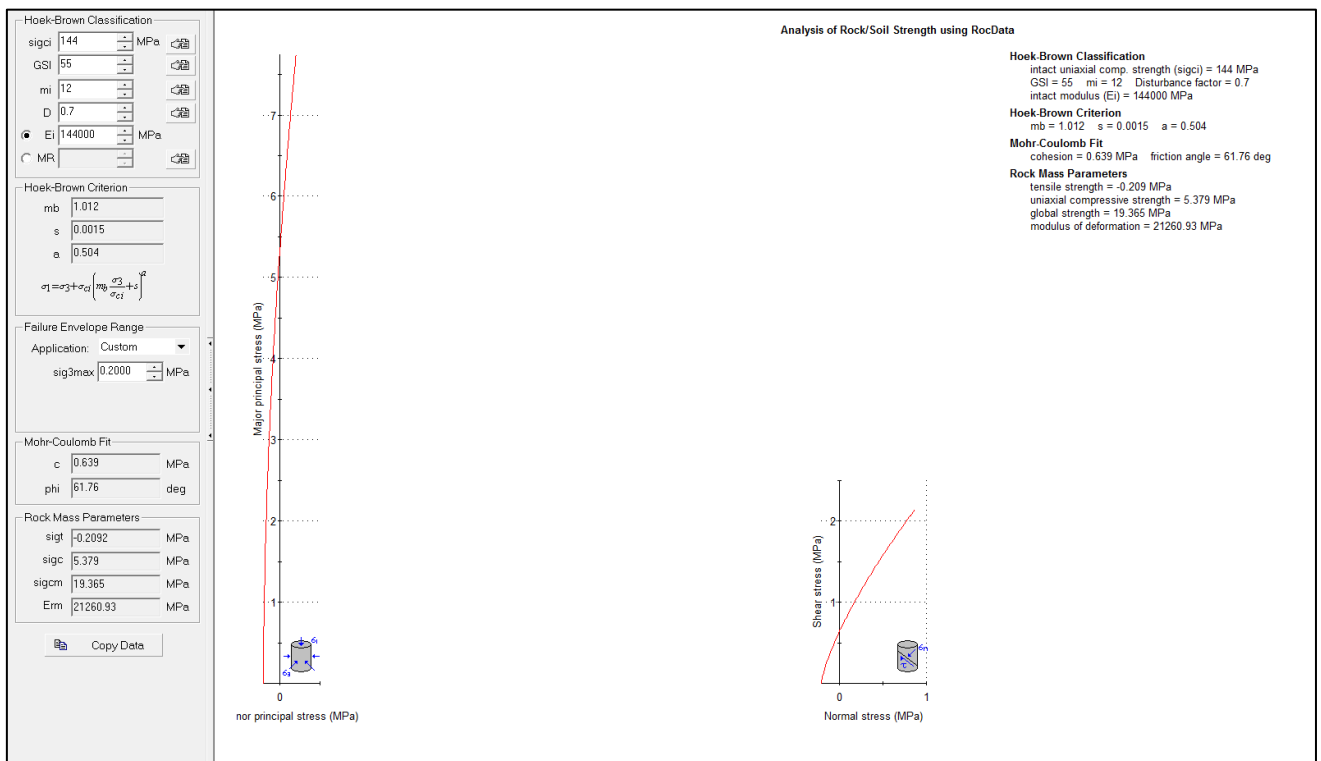
GABMW and GABW_ Deep Rock Mass



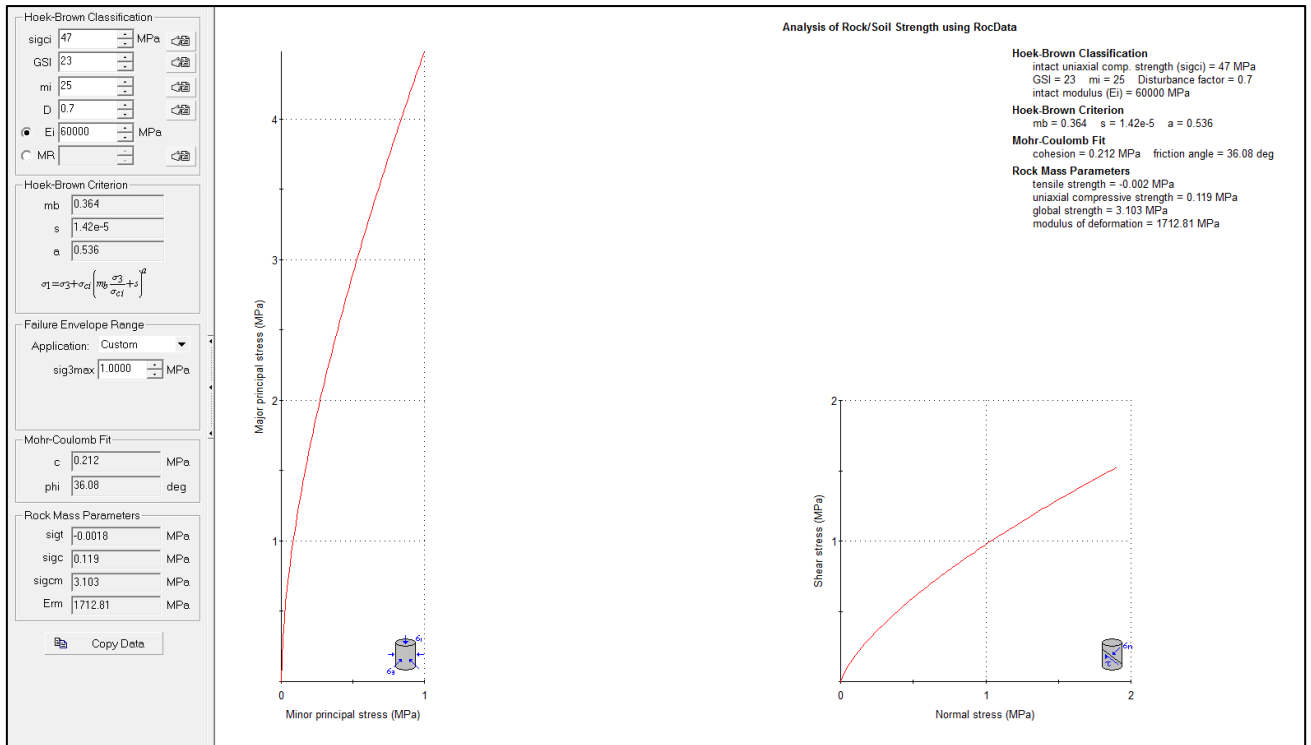
GABMW and GABW_ Shallow Rock Mass



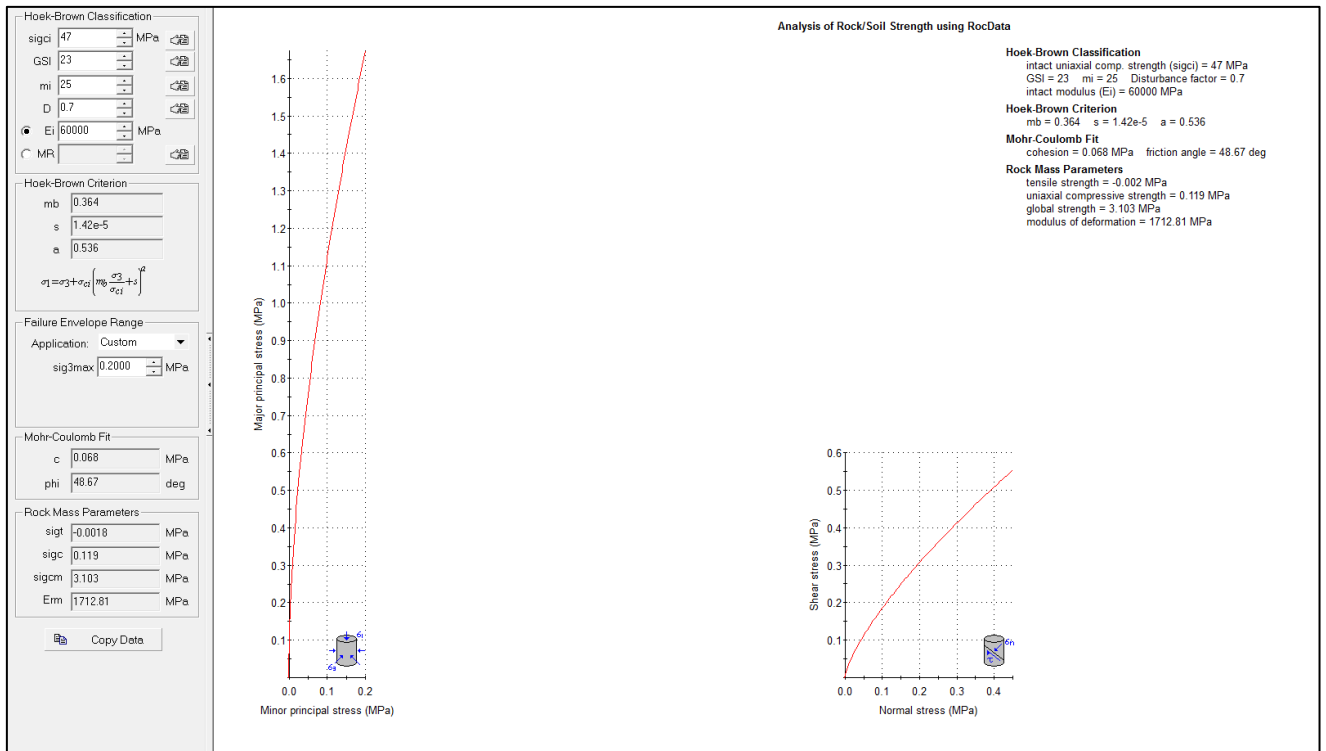
OFX_Deep Rock Mass



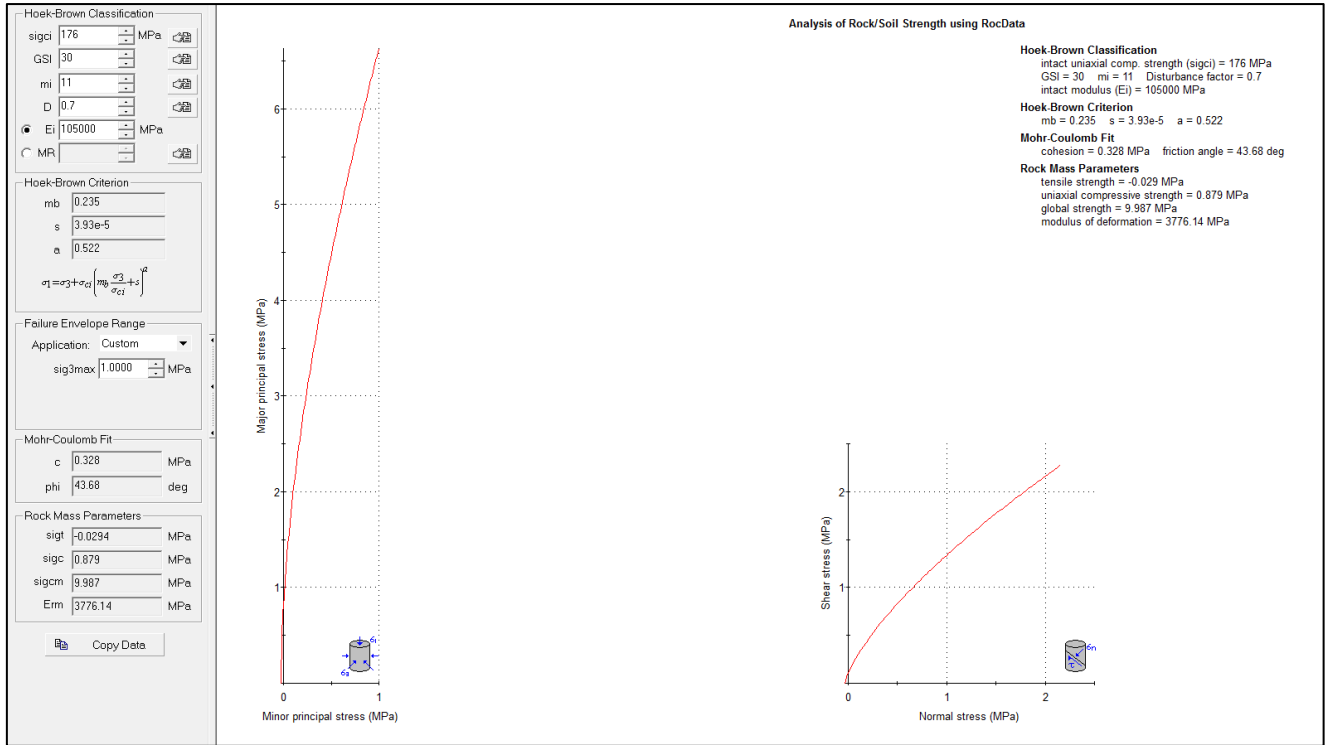
OFX_Shallow Rock Mass



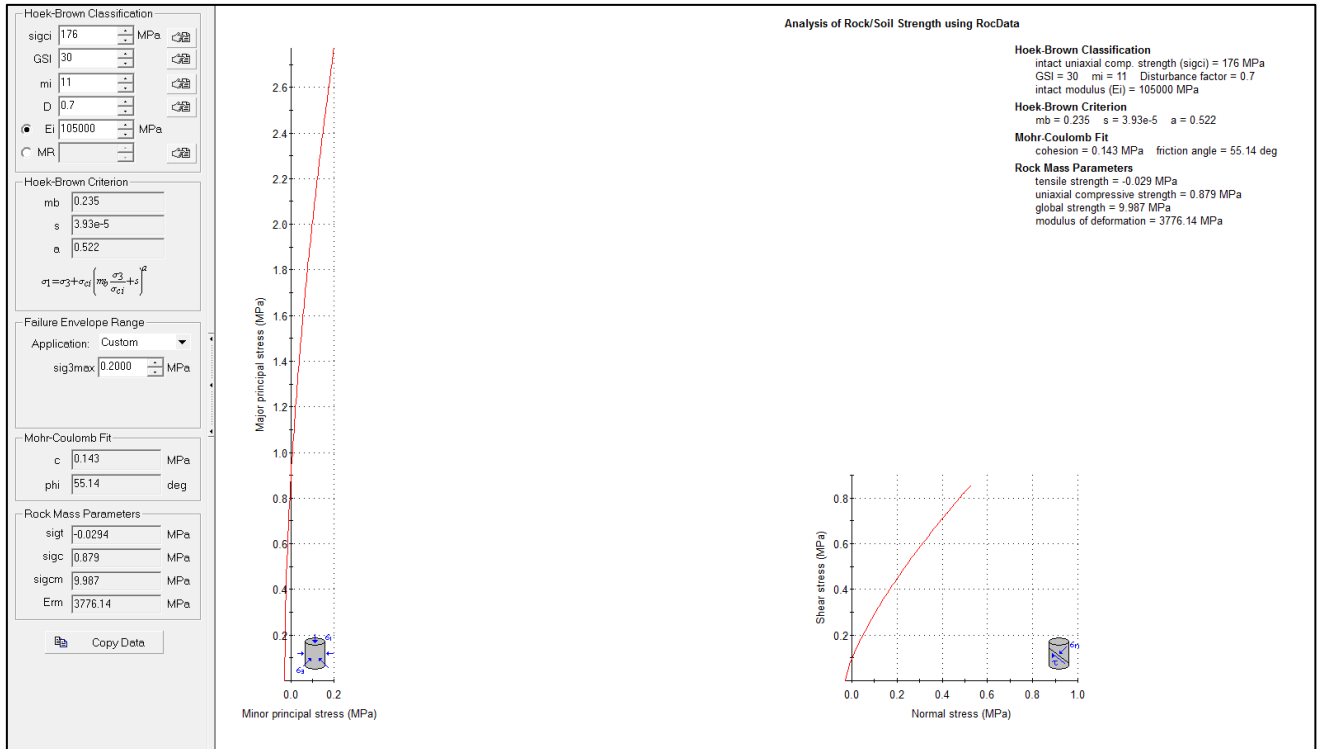
OFXMW and OFXW_ Deep Rock Mass



OFXMW and OFXW_ Shallow Rock Mass



GDO_ Deep Rock Mass



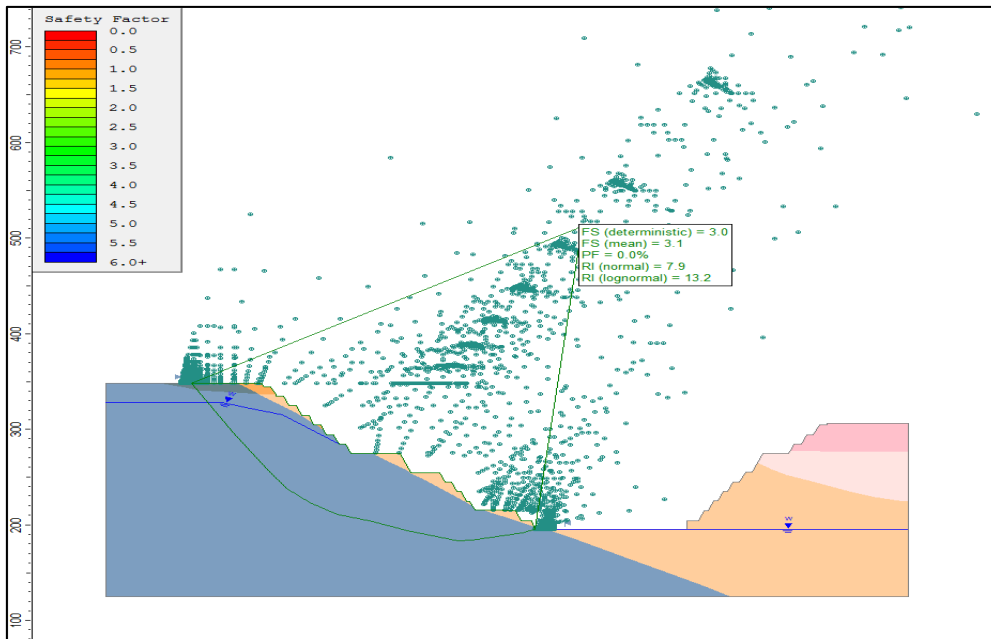
Appendix E: Barton Bandis

OFX Open Joint shear properties										
Scale	Unit	Case	Φ base (°)	Φ res (°)	JCS Field	JRC Field	Deep RM (Sign max=1MPa)		Shallow RM (Sign max=0.2MPa)	
							c (KPa)	Φ (°)	c (KPa)	Φ (°)
20m	OFX	Base	34	30	38	3.8	29	34.6	7	37.0
		(+)	37.5	32			30	36.6	7	39.0
		(-)	30.5	28			27	32.7	6	35.0
OFXW and OFX MW Open Joint shear properties										
Scale	Unit	Case	Φ base (°)	Φ res (°)	JCS Field	JRC Field	Deep RM (Sign max=1MPa)		Shallow RM (Sign max=0.2MPa)	
							c (KPa)	Φ (°)	c (KPa)	Φ (°)
20m	OFX W and OFX MW	Base	37	31	57	3.8	30	36.2	7	38.6
		(+)	37	33			31	38.2	7	40.6
		(-)	37	29			28	34.3	6	36.6
GDO Open Joint shear properties										
Scale	Unit	Case	Φ base (°)	Φ res (°)	JCS Field	JRC Field	Deep RM (Sign max=1MPa)		Shallow RM (Sign max=0.2MPa)	
							c (KPa)	Φ (°)	c (KPa)	Φ (°)
20m	GDO	Base	32	30	75	3.8	30	35.8	7	38.2
		(+)	33.5	32			31	37.8	7	40.2
		(-)	30.5	28			28	33.8	7	36.2
GAB Open Joint shear properties										
Scale	Unit	Case	Φ base (°)	Φ res (°)	JCS Field	JRC Field	Deep RM (Sign max=1MPa)		Shallow RM (Sign max=0.2MPa)	
							c (KPa)	Φ (°)	c (KPa)	Φ (°)

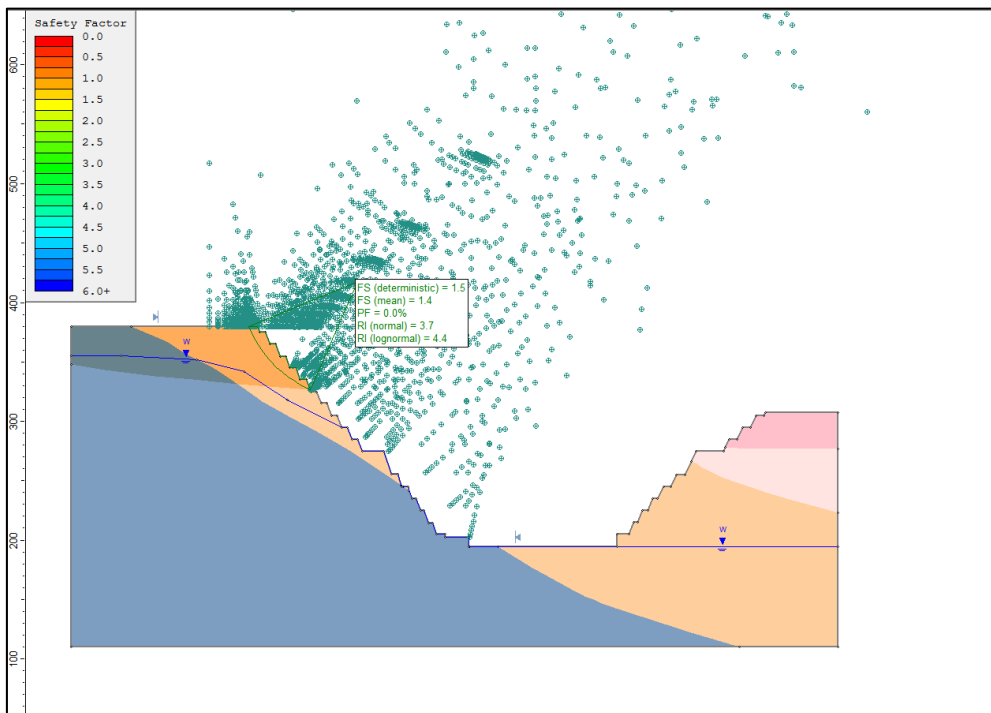
							c (KPa)	Φ (°)	c (KPa)	Φ (°)
20m	GAB	Base	33	24	43	3.8	25	28.8	6	31.1
		(+)	33	31			29	35.8	7	38.1
		(-)	33	17			22	21.8	5	24.1
GABMW and GABW Open foliation shear properties										
Scale	Unit	Case	Φ base (°)	Φ res (°)	JCS Field	JRC Field	Deep RM (Sign max=1MPa)		Shallow RM (Sign max=0.2MPa)	
							c (KPa)	Φ (°)	c (KPa)	Φ (°)
20m	GABMW and GABW	Base	30	24	28	3.8	24	28.1	6	30.4
		(+)	30	26			25	30.1	6	32.4
		(-)	30	22			24	26.1	5	28.4

GAN Open foliation shear properties										
Scale	Unit	Case	Φ base (°)	Φ res (°)	JCS Field	JRC Field	Deep RM (Sign max=1MPa)		Shallow RM (Sign max=0.2MPa)	
							c (KPa)	Φ (°)	c (KPa)	Φ (°)
20m	GAN	Base	33	31.2	34	3.8	29	35.6	7	38.0
		(+)	35.9	34.2			32	38.6	7	41.0
		(-)	30.1	28.2			27	32.6	6	35.0
GANMW and GANW Open foliation shear properties										
Scale	Unit	Case	Φ base (°)	Φ res (°)	JCS Field	JRC Field	Deep RM (Sign max=1MPa)		Shallow RM (Sign max=0.2MPa)	
							c (KPa)	Φ (°)	c (KPa)	Φ (°)
20m	GANW+ GANMW	Base	30	26	28	3.8	25	30.1	6	32.4
		(+)	30	26			25	30.1	6	32.4
		(-)	30	26			25	30.1	6	32.4

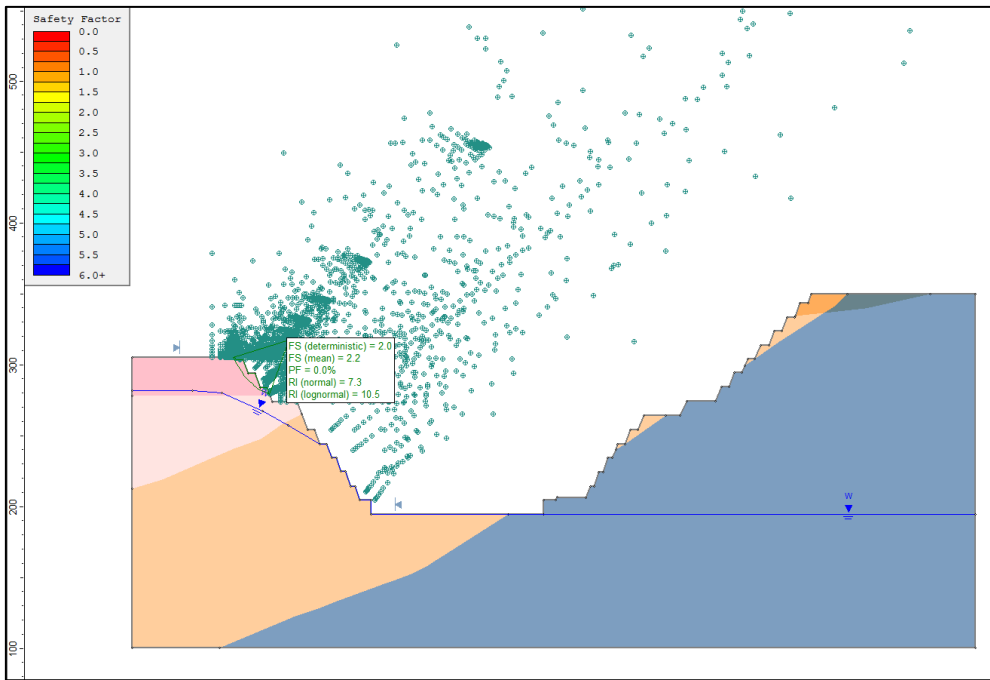
Appendix F: Slide Outputs



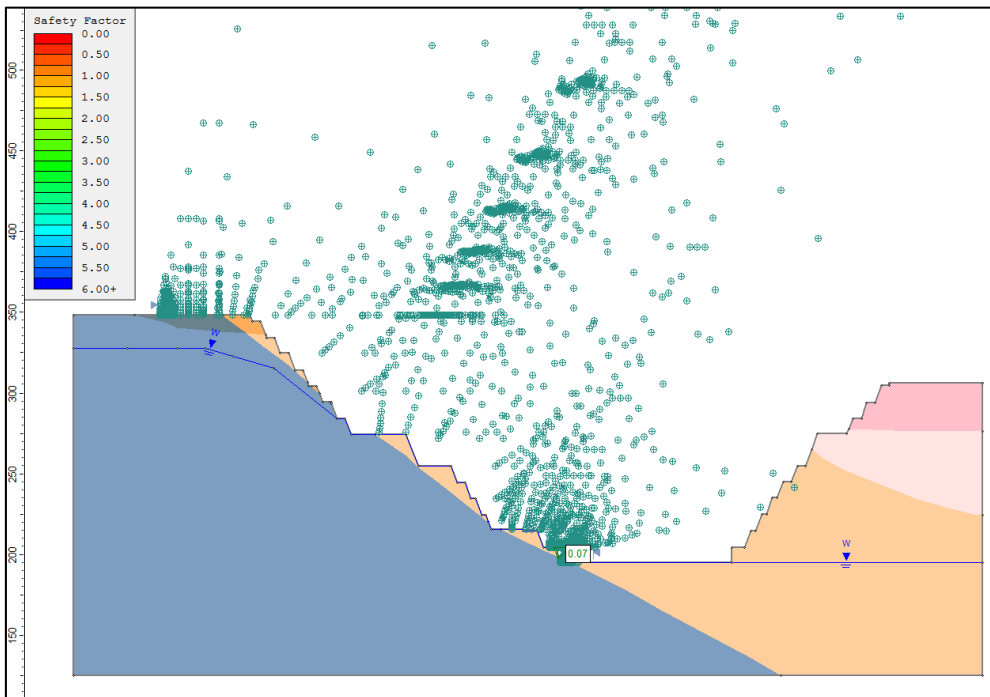
Section A_ Isotropic



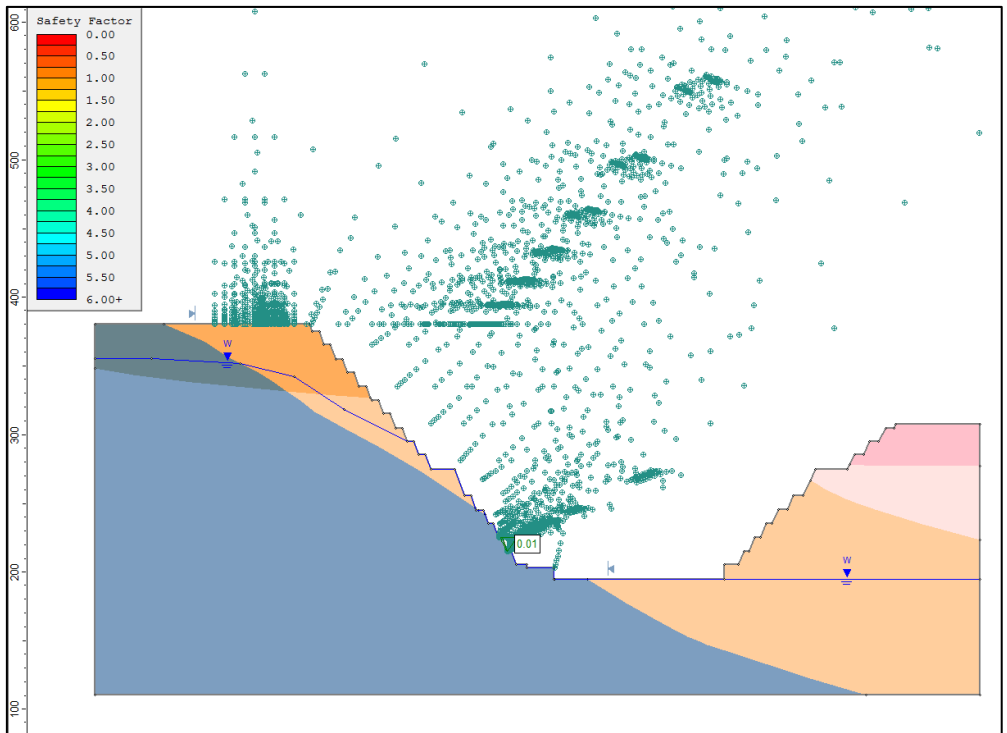
Section B_ Isotropic



Section C_Isotropic



Section A_Anisotropic



Section B_ Anisotropic